

# **Synthesis and characterization of surfmers for latex stabilization in RAFT-mediated miniemulsion polymerization**

by

**Howard Matahwa**

Thesis presented in partial fulfillment of the requirements for the  
degree of

**Master of Science (Polymer Science)**

at the

University of Stellenbosch

Promoter: Prof. R.D Sanderson

Co-promoter: Dr J.B McLeary

December 2005

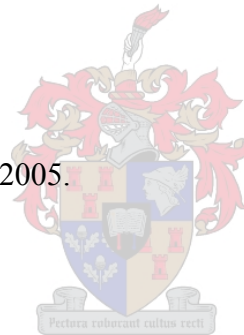
## *Declaration*

I, the undersigned, hereby declare that the work contained in this thesis is my own original work and that I have not previously in its entirety or in part submitted it at any university for a degree.

---

**Howard Matahwa**

Signed on the 30<sup>th</sup> day of November 2005.



Synthesis of two surfmers (cationic and anionic) was carried out and the surfmers were used to stabilize particles in miniemulsion polymerization. Surfmers were used to eliminate adverse effects associated with free surfactant in the final product e.g. films and coatings. The Reversible Addition Fragmentation chain Transfer (RAFT) polymerization process was used in miniemulsion polymerization reactions to control the molecular weight distribution. RAFT offers a number of advantages that include its compatibility with a wide range of monomers and solvents. Moreover block copolymer synthesis is possible via chain extension.

A comparative study between classical surfactants and surfmers was conducted in regard to reaction rates and molar mass distribution. The rates of reactions of surfmer stabilized RAFT miniemulsion polymerization of Styrene and MMA were similar (in most cases) to classical surfactant stabilized RAFT miniemulsion polymerization reactions. The final particle sizes were also similar for polystyrene latexes stabilized by surfmers and classical surfactants. However PMMA latexes stabilized by surfmers had larger particle sizes compared to latexes stabilized by classical surfactants.

The surfmers were also oligomerized in homogeneous media using the RAFT process and their  $M_n$  values were estimated using UV-VIS spectroscopy. The oligosurfmers were then used as emulsifiers in RAFT miniemulsion polymerization. The rates of reaction were slower than rates obtain when the surfmers (monomer or oligosurfmers) were used directly as emulsifiers in RAFT miniemulsion polymerization of styrene and MMA. The final latex particle sizes obtained with oligosurfmers were also larger than that of latex stabilized by their parent monomers.

The RAFT process was successfully applied in miniemulsion polymerization in both classical surfactant and surfmer stabilized miniemulsions. The molecular weight increased with conversion showing that the molecular weights of the polymers were controlled.

### Opsomming

Die sintese van twee seepmere (kationies en anionies) is uitgevoer en die seepmere is gebruik om partikels te stabiliseer in miniemulsiepolimerisasie. Die seepmere is gebruik om die negatiewe effekte van vrye seep in die finale produk d.w.s. films en deklae, te elimineer. Die Omkeerbare Addisie Fragmentasie ketting Oordrag (OAFO) polimerisasie proses is gebruik in miniemulsiepolimerisasiereaksies om die molekulere massa verspreiding te beheer. OAFO bied 'n verskeidenheid voordele wat monomeer- en oplosmiddelaanpasbaarheid insluit. Blokpolimeersintese is ook moontlik via kettingverlenging.

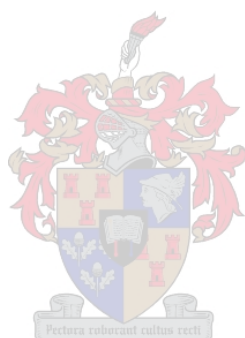
'n Vergelykende studie tussen klassieke sepe en seepmere met betrekking tot reaksietempo's en molekulere massa verspreiding is onderneem. Die reaksietempo's van die seepmeer-gestabiliseerde OAFO miniemulsiepolimerisasie van stireen en MMA was in die meeste gevalle soortgelyk aan die klassieke seep-gestabiliseerde miniemulsiepolimerisasiereaksies. Die finale partikelgroottes was ook soortgelyk vir die polistireen latekse wat gestabiliseer is deur seepmere en klassieke sepe. Die PMMA latekse wat gestabiliseer is deur seepmere het groter partikelgroottes gehad met betrekking tot die latekse wat gestabiliseer is deur klassieke sepe.

Oligomere is gesintetiseer van die seepmere in 'n homogene media via die OAFO proses en die  $M_n$ -waardes is bereken vanaf UV-VIS data. Die oligoseepmere is daarna geëmulgiseer deur OAFO miniemulsiepolimerisasie. Die reaksietempo's is stadiger as die tempos wat verkry is toe die seepmere (monomere en oligoseepmere) direk gebruik is by emulsie-agente in OAFO miniemulsiepolimerisasie van stireen en MMA. Die finale lateks partikelgroottes wat verkry is met die oligoseepmere was ook groter as die van die lateks wat gestabiliseer is deur die oorspronklike monomere.

Die OAFO proses is suksesvol gebruik in miniemulsiepolimerisasie van beide klassieke sepe en seepmeer-gestabiliseerde miniemulsies. Die molekulêre massa het toegeneem met omset wat daarop dui dat die molekulêre massa beheerd was.

*Dedication*

I dedicate this work to my family, friends and my beloved.



*List of Contents*

<i>Abstract</i> .....	iii
<i>Opsomming</i> .....	iv
<i>Dedication</i> .....	v
<i>List of Contents</i> .....	vi
<i>List of Figures</i> .....	xiv
<i>List of Schemes</i> .....	xx
<i>List of Tables</i> .....	xxi
<i>List of Symbols</i> .....	xxii
<i>List of Acronyms</i> .....	xxiv
<i>Acknowledgements</i> .....	xxv
<b>Chapter 1: Introduction and objectives</b> .....	<b>1</b>
1.1: Introduction .....	2
1.2: Aqueous dispersed free radical polymerization .....	2
1.3: Living radical polymerization .....	3
1.4: Polymerizable surfactants in aqueous dispersed polymerizations .....	4
1.5: Research leading to the project .....	4
1.6: Objectives .....	6
1.7: Layout of the thesis .....	6
1.8: References .....	8
<b>Chapter 2: Historical and theoretical background</b> .....	<b>10</b>
2.1: Free radical polymerization .....	11
2.1.1: General .....	11
2.1.2: Free radical kinetics .....	12
2.2: Living Free Radical Polymerization (LFRP) .....	17
2.2.1: Atom Transfer Radical Polymerization (ATRP) .....	18

## ***Index and tables***

---

---

2.2.2: Nitroxide Mediated Polymerization (NMP) .....	20
2.2.3: Reversible Addition Fragmentation chain Transfer (RAFT) .....	21
2.3: Aqueous dispersed polymerization .....	26
2.3.1: Conventional emulsion .....	26
2.3.2: Miniemulsion .....	26
2.3.2.1: General .....	26
2.3.2.2: Preparation of miniemulsions by ultrasound homogenization .....	27
2.3.2.3: Stability of miniemulsions .....	28
2.3.2.4: Effect of a hydrophobe .....	28
2.3.2.5: Mechanisms of particle nucleation .....	29
2.3.2.6: Mechanism and kinetics of miniemulsion polymerization .....	31
2.4: Polymerizable surfactants .....	33
2.4.1: General .....	33
2.4.2: Surfmers .....	34
2.4.3: Critical micelle concentration (CMC) .....	35
2.4.4: Surfactants and surfmers in aqueous dispersed polymerizations .....	35
2.5: References .....	38
<b>Chapter 3: Synthesis, characterization and homogeneous polymerization of polymerizable surfactants using the RAFT process .....</b>	<b>43</b>
3.1: Introduction .....	44
3.2: Synthesis of sulfate surfmer: Sodium 11-methacryloyloxyundecan-1-yl sulfate (SS) .....	45

3.2.1.1: Sodium methacrylate salt formation .....	45
3.2.1.2: Synthesis of 11-methacryloyloxyundecan-1-ol.....	46
3.2.1.3: Synthesis of sodium 11-methacryloyloxyundecan-1-yl sulfate .....	46
3.2.2: Characterization of sodium 11-methacryloyloxyundecan-1-yl sulfate .....	48
3.2.2.1: <sup>1</sup> H NMR spectroscopy of sodium 11-methacryloyloxyundecan-1-yl sulfate .....	48
3.2.2.2: Electro spray-mass spectroscopy (ES/MS) of sodium 11-methacryloyloxyundecan-1-yl sulfate.....	49
3.2.2.3: Infra-red (IR) spectroscopy of sodium 11-methacryloyloxyundecan-1-yl sulfate .....	50
3.3: Synthesis of the ammonium surfmer: Synthesis of 11-methacryloyloxyundecan-1-yl trimethyl ammonium bromide (AS) .....	51
3.3.1: Experimental .....	51
3.3.1.1: Synthesis of 11-methacryloyloxyundecan-1-yl bromide .....	51
3.3.1.2: Synthesis of 11-methacryloyloxyundecan-1-yl trimethyl ammonium bromide.....	52
3.3.2: Characterization of 11-methacryloyloxyundecan-1-yl trimethyl ammonium bromide.....	53
3.3.2.1: <sup>1</sup> H NMR spectroscopy of 11-methacryloyloxyundecan-1-yl trimethyl ammonium bromide .....	53
3.3.2.2: ES/MS spectroscopy of 11-methacryloyloxyundecan-1-yl trimethyl ammonium bromide .....	54
3.3.2.3: IR spectroscopy of 11-methacryloyloxyundecan-1-yl trimethyl ammonium bromide .....	55
3.3.3: Discussion: Surfmer synthesis (SS and AS) .....	55



3.4: Critical micelle concentration (CMC) of surfmers and surfactants .....	56
3.4.1: Experimental .....	56
3.4.2: Results .....	56
3.4.2.1: CMC of SDS and SS .....	56
3.4.2.2: CMC of CTAB and AS .....	57
3.5: Synthesis of the RAFT agent 4-cyano-4-(thiobenzoyl) sulfonyl pentanoic acid (CVADTB).....	59
3.5.1: Experimental .....	60
3.5.1.1: Preparation of the Grignard reagent.....	60
3.5.1.2: Preparation of dithiobenzoic acid.....	60
3.5.1.3: Preparation of bis (thiocarbonyl) disulfide .....	61
3.5.1.4: Preparation of the RAFT agent 4-cyano-4-(thiobenzoyl) sulfonyl pentanoic acid.....	61
3.6: Synthesis and characterization of oligosurfmers.....	62
3.6.1: General .....	62
3.6.2: Experimental .....	62
3.6.3: Characterization of oligosurfmers.....	64
3.6.3.1: Characterization of SS oligomer (SSO) by <sup>1</sup> H NMR spectroscopy.....	64
3.6.3.2: Characterization of AS oligomer (ASO) by <sup>1</sup> H NMR spectroscopy.....	65
3.6.3.3: Characterization of oligosurfmers (SSO & ASO) by UV spectroscopy .....	66
3.7: Conclusions .....	69
3.8: References .....	70

<b>Chapter 4: RAFT mediated miniemulsion polymerization of styrene and MMA</b> .....	<b>71</b>
4.1: Introduction .....	72
4.2: Experimental .....	72
4.2.1: Reagents .....	72
4.2.2: Analysis.....	73
4.2.3: General procedure .....	73
4.2.4: Polymerization .....	74
4.3: RAFT mediated miniemulsion polymerization of styrene.....	75
4.3.1: SDS and CTAB in RAFT mediated miniemulsion polymerization of styrene.....	75
4.3.1.1: Rates of reactions .....	76
4.3.1.2: Molecular weight distributions as determined by SEC.....	77
4.3.2: SS and AS in RAFT miniemulsion polymerization of styrene.....	79
4.3.2.1: Rates of reaction in styrene polymerization.....	79
4.3.2.2: Surfmer conversion in RAFT miniemulsion polymerization.....	80
4.3.2.3: Molecular weight distribution in RAFT mediated miniemulsion polymerization of styrene.....	82
4.3.2.4: UV-RI analysis of the SS reaction at 85°C .....	83
4.3.3: SDS and SS in RAFT mediated miniemulsion polymerization of styrene .....	87
4.3.3.1: Rates of reactions .....	87
4.3.3.2: Molecular weight distribution in styrene RAFT miniemulsion polymerization (SDS vs. SS).....	88
4.3.4: CTAB and AM in RAFT mediated miniemulsion polymerization of styrene.....	88

## *Index and tables*

---

---

4.3.4.1: Rates of reactions .....	88
4.3.4.2: Molecular weight distribution in RAFT mediated miniemulsion polymerization of styrene (CTAB vs AS).....	89
4.4: MMA RAFT mediated miniemulsion polymerization reactions .....	91
4.4.1: SDS and CTAB in RAFT mediated miniemulsion polymerization of MMA .....	92
4.4.1.1: Rates of reaction.....	92
4.4.1.2: Molecular weight distribution in MMA RAFT mediated miniemulsion polymerization.....	93
4.4.2: SS and AS in RAFT miniemulsion polymerization of MMA.....	95
4.4.2.1: Rates of reactions .....	95
4.4.2.2: Molecular weight distribution in RAFT mediated miniemulsion polymerization of MMA .....	96
4.4.2.3: UV-RI analysis of the SS and AS stabilized reactions at 80°C.....	99
4.4.3: SDS and SS in MMA RAFT miniemulsion polymerization.....	100
4.4.3.1: Rates of reaction.....	100
4.4.3.2: Molecular weight distributions as determined by SEC.....	101
4.4.4: CTAB and AM in RAFT miniemulsion polymerization of MMA .....	102
4.4.4.1: Rates of reaction.....	102
4.4.4.2: Molecular weight distribution in RAFT mediated miniemulsion polymerization of MMA .....	103
4.5: Analysis of copolymers of styrene and surfmers (2D-chromatography) .....	105
4.5.1: Introduction.....	105
4.5.2: Experimental conditions .....	106

4.5.3: Results.....	106
4.5.3.1: LCCC of SS-styrene.....	106
4.5.3.2: LCCC of AS-styrene.....	108
4.6: The use of oligosurfmers in RAFT mediated miniemulsion polymerization of styrene and MMA.....	109
4.6.1: Procedure.....	109
4.6.2: Sulfate surfmer oligomer (SSO) in RAFT miniemulsion of styrene and MMA.....	110
4.6.2.1: Rates of reactions.....	110
4.6.2.2: Molecular weight distribution in RAFT mediated miniemulsion polymerization of styrene and MMA with SSO as the emulsifier.....	111
4.6.3: Ammonium surfmer oligomer (ASO) in RAFT mediated miniemulsion polymerization of styrene.....	114
4.6.3.1: Rates of reaction.....	114
4.6.3.2: Molecular weight distribution curves for RAFT miniemulsion polymerization of styrene with ASO as the emulsifier.....	115
4.6.4: ASO in RAFT mediated miniemulsion polymerization of MMA.....	117
4.6.4.1: Rates of reaction.....	117
4.6.4.2: Stabilization of MMA using 1 g of ASO.....	118
4.6.4.3: Stabilization of MMA using 1.5 g of ASO.....	119
4.6.4.3: Comment on the use of RAFT oligosurfmers as emulsifiers.....	119
4.7: Particle sizes of styrene and MMA lattices.....	121
4.7.1: Dynamic Light Scattering (DLS) and Transmission Electron Microscopy (TEM).....	121

## *Index and tables*

---

---

4.7.1.1: Styrene latex particle sizes .....	121
4.7.1.2: MMA latex particle sizes .....	125
4.7.2: Capillary Hydrodynamic Fractionation (CHDF) .....	127
4.7.2.1: General .....	127
4.7.2.2: Results and discussion.....	128
4.7.2.3: Typical CHDF chromatograms .....	130
4.8: Conclusions .....	132
4.8.1: General .....	132
4.8.3: Molecular mass distributions .....	134
4.8.3: RAFT in miniemulsion polymerization .....	135
4.9: References .....	136
<b>Chapter 5: Conclusions and recommendations.....</b>	<b>138</b>
5.1: Conclusions .....	139
5.2: Recommendations for future research .....	142



*List of Figures*

Fig 2.1: Propagating polymeric radical with substituents R and X.....	11
Fig 2.2: Two commonly used azo- and peroxy- free radical initiators .....	12
Fig 2.3: The structures of 2,2,6,6-tetramethyl-1-piperidinyloxy free radical (TEMPO) and N-tert-butyl-N-(1-diethylphosphono-2,2-dimethylpropyl) nitroxide (DEPN).....	20
Fig 2.4: Basic structure of the RAFT agent <sup>30,37,38</sup> .....	21
Fig 2.5: (a) Examples of Z-groups and (b) R-groups of RAFT agents .....	22
Fig 2.6: Schematic representation of particle nucleation mechanisms possible for miniemulsion and emulsion <sup>59</sup> polymerizations .....	30
Fig 2.7: Kinetics of miniemulsion polymerization as revealed by calorimetry .....	31
Fig 2.8: The general structure of a classical surfactant e.g. sodium lauryl sulfate [hydrophobic tail is a C <sub>12</sub> and the hydrophilic head is the sulfate group with sodium as the counter ion (OSO <sub>3</sub> <sup>-</sup> Na <sup>+</sup> )] .....	33
Fig 2.9: Three different types of surfmers: [A] Diethyl maleate surfmer <sup>84</sup> [anionic (T- type)]; [B] 11-(acryloyloxy) undecyl trimethylammonium bromide <sup>83</sup> [cationic (H-type)] and [C] maleate surfmer <sup>84</sup> [nonionic (T-type)].....	34
Fig 3.1: <sup>1</sup> H NMR spectrum of sodium 11-methacryloyloxyundecan-1-yl sulfate (D <sub>2</sub> O solvent).....	48
Fig 3.2: ESMS spectrum of sodium 11-methacryloyloxyundecan-1-yl sulfate .....	49
Fig 3.3: Infra-red spectrum of sodium 11-methacryloyloxyundecan-1-yl sulfate .....	50
Fig 3.4: <sup>1</sup> H NMR spectrum of 11-methacryloyloxyundecan-1-yl trimethyl ammonium bromide (CDCl <sub>3</sub> solvent).....	53
Fig 3.5: ES/MS of 11-methacryloyloxyundecan-1-yl trimethyl ammonium bromide.....	54
Fig 3.6: Infra-red spectrum of 11-methacryloyloxyundecan-1-yl trimethyl ammonium bromide .....	55
Fig 3.7: A plot of logarithm of conductivity against concentration (M) for the determination of critical micelle concentration of sulfate surfmer (SS) and sodium dodecyl sulfate (SDS) .....	56
Fig 3.8: A plot of logarithm of conductivity against concentration (M) for the determination of critical micelle concentration of ammonium surfmer (AS) and CTAB .....	57
Fig 3.9: <sup>1</sup> H NMR spectra of SS oligosurfmer and the surfmer, showing the changes after polymerization of the sulfate surfmer (D <sub>2</sub> O solvent).....	64

Fig 3.10: <sup>1</sup> H NMR spectra of AS oligosurfmer and the AS surfmer showing the changes after homopolymerization of the ammonium surfmer (Solvents: D <sub>2</sub> O [ASO], (CD <sub>3</sub> ) <sub>2</sub> SO [AS]) .....	65
Fig 3.11: UV/VIS spectra: (A) sulfate oligomer (SSO) and sulfate surfmer (SS); (B) ammonium oligomer (ASO) and ammonium surfmer (AS) [Water was used as solvent (UV-cutoff 180 nm)] .....	66
Fig 3.12: (A) UV/VIS spectra of the RAFT agent [Toluene was used as solvent (UV-cutoff 285 nm)] and (B) calibration curve for the determination of <i>M<sub>n</sub></i> of oligosurfmers. [The dotted lines (labeled 1 to 4) are extrapolation lines (see Table 3.3)].....	66
Fig 4.1: 1st order rate kinetics for SDS and CTAB stabilized miniemulsion polymerization of styrene: 1 = SDS (85°C); 2 = CTAB (85°C); 3 = SDS (75°C); 4 = CTAB (75°C); 5 and 6 are initiator decay curves at 75°C and 85°C respectively .....	76
Fig 4.2: SDS stabilized RAFT mediated miniemulsion polymerization of styrene (reaction 2): A = molecular weight distribution for SDS stabilized reaction at 75°C and B = evolution of <i>M<sub>n</sub></i> and PDI for RAFT mediated miniemulsion polymerizations of styrene at 75°C .....	77
Fig 4.3: CTAB stabilized RAFT mediated miniemulsion polymerization of styrene (reaction 4): A = molecular weight distribution for CTAB stabilized reaction at 75°C and B = evolution of <i>M<sub>n</sub></i> and PDI for RAFT mediated miniemulsion polymerizations of styrene at 75° .....	71
Fig 4.4: 1st order rate kinetics for SS and AS stabilized miniemulsion polymerization of styrene: 7 = AS (85°C); 5 = SS (85°C); 8 = AS (75°C); 6 = SS (75°C). <i>I</i> <sub>1</sub> and <i>I</i> <sub>2</sub> are initiator decay curves at 75°C and 85°C, respectively. [The dotted lines on the rate curves are a guide to the eye].....	79
Fig 4.5: Conversion time graphs of SS & styrene (reaction 5, 85°C) and AS & styrene (reaction 7, 85°C) in RAFT miniemulsion polymerization of styrene. The solid line ( <i>I</i> <sub>2</sub> ) is the initiator decay curve at 85°C .....	80
Fig 4.6: Molecular weight distributions for SS and AS surfmer stabilized RAFT miniemulsion polymerization of styrene: A = SS at 85°C; B = AS at 85°C; C = SS at 75°C and D = AS at 75°C .....	82
Fig 4.7: UV-RI overlays: A, B and C, D are for the SS stabilized RAFT mediated miniemulsion polymerization of styrene at 85°C and 75°C respectively.....	84

Fig 4.8: UV-RI overlays: A, B and C, D are for the AS stabilized RAFT mediated miniemulsion polymerization of styrene at 85°C and 75°C, respectively. [Two plots per reaction for different conversions have been provided].....	86
Fig 4.9: 1st order rate kinetics for SDS and SS stabilized miniemulsion polymerization of styrene: 1= SDS (85°C); 5 = SS (85°C); 2 = SDS (75°C) and 6 = SS (75°C). I <sub>1</sub> and I <sub>2</sub> are initiator decay curves at 75°C and 85°C respectively. [The dotted lines are a guide to the eye] .....	87
Fig 4.10: Molecular weight distributions for SDS and SS surfmer stabilized RAFT miniemulsion polymerizations of styrene: A = SDS at 85°C and B = SS at 85°C .....	88
Fig 4.11: 1st order rate kinetics for CTAB and AS stabilized miniemulsion polymerization of styrene: 3 = CTAB (85°C); 7 = AS (85°C); 4 = CTAB (75°C) and 8 = AS (75°C). I <sub>1</sub> and I <sub>2</sub> are initiator decay curves at 75°C and 85°C respectively. ....	89
Fig 4.12: Molecular weight distribution for CTAB and AS stabilized RAFT mediated miniemulsion polymerization of styrene: A = CTAB at 85°C and B = AS at 85°C.....	89
Fig 4.13: Evolution of Mn and PDI for RAFT mediated miniemulsion polymerizations of styrene at 75°C with quaternary ammonium surfactants .....	90
Fig 4.14: 1st order rate kinetics for SDS and CTAB stabilized miniemulsion polymerization of MMA: 9 = SDS (80°C); 11 = CTAB (80°C); 10 = SDS (75°C) and 12 = CTAB (75°C)].....	92
Fig 4.15: Molecular weight distribution for SDS and CTAB stabilized RAFT mediated miniemulsion polymerization of MMA: A = SDS at 80°C and B = CTAB at 80°C.....	93
Fig 4.16: Evolution of $M_n$ and PDI for RAFT miniemulsion polymerizations of MMA: A = SDS and B = CTAB, reactions conducted at 80°C .....	94
Fig 4.17: 1st order rate kinetics for SS and AS stabilized RAFT mediated miniemulsion polymerization of MMA: 13= SS (80°C); 15 = AS (80°C); 14 = SS (75°C) and 16 = AS (75°C).....	95
Fig 4.18: Molecular weight distributions for SS and AS surfmer stabilized RAFT mediated miniemulsion polymerizations of MMA: A = SS at 80°C and B = AS at 80°C.....	96
Fig 4.19: Evolution of $M_n$ and PDI for RAFT miniemulsion polymerizations of MMA, using AS at 80°C .....	97

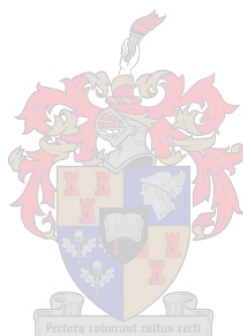


Fig 4.20: UV-RI overlays: A, B and C, D for SS and AS stabilized RAFT miniemulsion polymerization of MMA at 80°C, respectively. [Two plots were provide per reaction at different conversions].....	99
Fig 4.21: 1st order rate kinetics for SDS and SS stabilized miniemulsion polymerization of MMA: 9= SDS (80°C); 13 = SS (80°C); 10 = SDS (75°C) and 14 = SS (75°C). [The dotted lines are a guide to the eye].....	100
Fig 4.22: Molecular weight distributions for SDS and SS surfmer stabilized RAFT miniemulsion polymerization of MMA: A = SDS at 80°C and B = SS at 80°C.....	101
Fig 4.23: 1st order rate kinetics for CTAB and AS stabilized miniemulsion polymerization of MMA: 11 = CTAB (80°C); 15 = AS (80°C); 12 = CTAB (75°C) and 16 = AS (75°C). [The dotted lines are a guide to the eye].....	102
Fig 4.24: Molecular weight distribution for CTAB and AS surfmer stabilized RAFT miniemulsion polymerization of MMA: A = CTAB at 75°C and B = AS at 75°C....	103
Fig 4.25: Evolution of $M_n$ and PDI for RAFT miniemulsion polymerizations of MMA at 75°C: (a) and (b) are the theoretical $M_n$ values for CTAB and AS stabilized miniemulsions, reactions 12 and 16 respectively; (c) and (e) GPC $M_n$ and PDI respectively for AS stabilized miniemulsions (reaction 16); finally (d) and (f) GPC $M_n$ and PDI respectively for CTAB stabilized miniemulsion polymerization (reaction 12).....	104
Fig 4.26: Liquid adsorption chromatogram (1st dimension) for SS-styrene copolymer, reaction 5.....	107
Fig 4.27: 3-D chromatogram for SS-styrene copolymer reaction 5.....	107
Fig 4.28: Liquid adsorption chromatogram (1st dimension) for AS-styrene copolymer, reaction 7.....	108
Fig 4.29: 1st order rate kinetics for SSO stabilized miniemulsion polymerization of: A = styrene at 85°C and B = MMA at 80°C .....	110
Fig 4.30: Molecular weight distribution for SSO stabilized RAFT miniemulsion polymerization of: A = styrene at 85°C (reaction 17) and B = MMA at 80°C (reaction 18).....	111
Fig 4.31: Evolution of $M_n$ and PDI for SSO stabilized RAFT miniemulsion polymerization of: A = styrene at 85°C (reaction 17) and B = MMA at 80°C (reaction 18).....	112

Fig 4.32: UV-RI overlays for SSO stabilized RAFT miniemulsion polymerization of styrene at 85°C (reaction 17) at two different conversion: A =18.5% and B = 51.3% conversion.....	113
Fig 4.33:1st order rate kinetics for AS oligomer stabilized miniemulsion polymerization of styrene.....	114
Fig 4.34: Molecular weight distribution for ASO stabilized RAFT miniemulsion polymerization of styrene at 85°C: A = 1 g ASO and B = 1.5 g ASO.....	115
Fig 4.35: Evolution of $M_n$ and PDI for ASO stabilized RAFT miniemulsion polymerization of styrene at 85°C: A = 1 g of ASO and B = 1.5 g of ASO .....	115
Fig 4.36: UV-RI overlays; A, B and C, D for 1.0 g and 1.5 g ASO respectively in RAFT mediated miniemulsion polymerization of styrene at respective conversions.....	116
Fig 4.37: 1st order rate kinetics for AS oligomer stabilized miniemulsion polymerization of MMA: 22 = 1.5 g ASO, 21 = 1.0 g of ASO and I = initiator decay curve at 80°C.....	117
Fig 4.38: A = Molecular weight distribution for AS oligomer (1.0 g) stabilized RAFT miniemulsion polymerization of MMA; B = Evolution of $M_n$ and PDI for RAFT miniemulsion polymerization of MMA at 80°C; C and D are UV-RI overlays at respective conversions .....	118
Fig 4.39: A = molecular weight distribution for AS oligomer (1.5g) stabilized RAFT miniemulsion polymerization of MMA at 80°C; B = Evolution of $M_n$ and PDI for RAFT miniemulsion polymerization of MMA at 80°C; C and D are UV-RI overlays at respective conversions.....	119
Fig 4.40: TEM images for polystyrene latexes: A = SDS stabilized polystyrene particles; B = SS stabilized polystyrene particles; C = CTAB stabilized polystyrene particles; D = AS stabilized polystyrene particles (see Table 4.1 for compositions).....	122
Fig 4.41: TEM images for polystyrene latexes: A = SSO stabilized polystyrene particles; B = ASO stabilized polystyrene particles. (see Table 4.3 for compositions).....	124
Fig 4.42: TEM images for MMA latexes: A = SDS stabilized PMMA particles; B = SS stabilized PMMA particles; C = CTAB stabilized PMMA particles and D = AS stabilized PMMA particles. (see Table 4.2 for compositions).....	126
Fig 4.43: Overlaid number data and weight overlaid data (as labeled) for polystyrene latex stabilized by the sulfate surfmer (SS) .....	130

Fig 4.44: Overlaid number data and weight overlaid data (as labeled) for PMMA latex  
stabilized by the sulfate surfmer (SS) ..... 130

Fig 4.45: Overlaid number data and weight overlaid data (as labeled) for polystyrene  
latex stabilized by the ammonium surfmer (ASO) ..... 131



***List of Schemes***

Scheme 2.1: A coupling termination reaction.....	15
Scheme 2.2: A disproportionation reaction.....	16
Scheme 2.3: General formation of a dormant species in LFRP.....	18
Scheme 2.4: Schematic representation of the ATRP process.....	19
Scheme 2.5: Schematic representation of the NMP process.....	20
Scheme 2.6: Some of the elementary steps in the RAFT mechanism as reported by McLeary <i>et al</i> <sup>66</sup> .....	23
Scheme 2.7: Miniemulsion preparation <sup>71</sup> .....	28
3.2.1: Experimental.....	45
Scheme 3.1: Reaction pathway and conditions for the synthesis of sodium 11-methacryloyloxyundecan-1-yl sulfate (SS).....	45
Scheme 3.2: Reaction mechanism for the synthesis of 11-methacryloyloxyundecan-1-ol.....	46
Scheme 3.3: Reaction mechanism for the synthesis of sodium 11-methacryloyloxyundecan-1-yl sulfate.....	46
Scheme 3.4: Reaction pathway and conditions for the synthesis of sodium 11-methacryloyloxyundecan-1-yl trimethyl ammonium bromide.....	51
Scheme 3.5: Reaction mechanism for the synthesis of 11-methacryloyloxyundecan-1-yl bromide.....	51
Scheme 3.6: Reaction mechanism for the synthesis of 11-methacryloyloxyundecan-1-yl trimethyl ammonium bromide.....	52
Scheme 3.7: Reaction pathway used for the synthesis of 4-cyano-4-(thiobenzoyl) sulfonyl pentanoic acid.....	59
Scheme 3.8: Synthesis of oligosulfonates in solution.....	63

*List of Tables*

Table 2.1: Various methods of free radical generation .....	13
Table 3.1: The CMC values of SDS, SS, CTAB and AS, as determined by the conductivity method.....	57
Table 3.2: Reagents and quantities used for the synthesis of SS and AS oligosurfmers .....	63
Table 3.3: UV data for the determination of the $M_n$ of the oligosurfmers as well as the predicted $M_n$ (from equation 3.1).....	67
Table 4.1: The quantities of reagents and reaction temperature used in the miniemulsion polymerizations of styrene .....	75
Table 4.2: Reagents and reaction conditions used in miniemulsion polymerizations of MMA.....	91
Table 4.3: The masses of reagents and reaction temperatures used in miniemulsion polymerizations of styrene and MMA .....	110
Table 4.4: The particle sizes (nm) of styrene miniemulsion latexes for different surfactants and surfmers .....	121
Table 4.5: Styrene miniemulsion latex with SSO and ASO (oligomers) at 85°C.....	123
Table 4.6: The particle sizes (nm) of MMA miniemulsion latexes for different surfactants and surfmers .....	125
Table 4.7: MMA miniemulsion latex with SSO and ASO oligomers at 80°C.....	127
Table 4.8: Particle sizes (nm) of styrene miniemulsion latexes for different surfactants and surfmers.....	128
Table 4.9: Particle sizes (nm) of MMA miniemulsion latexes for different surfactants and surfmers.....	128

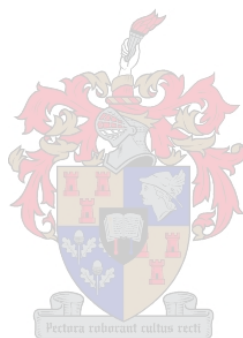
*List of Symbols*

X	Interaction parameter
$\mu$	Critical thermal increment
$\bar{n}$	Average number of radicals
$\phi_m$	Volume fraction of monomer
$\phi_h$	Volume fraction of hydrophobe
Mn	Number average molar mass
Mw	Weight average molar mass
M <sub>n,th</sub>	Calculated number average molar mass
I	Initiator
[I]	Initiator concentration
[I] <sub>0</sub>	Initial concentration of initiator
[M] <sub>0</sub>	Initial concentration of monomer
[RAFT] <sub>0</sub>	Initial concentration of RAFT agent
$\delta$	Droplet-water interfacial tension
$\bar{V}_m$	Molar volume of monomer
$\bar{V}_h$	Molar volume of hydrophobe
$\Delta G$	Gibbs free energy
M <sub>nh</sub>	Ratio of molar volume of monomer to hydrophobe
R <sub>p</sub>	Rate of polymerization
Q <sub>r</sub>	Heat of polymerization
V <sub>aq</sub>	Volume of aqueous phase
$\Delta H$	Molar heat of polymerization
$\overline{Mn}_{pred}$	Predicted number average molar mass
M <sub>w,monomer</sub>	Molecular weight of monomer
M <sub>w,RAFT</sub>	Molecular weight of RAFT agent
[Monomer]	Monomer concentration
[RAFT]	RAFT agent concentration
K <sub>d</sub>	Dissociation constant
$\lambda$	Fraction of termination by Disproportionation
$\langle Kt \rangle$	Average termination rate constant

## *Index and tables*

---

[M]	Concentration of monomer
$C_m$	Chain transfer constant
[S]	Concentration of the transfer agent
C	Transfer constant
$K_{tr}$	Transfer rate coefficient
$K_p$	Propagation rate coefficient
$K_t$	Termination constant
$\nu_t$	Rate of termination
$\nu_i$	Rate of initiation
f	Radical efficiency
t	Time



*List of Acronyms*

AIBN	2,2-azobis (isobutyronitrile)
AS	Ammonium surfmer
ASO	Ammonium surfmer oligomer
ATRP	Atom transfer radical polymerization
BPO	Benzoyl peroxide
CCD	Chemical composition distribution
CHDF	Capillary hydrodynamic fractionation
CMC	Critical micelle concentration
CTAB	Cetyl trimethyl ammonium bromide
DEPN	N-tert-butyl-N-(1-diethylphosphono-2,2-dimethylpropyl) nitroxide
DLS	Dynamic light scattering
ESR	Electron spin resonance
ESMS	Electro-spray mass spectrometry
<sup>1</sup> HNMR	Proton nuclear magnetic resonance spectroscopy
HPLC	High performance liquid chromatograph
IR	Infrared spectroscopy
LAC	Liquid adsorption chromatograph
LCCC	Liquid chromatograph at critical conditions
LFRP	Living free radical polymerization
M	Molar concentration
MMA	Methylmethacrylate
MMD	Molar mass distribution
NMP	Nitroxide mediated polymerization
RAFT	Reversible addition fragmentation chain transfer
RI	Refractive index detector
SDS	Sodium dodecyl sulfate
SEC	Size exclusion chromatograph
SS	Sulfate surfmer
SSO	Sulfate surfmer oligomer
TEMPO	2,2,6,6-tetramethyl-1-piperidinyloxy free radical
UV	Ultraviolet



## *Acknowledgements*

---

### *Acknowledgements*

Firstly, I would like to thank God for blessing me with the gift of life during my study. I know that God gave me guidance, courage, strength and joy in times of despair. May the honor and glory be unto Him.

I would like to thank the following people and organizations for their contributions to this project:

Prof. RD Sanderson for being my promoter, his knowledge input, motivation and encouragement during this study,

Dr JB McLeary for his unlimited input into this project;

Dr Grumel for GPC and HPLC analysis,

Dr Hartmann and Dr Weber for their contributions in the synthesis of surfmers,

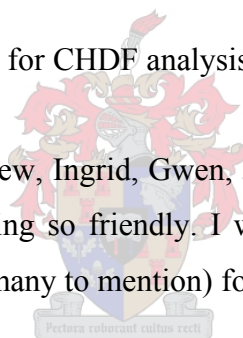
Dr Hurndall for assisting with preparing this manuscript,

Jean McKenzie for NMR analysis,

Ewan Sprong (University of Sydney) for CHDF analysis,

NRF and US for funding, and

The following people: Achille, Andrew, Ingrid, Gwen, JC, Marie-Claire, Vernon, Grehta and Austin for all their help and for being so friendly. I would also like to thank the Polymer Science Honours class of 2004 (too many to mention) for offering me encouragement.



Thank you all.

*May the good Lord bless you all, Amen*

## **Chapter 1: Introduction and objectives**

### **Abstract**

A short introduction to the contents of the thesis to allow the reader to understand the contents of each Chapter as well as the aims of the research presented in this thesis.



### **1.1: Introduction**

Polymers are a very important class of materials. They are found in almost all activities of modern life, from simple household utensils to advanced polymeric composites in high-tech engineering such as computers. The single most important characteristic of polymers is their diversity, which has its origins in the number of different types of molecular architecture and material forms. The term polymer describes a very large molecule that is made up of many basic units called monomers. The objectives of producing synthetic polymers were initially to imitate commercially important natural polymers, for example, the discovery of nylon as a substitute for silk and the production of synthetic rubber during world war two after a shortage of natural rubber.<sup>1</sup> It was from these beginnings that polymers with more desirable properties than natural polymers were designed. One of the most widely applied methods for commercial polymer synthesis is free radical polymerization. The method is applicable to all vinyl monomers and is compatible with most solvents. Much research in free radical polymerization is now focused on what is termed “living free radical polymerization” in order to obtain polymers with controlled molar mass, molar mass distributions and a wide variety of polymer architectures.

### **1.2: Aqueous dispersed free radical polymerization**

Synthesis of polymer nanoparticles that are dispersed in an aqueous phase has received considerable attention as it has numerous advantages over homogeneous bulk and solution polymerizations. Society today is moving away from the use of organic solvents because of security, health and environmental safety risks and the recent technological trend towards high solids contents at workable viscosities.<sup>2,3</sup> This has led to the development of a number of techniques for carrying out aqueous phase dispersed polymerizations. Some of the aqueous phase polymerization techniques include emulsion, miniemulsion, suspension and microemulsion polymerizations.<sup>4</sup> Polymeric dispersions are widely used in industry today in the production of paints, synthetic rubber, adhesives etc.<sup>5</sup> The application of polymeric dispersions also stretches to biomedical and pharmaceutical applications such as diagnostic tests and drug delivery systems.<sup>1,4-6</sup>

### **1.3: Living radical polymerization**

Conventional free radical polymerization (CFRP) has some major drawbacks, including the inability to produce polymers with controlled molar mass distribution and synthesis of block copolymers with tailored architecture. Various techniques of living free radical polymerization have been developed in order to overcome the major drawbacks associated with conventional free radical polymerizations.<sup>7</sup> These living/controlled techniques are based on either reversible termination of the propagating radicals to form dormant covalent species, as found with Nitroxide Mediated Polymerization (NMP) and Atom Transfer Radical Polymerization (ATRP), or Reversible Addition Fragmentation chain Transfer (RAFT).

Some of the advantages of living radical polymerization over conventional free radical polymerization include:

- ❖ Controlled molecular weight.
- ❖ Low polydispersity.
- ❖ The synthesis of block copolymers via chain extension.
- ❖ A variety of tailored architectures.
- ❖ The synthesis of polymers with specific end group functionalities.

Living/controlled free radical polymerizations have been applied to heterogeneous systems such as conventional emulsion<sup>8</sup> and miniemulsion<sup>4,6,9</sup> free radical polymerization. The use of CFRP in aqueous media may provide a novel and potentially inexpensive route to designing and obtaining polymers with controlled microstructure and narrow molecular weight distributions.<sup>10</sup> Moreover CFRP in aqueous dispersed polymerization may have synthetic and economic advantages over traditional homogeneous bulk and solution polymerization, such as the production of high solids content latexes at workable viscosities. However, applying living/controlled free radical polymerization in aqueous dispersions poses several challenges, originating from having two or even three phases in the reaction mixture.<sup>11</sup> Having more than one phase can lead to phase partitioning of the controlling agent, and difficulties in transport of the transfer agent between phases.

## ***Chapter 1: Introduction and objectives***

---

---

Moreover, the role of aqueous phase kinetics, and the phenomena of particle nucleation and colloidal stability are complicated. Nevertheless, living/controlled free radical systems have been successfully applied to aqueous dispersed radical polymerizations.<sup>4,9</sup>

### **1.4: Polymerizable surfactants in aqueous dispersed polymerizations**

Surfactants play a significant role in the synthesis and final products of emulsion polymerizations. The roles of the surfactant are to emulsify the monomer droplets and to keep the latex particles stable after polymerization (shelf life stability).<sup>7</sup> However, the presence of surfactants in the finished products has some disadvantages such as desorption from the latex causing destabilization. In some cases, surfactant removal is required as in styrene-butadiene rubber (SBR) and nitrile rubber (NBR).<sup>5</sup> This is done by washing the polymer with water which can be time consuming and costly. Where shelf life stability is of paramount importance, surfactant stabilized latexes will tend to flocculate with 'time' due to surfactant migration within the latex, which leads to destabilization of the latex particles. The use of polymerizable surfactants (surfmers) in aqueous dispersed polymerizations may eliminate such problems. In the final product, the surfmer will be covalently bonded to the polymer chains, thus no destabilization will occur due to surfmer migration.<sup>5</sup> However, this may lead to some changes in the overall properties of the desired product that can be either advantageous or disadvantageous.

### **1.5: Research leading to the project**

Living Free Radical Polymerization (LFRP) has been applied and reported for homogeneous free radical polymerization based on various living techniques including NMP,<sup>12-14</sup> ATRP,<sup>15</sup> RAFT.<sup>16,17</sup> Studies are now being focused on aqueous dispersed systems because they are widely used in industry today. Reversible Addition Fragmentation Chain Transfer (RAFT) polymerization has been viewed as the most robust and versatile method<sup>18</sup> for controlling molecular weight of polymers compared to ATRP and NMP. The RAFT process offers many advantages, which includes its tolerance to small amounts of impurities, compatibility with a variety of solvents, a wide range of working temperature and a variety of monomers.<sup>4</sup>

## ***Chapter 1: Introduction and objectives***

---

RAFT has been successfully applied in ab initio emulsion polymerizations and promising results have been obtained under starved feed conditions, allowing the synthesis of styrene-acrylate block polymers.<sup>8</sup> In batch emulsion polymerization systems, RAFT has yielded less satisfactory results compared to miniemulsion and seeded emulsion mainly because of diffusion and/or localization issues of the transfer agent, which can be overcome by avoiding transport of the transport agent through the aqueous phase.<sup>9</sup> Seeded emulsion and miniemulsion can easily eliminate the need for aqueous phase transport of the RAFT agent.<sup>4,6</sup> Results for seeded and miniemulsion were quite interesting in that reaction rates that were comparable to those of nonliving processes were obtained.<sup>6</sup> In these two polymerization systems (miniemulsion and seeded emulsion) with RAFT, the RAFT agent will be in the reaction loci from the beginning of polymerization; this allows all the growing chains an equal lifetime. In addition, the RAFT agent will be homogeneously distributed within the particles thereby yielding particles of similar average molecular weight. Moreover, there is a possibility of using water insoluble controlling agents, especially in miniemulsion polymerization.<sup>9</sup> Aqueous phase polymerization requires the use of surfactants to emulsify monomer droplets and lend stability to the particles. Work has been done on using polymerizable surfactants as substitutes for non-polymerizable surfactants in order to eliminate problems associated with surfactant migration in the final product e.g. latexes and films.<sup>7,10,19</sup> Polymerizable surfactants (surfmers) have been applied in emulsion,<sup>7,19</sup> as well as in miniemulsion polymerization.<sup>10</sup> The use of surfmers to stabilize aqueous dispersed systems during polymerization gives certain benefits in the resulting products. These benefits include high latex stability (even under high shear conditions) and reduction in processing cost in cases where free surfactant removal is of paramount importance. Studies performed in miniemulsion have shown that the rate of polymerization in surfmer-stabilized miniemulsions is lower compared to non-reactive/classical surfactant-stabilized miniemulsions.<sup>10</sup> High conversions were obtained in surfmer systems by adding a complementary classical surfactant. This shows that surfmers have advantages only on the final processing and shelf life of polymeric latexes and not during the polymerization stage. The challenge now is to apply RAFT in miniemulsion polymerization stabilized by surfmers in order to obtain polymeric latexes with controlled molecular weight as well as with properties obtained from the use of polymerizable surfactants.

### **1.6: Objectives**

This project explores a number of aspects of miniemulsion polymerization, including the control of molecular weight using the Reversible Addition Fragmentation chain Transfer (RAFT) process, the use of polymerizable surfactants (surfmers) and oligosurfmers in RAFT-mediated miniemulsion polymerizations, as well as a comparative study of the differences between classical surfactants and surfmers in RAFT-mediated miniemulsion polymerizations.

The objectives of the project are as follows:

- 1) To synthesize a surfmer that is capable of stabilizing particles in RAFT miniemulsion.
- 2) To compare surfmer-stabilized RAFT miniemulsion to classical surfactant stabilized RAFT miniemulsion
- 3) To synthesis oligosurfmers in RAFT-mediated solution polymerization and investigate the feasibility of forming RAFT terminated/functionalized oligosurfmers.
- 4) To use oligosurfmers as emulsifiers in miniemulsion polymerizations, this in turn allows chain extension of the oligosurfmers.
- 5) To characterize (molecular weight and composition) and investigate the properties of the copolymers (thermal and mechanical).



### **1.7: Layout of the thesis**

#### **❖ Chapter 1: Introduction and objectives**

A brief introduction to the major areas pertaining to this research which include; a description of aqueous dispersed polymerizations (emulsion and miniemulsion), controlled radical polymerizations and polymerizable surfactants in aqueous dispersed

## ***Chapter 1: Introduction and objectives***

---

---

phase polymerization. Chapter 1 also includes a short discussion on the research leading to this study, as well as the objectives of the research project.

### **❖ Chapter 2: Historical and theoretical background**

This is a review of the historical and theoretical aspects related to the research project. Included are important studies related to this research that have been done by other researchers to date. This enables the reader to understand all the important aspects and concepts relevant to this study/research.

### **❖ Chapter 3: Synthesis and characterization of polymerizable surfactants and the RAFT agent**

This Chapter covers the synthesis and characterization of two polymerizable surfactants; namely sodium 11-methacryloyloxyundecan-1-yl sulfate (anionic) and 11-methacryloyloxyundecan-1-yl trimethyl ammonium bromide (cationic), and the RAFT agent cyanovaleric acid dithiobenzoate (CVATB).

Solution polymerization of surfmers to form oligosurfmers and the characterization of oligosurfmers with special attention on the feasibility of using RAFT to control the molecular weight of the polysurfmers, are included.

### **❖ Chapter 4: Miniemulsion polymerization**

This Chapter is concerned with the polymerization of styrene and methyl methacrylate using classical surfactants, surfmers and oligosurfmers as emulsifiers in RAFT mediated miniemulsion polymerizations. Included in this Chapter is a comparative study of the rates of reactions as well as molecular weight distributions of the polymers. A comparison of the particle sizes between classical surfactants and polymerizable surfactants, as well as oligosurfmers in miniemulsion latexes, is included. The thermal behavior of the final polymers are compared and described.

### **❖ Chapter 5: Conclusions and recommendations for future work**

General conclusions to the study, covering achievements, and recommendations for future work are given.



### **1.8: References**

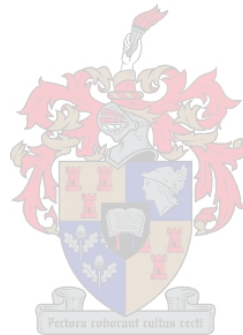
- (1) Guyot, A.; Tauer, K. In *Reactions and synthesis in surfactant systems*; J, T., Ed.; Marcel Dekker: New York, 2001; pp 547-575.
- (2) Asua, J. M. *Progress in Polymer Science* 2002, 27, 1283-1346.
- (3) Antonietti, M.; Landfester, K. *Progress in Polymer Science* 2002, 27, 689-757.
- (4) Brouwer, H.; Tsavalas, J. G.; Schork, J.; Monteiro, M. J. *Macromolecules* 2000, 33, 9239-9246.
- (5) Capek, I.; Chern, C.-S. *Advances in polymer science* 2001, 155, 101-125.
- (6) Butte, B.; Storti, G.; Morbidelli, M. *Macromolecules* 2001, 34, 5885-5896.
- (7) Unzue, M. J.; Schoonbrood, H. A. S.; Asua, J. M.; Gon, A. M.; Sherrington, D. C.; Stahler, K.; Goebel, K.; Tauer, K.; Sjoberg, M.; Holmberg, K. *Journal of Applied Polymer Science* 1997, 66, 1803–1820.
- (8) Monteiro, M. J.; Barbeyrac, J. *Macromolecules* 2001, 34, 4416-4423.
- (9) Lansalot, M.; Davis, T. P.; Heuts, J. P. A. *Macromolecules* 2002, 35, 7582-7591.
- (10) Guyot, A.; Graillat, C.; Favero, C. *C.R Chimie* 2003, 6, 1319-1327.
- (11) Tsavalas, J. G.; Schork, F. J.; Brouwer, H.; Monteiro, M. J. *Macromolecules* 2001, 34, 3938-3946.
- (12) Allinger, N. L.; Cava, M. P.; De Jongh, D. C.; Johnson, C. R.; Lebel, N. A.; Stevens, C. L. In *Organic Chemistry*, 1971; p 670.
- (13) Veregin, R. P. N.; Georges, M. K.; Kazmaier, P. M.; Hamer, G. K. *Macromolecules* 1993, 26, 5316-5320.
- (14) Kazmaier, P. M.; Moffat, K. A.; Georges, M. K.; Veregin, R. P. N.; Hamer, G. K. *Macromolecules* 1995, 28, 1841-1846.
- (15) Wang, J.-S.; Matyjaszewski, K. *Journal of the American Chemical Society* 1995, 117, 5614-5615.
- (16) Chiefari, J.; Chong, Y. K. B.; Ercole, F.; Krstina, J.; Jeffery, J.; Le, T. P. T.; Mayadunne, R. T. A.; Meijs, G. F.; Moad, C. L.; Moad, G.; Rizzardo, E.; Thang, S. H. *Macromolecules* 1998, 31, 5559-5562.
- (17) Chong, Y. K. B.; Krstina, J.; Le, T. P. T.; Moad, G.; Postma, A.; Rizzardo, E.; Thang, S. H. *Macromolecules* 2003, 36, 2256-2272.
- (18) Zhu, J.; Zhu, X.; Zhou, D.; Chen, J. *e-polymers* 2003, 43, 1618-7229.

## ***Chapter 1: Introduction and objectives***

---

---

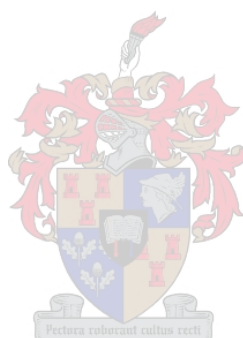
- (19) Bele, S.; Sjoberg, M.; Hamaide, T.; Zicmanis; Guyot, A. *Langmuir* 1997, 13, 176-181.



## **Chapter 2: Historical and theoretical background**

### **Abstract**

A concise introduction to free radical polymerization in emulsion and miniemulsion, with a special emphasis on Living Free Radical Polymerization (LFRP), primarily the RAFT process. The Chapter also gives an overview of the use surfmers in aqueous dispersed polymerization and their advantages over classical surfactants.



### 2.1: Free radical polymerization

#### 2.1.1: General

Free radical polymerization is one of the most common and useful techniques for synthesizing polymers and is limited only to monomers containing the vinyl group ranging from small molecules to macromonomers. Polymers made by free radical polymerization include polystyrene, poly(methyl methacrylate) and branched polyethylene. The major advantages of free radical polymerization over other polymerization techniques are that it is compatible with a wide range of vinyl monomers and insensitive to small traces of impurities such as oxygen, metal ions and water. The drawbacks of free radical polymerization are that the reaction is not enantioface selective (which implies that it only produces atactic polymers); it produces polymers with a wide molar mass distribution (high polydispersity)<sup>1,2</sup> and preparation of multiblock copolymers is not facile.

The reactivities of vinyl monomers in a free radical polymerization reaction depend on the ability of the substituents (R and X) to stabilize the propagating radical.

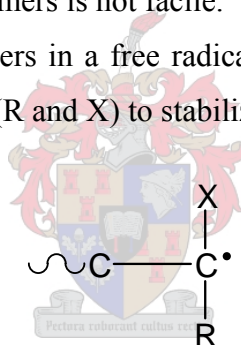


**Fig 2.1: Propagating polymeric radical with substituents R and X**

The less stable propagating radicals (where R is a poor radical stabilizer) are very reactive compared to the more stable radicals. As an example, in styrene where  $R = C_6H_5$  group and  $X = H$ , the radical formed is well stabilized by inductive effects compared to vinyl chloride when  $R = Cl$  and  $X = H$ . As a result the rate coefficient is larger in the vinyl chloride polymerization than in the styrene polymerization. Thus different monomers have different radical reactivities and thus have different propagating rate coefficients.<sup>3</sup> However, comparing the monomers themselves, the styrene monomer is more reactive than the vinyl chloride since the benzene ring activates the double bond by positive inductive effects whereas the chloride exerts negative induction on the double bond thus deactivating the double bond.

### 2.1.2: Free radical kinetics

Free radical polymerization is generally divided into three reaction steps: initiation, propagation and termination.

#### Step 1: Initiation

Initiation involves the homolytic dissociation of an initiator molecule forming two radicals capable of initiating polymerization. Most common initiators are the azo and peroxy compounds (Fig 2).

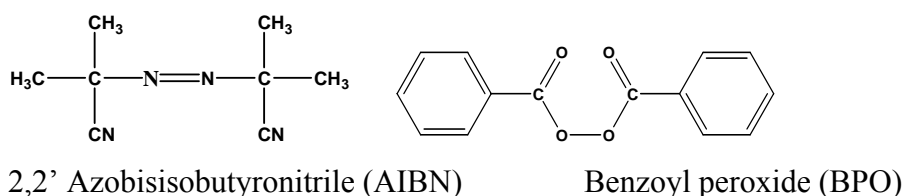


**Fig 2.2: Two commonly used azo- and peroxy- free radical initiators**

These compounds decompose when thermal energy is supplied to them and each initiator type has a unique half life which is temperature dependent. It follows that the nature and type of initiator to be used depends on the conditions required for a specific polymerization system. Solubility of the initiator in the polymerization medium is also a factor that should be considered when choosing an initiator. Potassium persulfate [ $(K^+)_2(SO_4^-)_2$ ] is an example of a water soluble initiator that also thermally decomposes to form two initiator radicals. Generally, there are four principal free radical initiating systems: thermo-initiated, chemically initiated (redox), photo-initiated and radiation-initiated polymerization.<sup>4</sup> A brief summary of some of the techniques used for the generation of free radicals is shown in Table 2.1.

## Chapter 2: Historical and theoretical background

**Table 2.1: Various methods of free radical generation**

Technique	Description	Example/s
Thermal	$\text{ROOR} \xrightarrow{\Delta} 2\text{RO}^\bullet$ $\text{RN=NR} \xrightarrow{\Delta} 2\text{R}^\bullet + \text{N}_2$	1) Peroxides (hydrogen peroxide) 2) Azo-compounds (AIBN)
Redox	$\text{Fe}^{2+} + \text{ROOH} \longrightarrow \text{RO}^\bullet + \text{HO}^- + \text{Fe}^{3+}$	1) Peroxides ( $\text{H}_2\text{O}_2$ ) 2) Hydroperoxides 3) Potassium persulfate
Ultra-violet	$\text{RCOCOR} \xrightarrow{\text{UV}} 2\text{RCO}^\bullet$	Benzil (R = Benzene)
Electrochemical	$\text{RCOO}^- \xrightarrow{\text{anode}} \text{RCOO}^\bullet - e^-$	Alkali-metal carbonates

Some of the radical generation techniques which are not commonly used include, particulate ( $\alpha$  and  $\beta$  particles), high energy radiation ( $\gamma$ -radiation), sonic and mechanical. A disadvantage of electromagnetic and high energy radiation in radical generation is that more than one species (radicals, ionic species) can be formed. This complicates the mechanism of initiation since the ionic species are also capable of initiating polymerization.

Initiator dissociation reaction



Rate of consumption of the initiator is given by the Equation:

$$\frac{d[I]}{dt} = -k_d [I] \quad (2.2)$$

The initiator decomposition can be described by the following Equation (2.3), which has been derived from Equation 2.2. A plot of initiator concentration against time is an exponential decay curve with the concentration intercept equal to  $[I]_0$ , i.e. at  $t = 0$ .

$$[I] = [I]_0 e^{-k_d t} \quad (2.3)$$

where  $[I]_0$  is the initial initiator concentration,  $[I]$  is the initiator concentration at time  $t$ . and  $k_d$  is the decomposition rate coefficient.

## Chapter 2: Historical and theoretical background

---

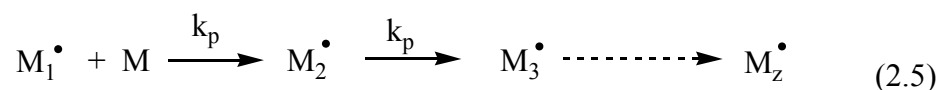
The rate of initiation ( $v_i$ ) is given by:

$$v_i = 2k_d f [I] \quad (2.4)$$

where the factor 2 accounts for the fact that two radicals are generated from one initiator molecule (but it is not always the case),  $f$  is the fraction of radicals that can effectively initiate polymerization. The factor  $f$  accounts for the geminate reactions which are basically a combination of primary radicals with other molecules such as oxygen to form stable molecules/compounds. The factor  $f$  also accounts for the “cage effect” which is basically the recombination of primary and split initiator radicals (as they are formed by dissociation and subsequent  $\text{CO}_2$  loss) forming the non reactive molecules. The cage effect is due to the fact that the formed radicals can remain in close proximity to each other and result in a percentage of recombination.

### Step 2: Propagation

Propagation reactions follow after the initiation step has taken place. The monomer is sequentially added to the growing polymer chain via the process of electron transfer. The entire propagation of a single radical occurs within a fraction of a second and it stops when termination of the growing chain occurs. Since the radicals are continuously generated by the dissociation of the initiator, which follows a decay curve described by Equation 2.3, polymerization continues until it is limited by other factors such as monomer and initiator depletion or in extreme cases the viscosity of the reaction medium (mainly in bulk conditions).



Rate of propagation  $v_p$  is given by:

$$v_p = k_p [M] [M_1^\bullet] \quad (2.6)$$

The propagation rate coefficient is temperature and chain length<sup>5</sup> dependent. The temperature dependency of the propagating rate coefficient is described by the Arrhenius Equation for any chemical reaction, as given below:

$$\ln[k_2/k_1] = \frac{\mu}{R} \left( \frac{1}{T_1} - \frac{1}{T_2} \right) \quad (2.7)$$

where  $T_1$  and  $T_2$  are the absolute temperatures corresponding to reaction velocities  $k_1$  and  $k_2$ ,  $R$  is the gas constant, and  $\mu$  is the critical thermal increment: a constant characterising the particular reaction. The Arrhenius Equation 2.7 relates the reaction

## Chapter 2: Historical and theoretical background

---

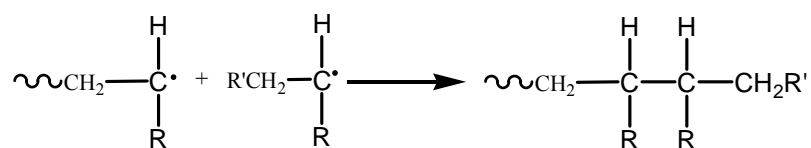
rate values of  $k_1$  and  $k_2$  to their corresponding reaction temperatures  $T_1$  and  $T_2$  respectively. An increase in reaction temperature i.e. ( $T_2 > T_1$ ) results in an increase in the reaction rate  $k_2$ . Thus the rate of polymerization increases with increasing temperature. The propagation rate is also affected by the bulkiness of the propagating radical in that the radical will be sterically hindered (longer chains), such that it cannot easily find the monomer. This gives rise to a reduction in the propagation rate coefficient. Argued differently, the monomer which moves more easily is hampered by the increased viscosity surrounding the active radical which is shielded by the coils of the polymer.

### Step 3: Termination

In theory, the propagation should continue until the supply of the monomer is exhausted. However this is not the case as side reactions do occur which lead to premature termination. The chain length also affects the termination rate coefficient<sup>7,8</sup> in that, as the chain grows, there is a decrease in the rate of radical chain end diffusion leading to a reduction in the probability of finding another radical for termination. The longer the chains become the lower is the rate of diffusion and the rate of termination is reduced. The major processes in which chain termination occurs are namely, radical coupling/combination, disproportionation and transfer reactions.

#### Coupling/combination reaction

Coupling occurs when two radicals find each other to form a single chain. This can occur with any growing chain and is the reason for the observation of high molecular weights when analyzed by chromatographic techniques. The molecular masses would be in the range of double the mass of the individual growing chains for controlled free radical polymerization. This is because premature termination is suppressed, implying that the majority of the radicals are long, hence coupling of these radicals leads to chains of twice the Mw of the individual chains.



**Scheme 2.1: A coupling termination reaction**



## Chapter 2: Historical and theoretical background

---

Polymer chains from monomers with a bulky R group and a radical on a tertiary carbon, such as methacrylates, do not normally undergo termination by coupling due to the steric effects.

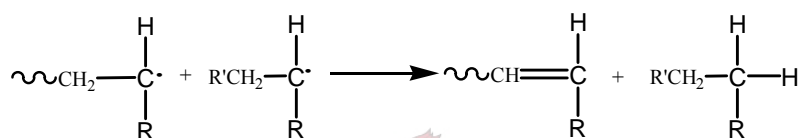
Rate of termination by coupling is given by:

$$V_t = k_{tc}[M^\bullet]^2 \quad (2.8)$$

where  $V_t$  is rate of termination and  $k_{tc}$  is termination by coupling rate constant

### Disproportionation reaction

Disproportionation stops the propagation reaction when a radical abstracts a hydrogen atom from a carbon atom  $\beta$  to the active center. This leads to a formation of a carbon-carbon double bond.



### Scheme 2.2: A disproportionation reaction

Rate of termination ( $\nu_t$ ) is then given by:

$$\nu_t = k_{td}[M^\bullet]^2 \quad (2.9)$$

where  $[M^\bullet]$  is the free radical concentration, the factor 2 is included since two radicals are lost in one reaction and  $k_{td}$  is the termination by disproportionation rate constant.

To take account of both coupling and disproportionation:

$$V_t = 2k_t[M^\bullet]^2 \quad (2.10)$$

where  $2k_t = k_{td} + k_{tc}$

### Steady state approximation

When steady state is reached, the radical concentration becomes essentially constant and the rate of termination is equal to the rate of initiation ( $\nu_t = \nu_i$ ). Therefore the rate of propagation is given by the Equation below, derived from Equations 2.4, 2.6 and 2.10.

$$\nu_p = k_p \left( \frac{fk_d[I]}{k_t} \right)^{0.5} [M] \quad (2.11)$$

## Chapter 2: Historical and theoretical background

---

and the subsequent monomer consumption is described by the following Equation, which has been derived from Equation 2.11

$$[M] = [M]_0 e^{-k_p \left( \frac{fk_d}{k_t} \right)^{0.5} [I]^{0.5} t} \quad (2.12)$$

The assumption is that the initiator concentration  $\frac{dI}{dt}$  is small throughout the propagation step.

### Transfer reactions

Practically, there are a number of transfer reactions (transfer to monomer, solvent, initiator or a transfer agent, either an impurity or a deliberately added transfer agent) that can also complicate the system. The chain transfer constants depend on different parameters such as temperature, solvent, or type of monomer. The general transfer constant C is given by:

$$C = \frac{k_{tr}}{k_p} \quad (2.13)$$

These transfer reactions do not necessarily lead to a reduction in radical concentration but have a tendency of limiting the molecular weight of the polymer chains. In transfer reactions, the active center of a propagating radical is transferred to another molecule (monomer, solvent, transfer agent, etc). Transfer reactions result in the preservation of the propagating radical concentration and termination of the former propagating species. The number-average degree of polymerization ( $DP_n$ ) is given by the following Equation 2.14:

$$\frac{1}{DP_n} = \frac{(1 + \lambda) \langle k_t \rangle [R^\bullet]}{k_p [M]} + C_M + C_S \frac{[S]}{[M]} \quad (2.14)$$

In this expression,  $\lambda$  is the fraction of termination by disproportionation,  $\langle k_t \rangle$  the average termination rate coefficient,  $[R^\bullet]$  the overall radical concentration,  $[M]$  monomer concentration,  $C_M$  the chain transfer constant for chain transfer to monomer, and  $[S]$  the concentration of chain transfer agent.<sup>9</sup>

## 2.2: Living Free Radical Polymerization (LFRP)

In the last few years, 'living'/controlled free radical polymerization has been shown to be a convenient method to obtain polymers with low polydispersity, tailored molecular weight and well defined architectures.<sup>10,11,12</sup> Controlled/living radical

## Chapter 2: Historical and theoretical background

---

polymerization processes are of great interest in macromolecular chemistry, both in academy as well as in industry. Since the first reports on CFRP appeared, the research area has become one of the most rapidly growing areas of polymer chemistry. The main idea is to reversibly trap most of the growing chains by adding “trapping species”, so as to reduce the radical concentration thereby preventing bimolecular terminations as shown below:



### Scheme 2.3: General formation of a dormant species in LFRP

In LFRP systems, equilibrium between propagating active species and dormant species is formed. The exchange between the active and dormant species must be fast, such that the rate of deactivation is faster than the rate of propagation. This allows polymerization to occur via the mechanism of Mw control, leading to a high degree of control and low polydispersity because all the chains are given equal chances to grow. Most of the chains exist in the dormant state to ensure that the active species does not undergo termination by coupling or disproportionation reactions. However it must be noted that these techniques are not “truly living”, some chains will terminate. Although termination is diffusion controlled, the presence of a transfer agent results in the reduction of the number of radicals and termination becomes less prevalent. The terminated/dead chains are not capable of undergoing chain extension in the case of block copolymerization via chain extension. In principle, controlled/living radical polymerizations provide molecular weights that are predetermined by reagent concentrations and, most importantly, give polymer products that can be reactivated for chain extension or block synthesis.<sup>13</sup> Several CFRP techniques have been developed; they are mainly based on degenerative transfer, reversible addition transfer reactions and reversible end capping. Recently, research was focused on the application of CFRP in aqueous media because of society’s bias towards non-organic volatiles.

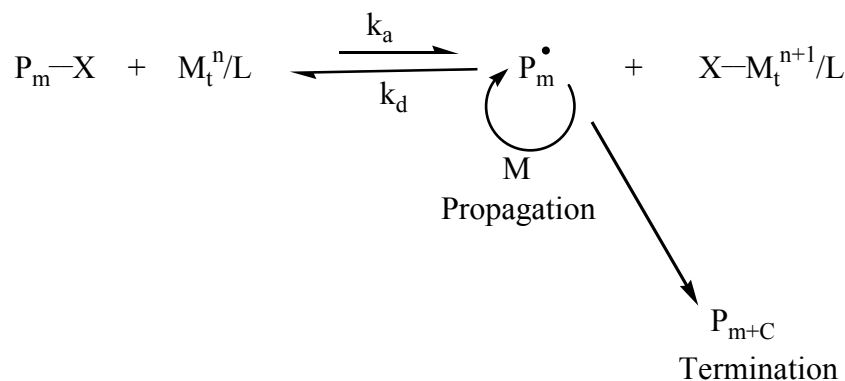
#### 2.2.1: Atom Transfer Radical Polymerization (ATRP)

Atom transfer radical polymerization (ATRP) is a “living” polymerization technique, discovered by Matyjaszewski<sup>14</sup> and Sawamoto<sup>15</sup> in 1995. This technique is based on a reversible exchange between a low concentration of growing radicals and a dormant

## Chapter 2: Historical and theoretical background

---

species. Reactivation of the dormant species allows the polymer chains to grow and deactivate again. The radical formation occurs by a transition metal catalyst (in the lower oxidation state) that activates the initiator (either alkyl halide or substituted arylsulfonyl halide<sup>16,27</sup>) or dormant species by abstracting the halide at the chain end.



### Scheme 2.4: Schematic representation of the ATRP process

where X represents the halide atom, M is the metal atom, L represents the ligands and  $\text{P}_m^\bullet$  is the propagating chain.

The process results in a polymer chain that grows slowly and steadily and has a well-defined end group, because, under appropriate conditions, the contribution of termination is small. ATRP is capable of polymerizing a wide variety of monomers and is tolerant of trace impurities, but the metal is sensitive to other redox reactions. Aqueous ATRP is possible, although monomer choice is limited to methacrylates and certain styrenics. A major disadvantage of ATRP is the need to remove the metal ions in the final product.

### 2.2.2: Nitroxide Mediated Polymerization (NMP)

The use of stable radicals in polymerizations was pioneered by Rizzardo *et al.* during the early 1980s, and how the stable radicals interact with olefins was investigated.<sup>17</sup> Georges *et al.* prepared narrow molecular weight resins using nitroxide stable free radicals.<sup>18</sup> The process is suitable for acrylates, styrenes, and dienes. Nitroxide-mediated CRFP has been successfully applied to control the polymerization of styrene under heterogeneous conditions such as dispersion<sup>19</sup>, seeded emulsion<sup>20</sup>, batch emulsion<sup>21</sup>, and miniemulsion<sup>22</sup> polymerization. Below are examples of nitroxide free radicals used in NMP.

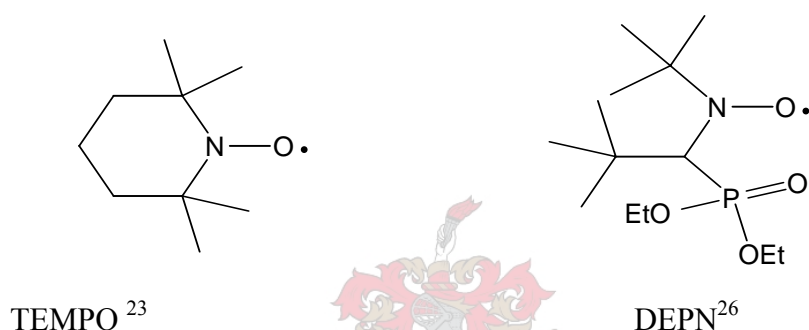
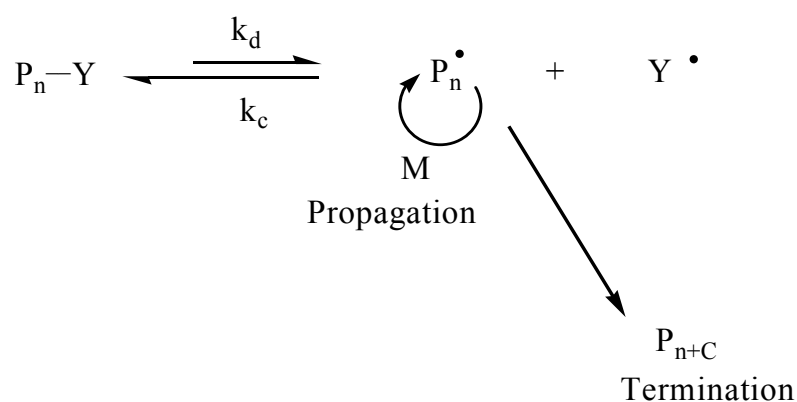


Fig 2.3: The structures of 2,2,6,6-tetramethyl-1-piperidinyloxy free radical (TEMPO) and N-tert-butyl-N-(1-diethylphosphono-2,2-dimethylpropyl) nitroxide (DEPN)

The nitroxide radical is generated by homolytic cleavage of the alkoxide amine by thermal means. The nature of the mediating radical species is of great importance as initiation is expected to occur only via the desired initiating species<sup>23</sup> and not the mediating radical.



$Y^\bullet$  is the nitroxide radical and  $P_n$  is the propagating radical

Scheme 2.5: Schematic representation of the NMP process

## Chapter 2: Historical and theoretical background

---

In this technique, the reversible termination of the growing polymeric radical ( $P_n$ ) is the most important step. The concentration of the propagating radicals is reduced by the reversible chain end capping; thus, termination of growing chains is suppressed. Although NMP can be successfully used for making block copolymers based on styrene and derivatives, it appears to have less utility for other systems.<sup>24,25</sup> A major disadvantage of NMP is that the required optimum temperatures are usually high. This is due to the fact that the C-O bond formed between the nitroxide compound and the propagating radical is relatively stable and requires a substantial amount of energy to break it.

### 2.2.3: Reversible Addition Fragmentation chain Transfer (RAFT)

Rizzardo *et al.*<sup>29</sup> (1998) reported a novel “living” free radical polymerization technique that is based on Reversible-Addition Fragmentation chain Transfer and designated it the RAFT process. The polymerization conditions are the same as those employed in conventional free radical polymerizations (monomers, initiation, solvents and temperature). The RAFT process involves free radical polymerization in the presence of a transfer agent mainly dithioesters<sup>31-36</sup>, xanthates<sup>30,37-39</sup>, and trithiocarbonates<sup>30,40-44</sup> as the RAFT agents.

The basic structure of the transfer agents used in the RAFT process is shown in Fig 2.4. Z refers to the stabilizing group, and R refers to the leaving group.

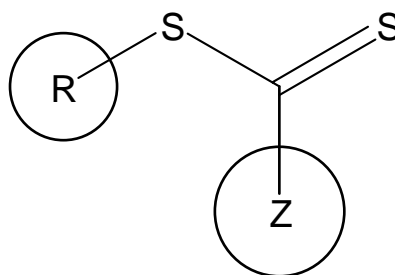
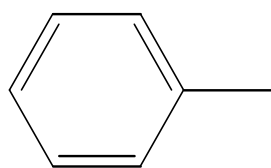


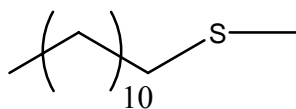
Fig 2.4: Basic structure of the RAFT agent<sup>30,37,38</sup>

## Chapter 2: Historical and theoretical background

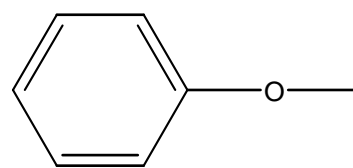
### (a) Examples of Z-groups



Z= Benzene  
(Dithioesters)

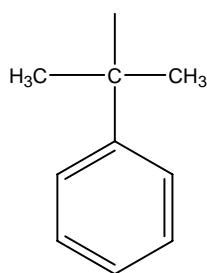


Z bonds via sulfur atom  
(trithiocarbonates)

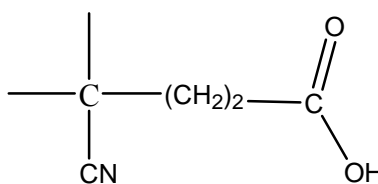


Z bonds via oxygen atom  
(Xanthates)

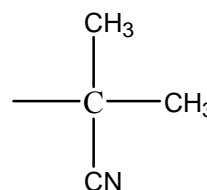
### (b) Examples of R-groups



cumyl



cyanovaleric acid



cyanoisopropyl

Fig 2.5: (a) Examples of Z-groups and (b) R-groups of RAFT agents

### Important aspects of Z and R

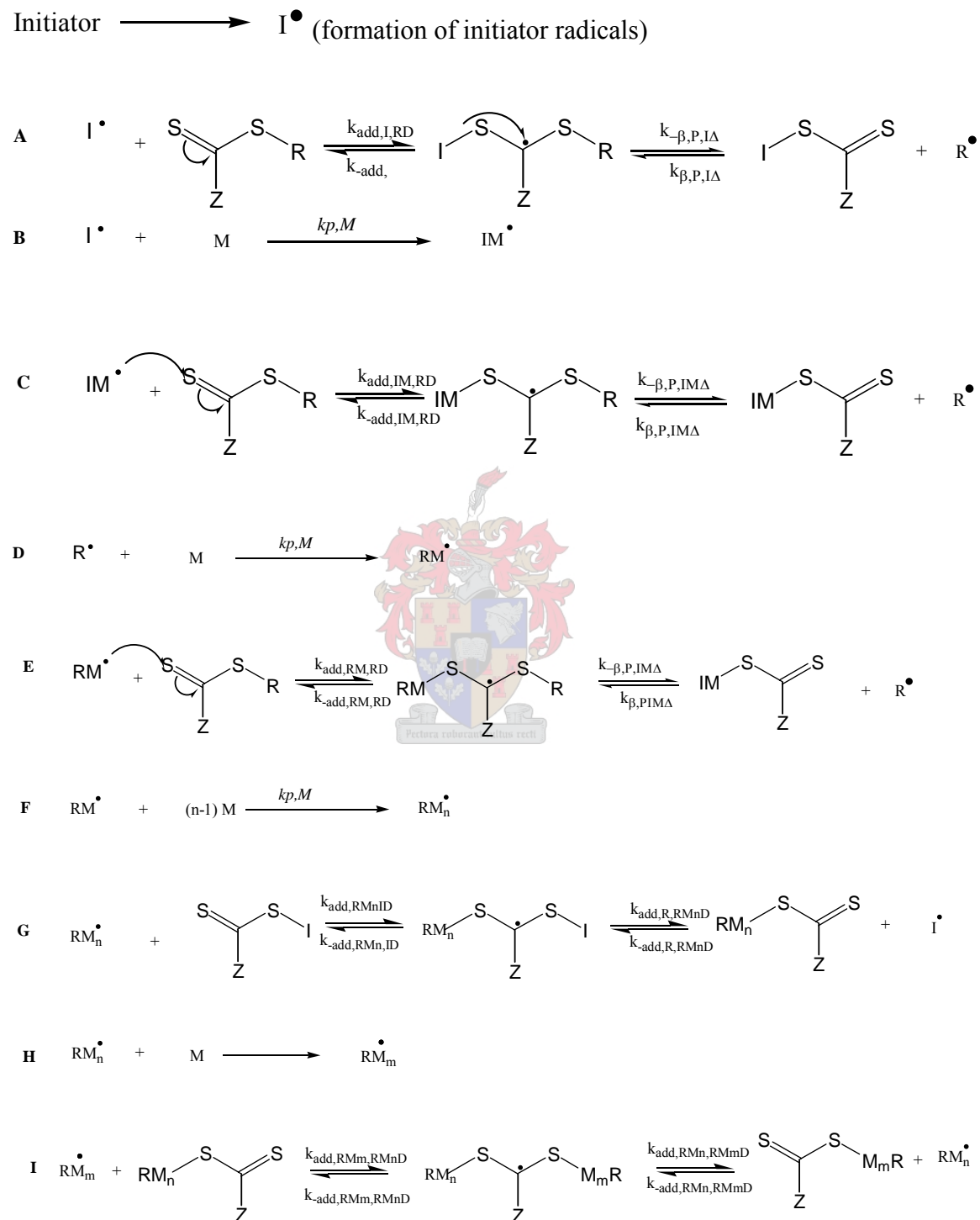
The Z-group should be able to activate the dithioester double bond for fast addition of the propagating polymeric radicals.<sup>45,46</sup> Some studies show that the rate of addition to the RAFT agent is different for different monomers<sup>48</sup> and that different Z groups have different effects on the addition of the propagating radicals.<sup>47</sup> For example, when a phenyl group is used as the activation group in styrene polymerization, a high rate of addition of polystyryl propagating radicals to the RAFT agent is obtained but the same group will be less effective when vinyl acetate is polymerized. The chain transfer coefficients decrease in the series where Z is Ph >SCH<sub>2</sub>Ph ~ SMe ~ Me ~ N-pyrrolo >> OC<sub>6</sub>F<sub>5</sub> > N-lactam > OC<sub>6</sub>H<sub>5</sub> > O (alkyl) > N (alkyl).<sup>47</sup>

The nature of the R group on the RAFT agent affects the chain transfer constant.<sup>45</sup> The choice of the R group depends on the monomer being polymerized. R should be a good leaving group, capable of reinitiating polymerization.<sup>46,49</sup> If R is not efficient in reinitiating, retardation and inhibition may occur.<sup>50</sup> This may lead to slow conversion of the RAFT agent and broad molar mass distribution. The leaving group ability decreases in the series R=tertiary >> secondary > primary.

## Chapter 2: Historical and theoretical background

### Mechanism

Evidence for the RAFT mechanism has been shown using techniques such as NMR, UV/visible<sup>46</sup> and ESR.<sup>51</sup> The mechanism is given in Scheme 2.6:



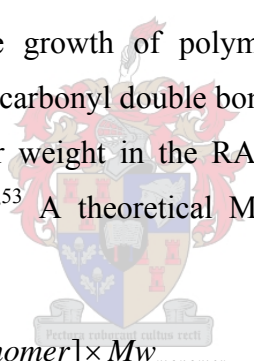
Scheme 2.6: Some of the elementary steps in the RAFT mechanism as reported by McLeary *et al*<sup>66</sup>



## Chapter 2: Historical and theoretical background

---

The first step in the RAFT polymerization is the decomposition of the initiator to form free radicals. The radicals can then either react with the S = C moiety of the RAFT agent or with the monomer to form propagating single monomer radicals (IM). The reaction of the radicals with the S = C is the rate determining step in the RAFT process because it is a fast reaction compared to propagation reactions. An intermediate radical is formed upon every addition of a radical to the RAFT agent and, at this stage, fragmentation of one of the arms follows, to form a temporarily deactivated polymeric RAFT agent. The cleaved arm will propagate, and then add again to the RAFT agent, forming an intermediate radical which will then fragment, releasing any one of the arms and the process continues in this manner. The subsequent addition of the growing polymeric radicals to the dithiocarbonyl double bond of the dormant polymeric RAFT agent forming the intermediate radical has been directly observed by electron spin resonance spectroscopy.<sup>51</sup> The existence of the intermediate radical shows that there is indeed addition to the S = C double bond of the RAFT agent. For stepwise growth of polymer chains, the addition of the propagating radicals to the dithiocarbonyl double bond should be fast compared to the rate of propagation.<sup>52</sup> Molecular weight in the RAFT process is controlled by the stoichiometry of the reaction.<sup>49,53</sup> A theoretical Mw predicting Equation is given below:


$$Mw_{Pred} = \frac{X \times [monomer] \times Mw_{monomer}}{[RAFT] + 2f[I]_0(1 - e^{-kdt})} + Mw_{RAFT} \quad (2.15)$$

where  $Mw_{pred}$  is the predicted molecular weight, X is the % conversion, [monomer] is the number of moles of monomer consumed, [RAFT] is the number of moles of the RAFT agent used,  $Mw_{monomer}$  and  $Mw_{RAFT}$  are the molecular weights of the monomer and RAFT agent respectively.

### Retardation in the RAFT process

The rate retardation phenomenon has been explained differently by different research groups. Rate retardation has been observed in certain RAFT systems while in other systems there are no signs of retardation. For example, the cumyl dithiobenzoate mediated RAFT polymerization showed retardation while the cumyl phenyl-dithiobenzoate showed no retardation.<sup>60</sup> Retardation in the RAFT process has been explained to be due to slow fragmentation of the intermediate radical (2) [see

## ***Chapter 2: Historical and theoretical background***

---

mechanism of RAFT, Scheme 2.6]. The postulation is that the intermediate radical is stable enough to cause no polymerization<sup>61,62</sup> especially at temperatures below 60°C. Thus, it was observed that if the Z-group is not a good radical stabilizer no retardation occurs during polymerization because there will be fast fragmentation of the intermediate radical leading to normal propagation. When the intermediate radical is stable, the rate of propagation is slow since the propagating radicals spend most of the time in the dormant state hence retardation is observed in such systems especially at temperatures below 60°C. Moreover, other research groups explained the retardation phenomenon to be due to the termination of the intermediate radical.<sup>63-65</sup> Monteiro *et al.*<sup>63</sup> found that, UV irradiation of polystyryl dithiobenzoate in the absence of a monomer yielded polymers with molecular masses thrice the expected values, suggesting termination of the intermediate radical by coupling. The formation of such values of molecular mass or the observation of molecular masses equivalent to a three-arm star polymer from GPC curves was also confirmed by Kwak.<sup>64</sup> Calitz *et al.*<sup>65</sup> observed the termination of the intermediate radical in cumyl dithiobenzoate-mediated free radical polymerization of styrene. A <sup>13</sup>C labeled dithioester at the carbon where the reaction of the intermediate radical is expected to occur was followed in situ. The products of the intermediate termination were observed and the results were consistent with the data observed from ESSR and <sup>1</sup>H NMR. McLeary *et al.*<sup>66</sup> conducted <sup>1</sup>H NMR studies on RAFT mediated polymerizations which resulted in the introduction of the concept of initialization. Results of NMR studies indicated that the RAFT system shows an initialization period which is different from the known inhibition period. The initialization period has been attributed to be related to the reactivities of different radicals and radical stabilities which affect relative addition and fragmentation rate coefficients of monomer adducts and the R group of the RAFT agent.<sup>66</sup>

### **RAFT in aqueous dispersed polymerization**

Recently, increased attention has been paid to process development of controlled radical polymerizations in aqueous dispersed emulsion or miniemulsion systems. Such processes will be more suitable for commercial large-scale production on account of better mixing and heat transfer than in the bulk or solution systems. Although little progress has been made with emulsion polymerization<sup>30,54-56</sup> considerable success has been achieved using miniemulsion polymerization with living radical systems.<sup>57,82,76,86-87</sup> In miniemulsion, mass transport, which is a

## ***Chapter 2: Historical and theoretical background***

---

requirement in conventional emulsion, is eliminated by the fact that the droplets themselves are nucleated.

### **2.3: Aqueous dispersed polymerization**

#### **2.3.1: Conventional emulsion**

Emulsion polymerization is a widely used industrial process; it is used to make products such as coatings, paints, adhesives and resins.<sup>72</sup> The simplest recipe for an emulsion polymerization constitutes water, surfactant, sparingly water soluble monomer (e.g. styrene) and a water soluble initiator such as potassium persulfate. A mixture of these ingredients is stirred to form an emulsion. Polymerization is initiated by thermally decomposing the initiator to form initiator radicals which will then initiate polymerization. The final product of polymerization is a latex comprising polymer particles dispersed in aqueous phase. Typical particle sizes obtained by conventional emulsion polymerization are in the range of 50 to 300 nm.<sup>58</sup>

#### **Mechanism of conventional emulsion polymerization**

The surfactant is normally above its critical micelle concentration (CMC). A high concentration of monomer swollen micelles is present in the aqueous phase. Some large monomer droplets are also present in the aqueous phase but their total surface area is a lot smaller than that of the micelles, hence polymerization is considered to occur mainly in monomer swollen micelles (heterogeneous nucleation).<sup>59,71,72</sup> However, polymerization can also occur in the aqueous phase (homogeneous nucleation<sup>59</sup>) as shall be explained later. Heterogeneous nucleation is the major process by which particle nucleation occurs. In this process, the surface active radicals will enter the monomer swollen micelles and initiate polymerization, whilst water soluble radicals remain in the aqueous phase.<sup>59</sup> Particle nucleation continues until most micelles are nucleated. The monomer from droplets diffuses into the growing particle, thus the monomer droplet acts as a monomer reservoir.<sup>73-74</sup>

#### **2.3.2: Miniemulsion**

##### **2.3.2.1: General**

Miniemulsions are dispersions of critically stabilized oil droplets with a size of between 50 and 500 nm<sup>73,75</sup> prepared by shearing a system containing oil (monomer), water, surfactant, initiator and a hydrophobe. Miniemulsion polymerization shares

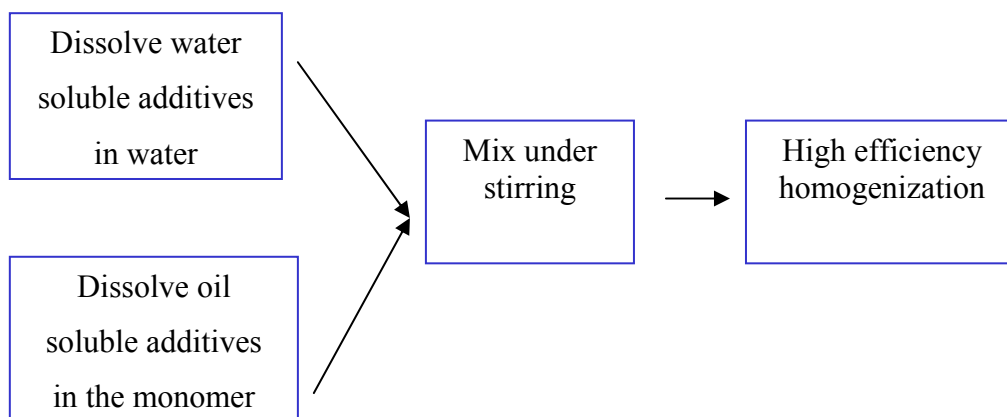
## ***Chapter 2: Historical and theoretical background***

---

many similarities with conventional emulsion polymerization, including the idea of compartmentalization.<sup>76</sup> Compartmentalization means that the polymerization occurs in small “individual reactors”, taken to be monomer swollen micelles (emulsion) and monomer droplets (miniemulsion). The final miniemulsion latex can have the same particle size as that of conventional emulsion.<sup>76</sup> The major difference between conventional emulsion and miniemulsion is the mechanism for particle nucleation. In miniemulsions, particle nucleation occurs in the stabilized monomer droplet<sup>79,80</sup> whereas in conventional emulsion polymerizations micellar nucleation occurs above the CMC. Thus, the reaction kinetics are simpler for miniemulsion compared to conventional emulsion polymerization because the monomer diffusion to the reaction sites is of no kinetic importance in miniemulsion since there is already the maximum monomer concentration at all reaction sites.<sup>76,81</sup> Ideally, polymerizations in miniemulsions result in latex particles which have about the same size as the initial droplets.<sup>75-77</sup> Unlike emulsion polymerization, miniemulsion can be used to produce composite particles since additives that are not capable of aqueous phase transport, such as pigments and water insoluble materials, can be added to monomer prior to dispersion.<sup>76</sup>

### **2.3.2.2: Preparation of miniemulsions by ultrasound homogenization**

Preparation of miniemulsions starts with mechanically mixing the oil phase constituting monomer, hydrophobe, initiator (if oil soluble) and water, which contains the other additives such as surfactant and initiator (if water soluble initiator is used). The additives are dissolved in either of the phases depending on their solubility in respect to the two phases. After this mechanical mixing, the contents are then subjected to a high energy homogenizer (e.g. ultrasound homogenization).<sup>71,73,78</sup> During this process, a series of fission-fusion occurs until the miniemulsion reaches a steady state.



**Scheme 2.7: Miniemulsion preparation**<sup>71</sup>

The polydispersity of the droplet size decreases with time of sonication. The droplet size is determined by the amount of monomer, water, surfactant and the amount of hydrophobe.<sup>71</sup> It was found that the initial droplet size depends on the mechanical agitation.<sup>78</sup>

### 2.3.2.3: Stability of miniemulsions

Stability of the miniemulsion is accomplished by the use of a surfactant and a hydrophobe.<sup>75</sup> As in emulsion polymerization, surfactants emulsify the monomer droplets. In emulsion polymerization, stabilization is via the repulsive forces between micelles. However, in miniemulsion, the monomer droplet is critically stabilized against coalescence and it is necessary to add an ultrahydrophobe. The hydrophobe is a long chain alkane e.g. hexadecane, which enhances droplet stability. The hydrophobe is water insoluble and it is housed inside the monomer droplets. The hydrophobe prevents Oswald ripening, which is a process by which large droplets grow at the expense of smaller droplets via diffusion, and sometimes it is referred to as diffusion degradation.<sup>71</sup>

### 2.3.2.4: Effect of a hydrophobe

In miniemulsion, the hydrophobe is added to monomer to prevent diffusion degradation. The hydrophobe increases the osmotic pressure inside the droplets and a chemical potential equilibrium is set between the monomer droplets, thereby preventing diffusion degradation (i.e. Oswald ripening).<sup>82</sup> The effect of a hydrophobe is qualitatively observed by applying thermodynamics for the stabilization of

## Chapter 2: Historical and theoretical background

---

monomer miniemulsions. The partial molar Gibbs free energy of monomer in a droplet containing a water soluble initiator is given by the following Equation<sup>71</sup>:

$$\frac{\overline{\Delta G}_m}{RT} = \ln(\phi_m) + (1 - m_{mh})\phi_h + X_{mh}(\phi_h)^2 + \frac{2\overline{V}_m\sigma}{rRT} \quad (2.16)$$

where  $\phi_m$  and  $\phi_h$  are the volume fractions of the monomer and hydrophobe in the monomer droplets respectively,  $m_{mh}$  is the ratio of the molar volume of monomer ( $\overline{V}_m$ ) to that of hydrophobe ( $\overline{V}_h$ ),  $X_{mh}$  is the interaction parameter of monomer and hydrophobe,  $\sigma$  is the droplet-water interfacial tension and  $r$  is the volume of the droplet.

When  $\Delta G = 0$ , the swelling capacity of the droplets in the presence of a hydrophobe can be calculated, hence the effect of droplet size and the type of hydrophobe on the maximum swelling can then be evaluated.<sup>71</sup> It has been suggested theoretically that low molecular weight and water insoluble hydrophobes lead to super-swelling.<sup>71</sup> The problem with the use of such low molecular weight hydrophobes is in the finished products such as films where they can easily leach out of the film. Therefore, it is advantageous to use high molecular weight hydrophobes. Work has been done to try to use a polymerizable small molecule hydrophobe in miniemulsion in order to prevent the problem of leaching out of the hydrophobes.<sup>68</sup>

### 2.3.2.5: Mechanisms of particle nucleation

#### Droplet nucleation

A radical in the aqueous phase (if water soluble initiator is used) polymerizes in the aqueous phase to form an oligoradical. The oligoradical will then enter the droplet and become the locus for polymerization. This is the prominent mechanism of droplet nucleation in miniemulsion<sup>59</sup>, since in miniemulsion polymerization occurs in each of the stabilized monomer droplets and micelle formation is prevented. Most, if not all, monomer droplets are nucleated and monomer diffusion to the reaction loci (which is the case with emulsion polymerization) is eliminated.

## Chapter 2: Historical and theoretical background

### Homogeneous nucleation

It is possible for nucleation in miniemulsion to occur via homogeneous nucleation. In homogeneous nucleation the oligoradical growing in the aqueous phase will reach its limiting solubility and precipitate out of solution.<sup>71</sup> The precipitated oligoradicals are stabilized by adsorbed surfactant and they will coagulate, forming a center for particle nucleation and growth via adsorption of monomer. The latex seeds will start from oligoradicals in the aqueous phase and monomer diffusion occurs from droplets to the reaction site. However droplet nucleation is the major particle nucleation mechanism in miniemulsion; and homogeneous nucleation is usually neglected. In miniemulsion, nucleation in the aqueous phase results in the formation of secondary particles. Secondary particles in the RAFT polymerization system are normally uncontrolled and are of higher molecular weight because transport of the RAFT agent in the aqueous phase is not efficient.

### Micellar nucleation

The oligoradical formed in the aqueous phase enters the micelle and the micelle becomes the reaction locus. This mechanism is prominent in emulsion polymerization where the number of micelles is by far much larger than the number of monomer droplets. In which case, it is more probable that the radical will enter into a micelle than a monomer droplet. However if micelles are present in a miniemulsion, micellar nucleation may occur. A summary of the types of particle nucleation mechanisms (miniemulsion and emulsion) is given schematically below

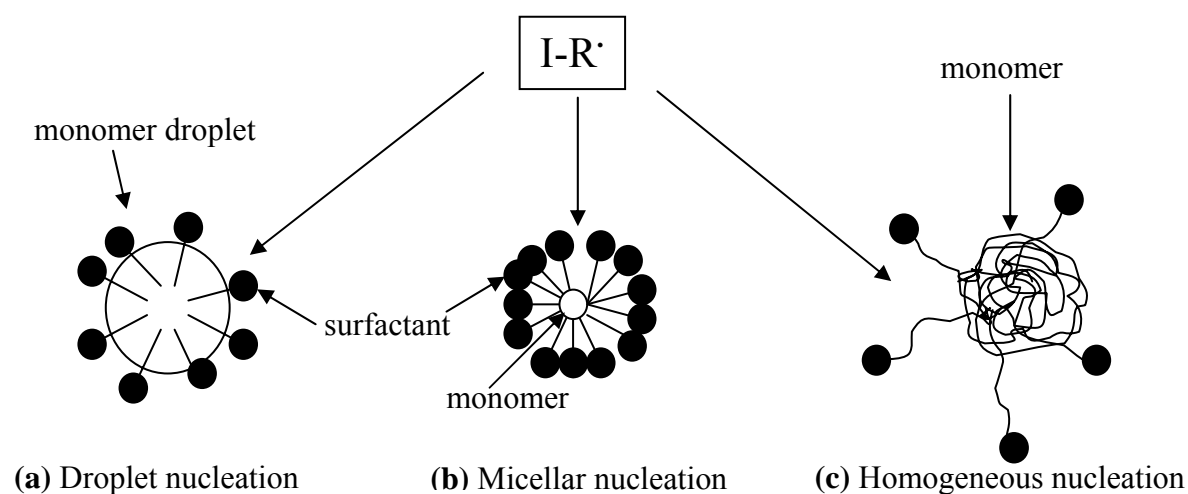


Fig 2.6: Schematic representation of particle nucleation mechanisms possible for miniemulsion and emulsion<sup>59</sup> polymerizations

## Chapter 2: Historical and theoretical background

### 2.3.2.6: Mechanism and kinetics of miniemulsion polymerization

Using calorimetry, Bechthold *et al.*<sup>59, 73</sup> examined the kinetic behavior of miniemulsion polymerization using water-soluble initiators. The objective was to further unravel the miniemulsion polymerization process by selectively changing parameters such as the amount of initiator and surfactant. The calorimeter measures the heat of reaction which is then converted to the rate of polymerization by the following Equation<sup>59,73</sup>:

$$R_p = \frac{Qr}{V_{aq}\Delta H_p} \quad (2.17)$$

where:  $R_p$  is the rate of polymerization,  $Qr$  is the heat of polymerization,  $V_{aq}$  is the volume of the aqueous phase and  $\Delta H_p$  is the molar heat of polymerization

Below is a typical kinetic curve obtained from calorimetric techniques<sup>59,73</sup>

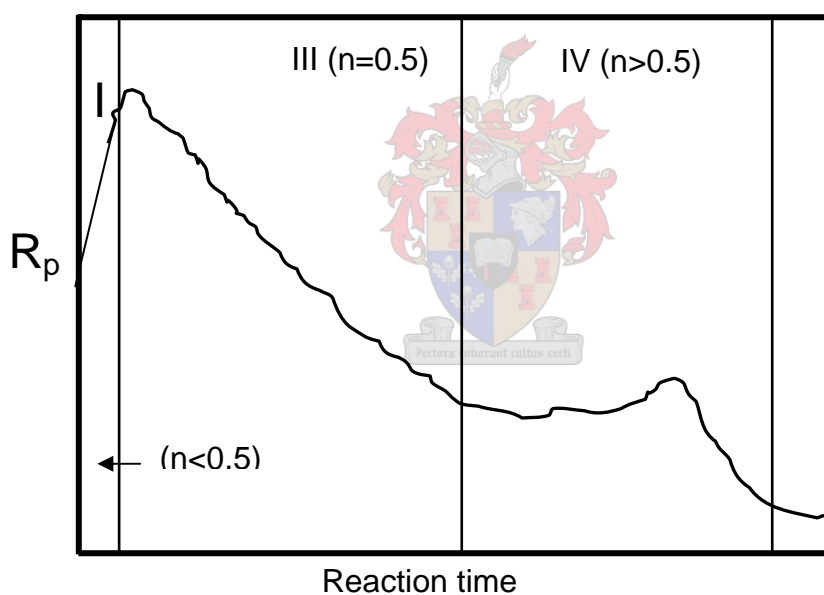


**Fig 2.7: Kinetics of miniemulsion polymerization as revealed by calorimetry**

Three distinguished intervals can be categorized for miniemulsion polymerization kinetic courses (Fig 2.6). As derived from Harkins' definition for macroemulsion polymerization,<sup>69</sup> only intervals I and III are found in the miniemulsion process. Intervals I and III can be defined by the average number of radicals per particle: during interval I, the average number of radicals per particle ( $\bar{n}$ ) increases until a plateau is reached at the onset of interval III ( $\bar{n} = 0.5$ ) (assuming zero-one conditions



## ***Chapter 2: Historical and theoretical background***

---

for styrene miniemulsion polymerization). The droplet nucleation interval (interval I) is very short, meaning that every droplet is nucleated within a short period of time and the average number of radicals per particle = 0.5 is reached. The slow increase in the average number of radicals per particle is due to a slow radical flux through the droplet interface. Therefore, it follows that the start of the polymerization in each miniemulsion droplet is not simultaneous. Each miniemulsion droplet is regarded as an individual nanoreactor, which does not interfere with others droplets (compartmentalization). The end of interval I is characterized by the maximum velocity ( $v_{\max}$ ) indicating the establishment of an equilibrium concentration of radicals per particle. Interval III reveals the similarity towards a suspension polymerization.<sup>59</sup> The value of the average number of radicals per particle ( $\bar{n}$ ) is 0.5 during interval III and is independent of the amount of initiator, and therefore, any increase in the initiator concentration does not result in an acceleration of the polymerization process in this interval. Only the number of active sites defines the net polymerization time: the higher the number of particles the shorter the net polymerization time. Additionally, interval IV describes the gel peak. There is an increase in  $\bar{n}$  which is due to an increase in the internal viscosity of the particles leading to localization of heat. The rate of termination is reduced due to reduction in the rate of diffusion of the propagating chains (due to increase in viscosity). In this region, the steady-state approximation does not hold ( $R_i \gg R_t$ ), hence there is an increase in the rate of propagation. This effect is known as the Trommsdorff effect and this usually occurs at high monomer conversions. In conventional emulsion polymerization three intervals are obtained (I, II and III). Intervals I and III are similar to the ones described above for miniemulsion. Interval II describes the process of monomer diffusion from large monomer droplets into the growing particle.<sup>70</sup> In this interval, the rate of monomer consumption in the particle is constant since the particle is constantly replenished with monomer from large monomer droplets. When the monomer droplets are exhausted, there will be an exponential decrease in the reaction rate (interval III)<sup>70</sup> and the Trommsdorff effect can be observed in some cases.<sup>59</sup>

### 2.4: Polymerizable surfactants

#### 2.4.1: General

Polymerizable surfactants are also referred to as reactive surfactants. This terminology refers to surfactants that participate in a chemical reaction during polymerization. Reactive surfactants contain a polymerizable group and a surfactant moiety which mimics the properties of classical surfactants. A classical surfactant has a long hydrocarbon chain (hydrophobic tail) and a hydrophilic head and is a surface active molecule (amphiphilic). The general structure of a classical surfactant is shown in Fig 2.8.

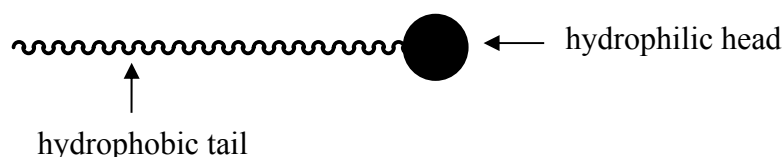


**Fig 2.8: The general structure of a classical surfactant e.g. sodium lauryl sulfate [hydrophobic tail is a C<sub>12</sub> and the hydrophilic head is the sulfate group with sodium as the counter ion (OSO<sub>3</sub><sup>-</sup>Na<sup>+</sup>)]**

The hydrophilic head can be either charged (cationic or anionic) or non-ionic (polyethylene oxide moiety). These features are the same as those found on the surfactant moiety of a reactive surfactant i.e. a reactive surfactant can be designed so that its hydrophilic head is the same as that of any classical surfactant. The main difference between classical and polymerizable surfactants is that the latter possess a polymerizable group either at the tail-end or anywhere along the hydrophobic chain. There are three classes of polymerizable surfactants<sup>31</sup>:

- Inisurf: Combining the initiator molecule with a surfactant moiety. The molecule fragments forming two radicals capable of initiating polymerization.
- Transurf: Combining a transfer agent with a surfactant moiety. The reactive surfactant acts as a transfer agent and participates in transfer reactions which are chemical (reversible/irreversible) reactions.

## Chapter 2: Historical and theoretical background

- c) Surfmer: Combining a surfactant with a monomer, the reactive surfactant behaves like a monomer during polymerization and is incorporated into the polymer chains.

With all three of the above types, the surfactant moiety is chemically bound to the polymer chains and still acts as a surfactant in particle stability.

### 2.4.2: Surfmers

An advantage of surfmers over insurfs and transurfs is that they can be used without any restriction in the critical amount that can be used. Thus, the amount of the insurf or transurf to be used depends on the amount of initiator or transfer agent required for the polymerization. The most common surfmers are the H-type (polymerizable group is located at the hydrophobic tail end) and the T-type (polymerizable group is located close to the hydrophilic head).<sup>88</sup>

#### Examples of surfmers

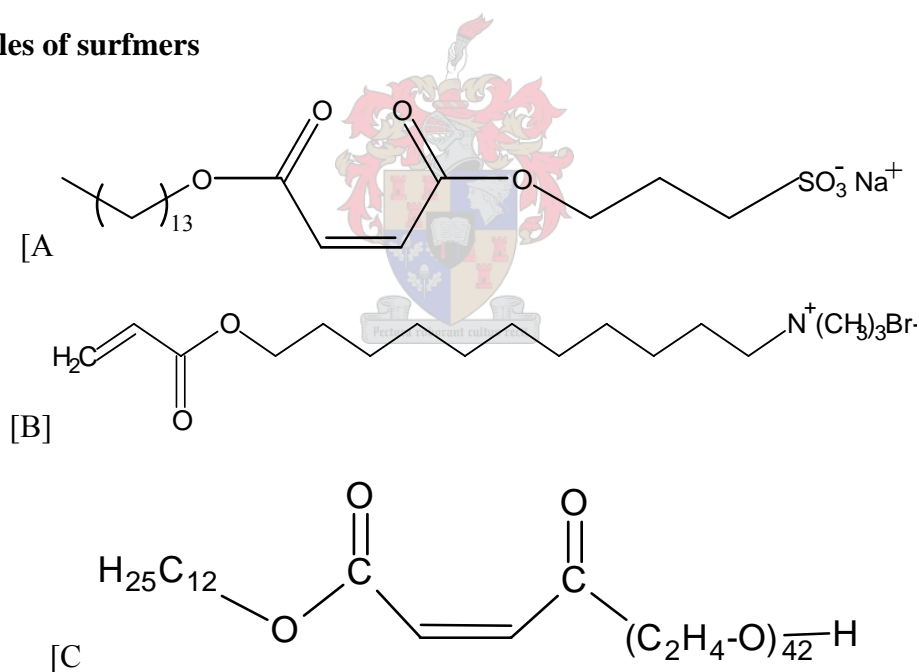


**Fig 2.9: Three different types of surfmers: [A] Diethyl maleate surfmer<sup>84</sup> [anionic (T-type)]; [B] 11-(acryloyloxy) undecyl trimethylammonium bromide<sup>83</sup> [cationic (H-type)] and [C] maleate surfmer<sup>84</sup> [nonionic (T-type)]**

Like classical surfactants, surfmers are water soluble and form micelles at concentrations greater than or equal to their critical micelle concentrations.

### **2.4.3: Critical micelle concentration (CMC)**

Surface active compounds contain two distinct components which differ in their affinity for solutes. The part of the molecule which has an affinity for polar solutes, such as water, is said to be hydrophilic. The part of the molecule which has an affinity for non-polar solutes, such as hydrocarbons, is said to be hydrophobic. Molecules containing both types of components are said to be amphiphilic. An amphiphilic molecule can arrange itself at the surface of the water such that the polar part interacts with the water and the non-polar part is held above the surface (either in the air or in a non-polar liquid). The presence of these molecules on the surface disrupts the cohesive energy at the surface and thus lowers the surface tension (surface tension measurements can give the CMC of solutions containing surface active agents).<sup>88</sup> Another arrangement of these molecules can allow each component to interact with its favored environment. Molecules can form aggregates in which the hydrophobic portions are oriented within the cluster and the hydrophilic portions are exposed to the solvent<sup>88</sup> and such aggregates are called micelles. There is a relatively small range of concentrations separating the limit below which virtually no micelles are detected and the limit above which virtually all additional surfactant molecules form micelles. Many properties of surfactant solutions (e.g. conductivity and surface tension), if plotted against the concentration, appear to change at a different rate above and below this range.<sup>84</sup> By extrapolating the loci of such a property above and below this range until they intersect, a value may be obtained known as the critical micelle concentration (CMC). As values obtained using different properties are not quite identical, the method by which the CMC is determined should be clearly stated.

### **2.4.4: Surfactants and surfmers in aqueous dispersed polymerizations**

In aqueous dispersed systems (emulsion, miniemulsion and microemulsion), surfactants are used to emulsify monomer droplets. Emulsification prevents the droplets from coalescing and is the basis of emulsion and microemulsion, whereby inter-micelle repulsions provide stability to the 'emulsion'. In miniemulsion, surfactants are also used but the stability of the miniemulsion is due to both the surfactant and a hydrophobe as previously mentioned in this Chapter, Section 2.3.2.3. The use of surfactants in aqueous dispersed polymerization may cause problems in the

## ***Chapter 2: Historical and theoretical background***

---

final product.<sup>84,83</sup> These problems are mainly due to the free migration of the surfactant within the latex or film product.<sup>84</sup> For example, where shelf life stability of the latex is of paramount importance, the physically bound surfactant can migrate within the latex and this may lead to destabilization of the latex particles. In films and coatings, surfactant migration may also lead to an increase in water percolation.<sup>84</sup> Research is currently also being done on aqueous dispersed polymerizations stabilized by polymerizable surfactants. This can also give economic advantages, for example in the rubber industry, where emulsion polymerization is used to synthesize rubber.<sup>83</sup> If surfactants are used, there is a need to remove the surfactant to avoid problems associated with its leaching out from the final product and this is done by washing using water and the process is costly. Moreover, surfactant removal may also lead to environmental pollution. When surfmers are used they are incorporated into the polymer chains, but still retain their surface activity.<sup>85</sup> The result is that the surfactant moiety is chemically bound to the polymer chains (copolymerization) and there is no free migration of the surfmer. A prominent difference is that there might be a considerable change in the properties of the polymer when a surfmer is used. The degree of property change depends on the amount of surfmer used and can be an advantage or a disadvantage.

### **Advantages of using surfmers are:**

- ❖ Improved particle stability (shelf life stability)
- ❖ No surfmer migration can occur in the final product
- ❖ Improved shear stability of latexes (no desorption due to shear constraints)
- ❖ No environmental pollution due to waste dumping
- ❖ Improved reduction in sensitivity to moisture (e.g. in coatings).

### **Disadvantages:**

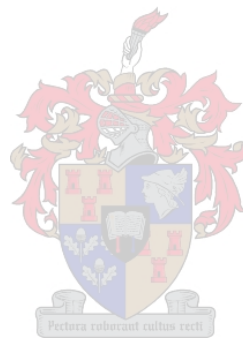
- ❖ Not easy to synthesize compared to classical surfactants
- ❖ Rates of polymerization are normally lower than when classical surfactants are used.

## ***Chapter 2: Historical and theoretical background***

---

---

Polymerizable surfactants have been used in both emulsion<sup>84</sup> and miniemulsion<sup>85</sup> polymerization. It has been shown that the latexes produced by surfmer stabilized emulsion polymerization are more stable under shear and stable even after being subjected to freezing conditions.<sup>83</sup>



### **2.5: References**

- (1) Isobe, Y.; Fujioka, D.; Habaue, S.; Okamoto, Y. *Journal of the American Chemical Society* 2001, 123, 7180-7181.
- (2) Ray, B.; Isobe, Y.; Morioka, K.; Habaue, S.; Okamoto, Y.; Kamigaito, M.; Sawamoto, M. *Macromolecules* 2003, 36, 543-545.
- (3) Beuermann, S.; Buback, M. *Progress in Polymer Science* 2002, 27, 191-254.
- (4) Bai, R.-K.; You, Y.-Z.; Pan, C.-Y. *Macromolecular Rapid Communications* 2001, 22, 315-319.
- (5) Olaj, O. F.; Vana, P.; Zoder, M. *Macromolecules* 2002, 35, 1208-1214.
- (6) Henriquez, C.; Bueno, C.; Lissi, E. A.; Encinas, M. V. *Polymer* 2003, 44, 5559-5561.
- (7) Russell, G. T.; Gilbert, R. G.; Napper, D. H. *Macromolecules* 1992, 25, 2459-2469.
- (8) Russell, G. T.; Gilbert, R. G.; Napper, D. H. *Macromolecules* 1993, 26, 3538-3552.
- (9) Heuts, J. P. A.; Davis, T. P.; Russell, G. T. *Macromolecules* 1999, 32, 6019-6030.
- (10) Pradel, J. L.; Boutevin, B.; Ameduri, B. *Journal of Polymer Science: Part A: Polymer Chemistry* 2000, 38, 3293-3302.
- (11) Miura, Y.; Nakamura, N.; Taniyuchi, I. *Macromolecules* 2001, 34, 447-455.
- (12) De Brouwer, H.; Schellekens, M. A. J.; Klumperman, B.; Monteiro, M. J.; German, A. L. *Journal of Polymer Science: Part A: Polymer Chemistry* 2000, 38, 3596-3603.
- (13) Moad, G.; Chiefari, J.; Chong, B. Y.; Krstina, J.; Mayadunne, R. T.; Postma, A.; Rizzardo, E.; Thang, S. H. *Polymer International* 2000, 49, 993-1001.
- (14) Wang, J.-S.; Matyjaszewski, K. *Journal of the American Chemical Society* 1995, 117, 5614-5615.
- (15) Kato, M.; Kamigaito, M.; Sawamoto, M.; Higashimura, T. *Macromolecules* 1995, 28, 1721-1723.
- (16) Percec, V.; Barboiu, B.; Kim, H.-J. *Journal of the American Chemical Society* 1998, 120, 305-316.
- (17) Moad, G.; Rizzardo, E.; Solomon, D. H. *Macromolecules* 1982, 15, 909-914.

## ***Chapter 2: Historical and theoretical background***

---

- (18) Georges, M. K.; Veregin, R. P. N.; Kazmaier, P. M.; Hamer, G. K. *Macromolecules* 1993, 26, 2987-2988.
- (19) Gabaston, L. I.; Jackson, R. A.; Armes, S. P. *Macromolecules* 1998, 31, 2883-2885.
- (20) Bon, S. A. F.; Bosveld, M.; Klumperman, B.; German, A. L. *Macromolecules* 1997, 30, 324-326.
- (21) Marestin, C.; Noel, C.; Guyot, A.; Claverie, J. *Macromolecules* 1998, 31, 4041-4044.
- (22) Farcet, C.; Lansalot, M.; Charleux, B.; Pirri, R.; Vairon, J. P. *Macromolecules* 2000, 33, 8559-8570.
- (23) Hawker, C. J.; Bosman, A. W.; Harth, E. *Chemical Reviews* 2001, 101, 3661-3688.
- (24) Fukuda, T.; Terauchi, T.; Tsujii, Y.; Miyamoto, T. *Macromolecules* 1996, 29, 3050-3052.
- (25) Yoshida, E.; Ishizone, T.; Hirao, A.; Nakaharna, S.; Takataj, T.; Endo, J. T. *Macromolecules* 1994, 27, 3119-3124.
- (26) Craig J. Hawker, A. W. B.; Harth E. *Chem. Rev.* 2001, 101, 3661-3688.
- (27) Percec, V.; Barboiu, B. *Macromolecules* 1995, 28, 7970-7972.
- (28) Matyjaszewski, K.; Xia, J. *Chem. Rev.* 2001, 101, 2921-2990.
- (29) Chiefari, J.; Chong, Y. K.; Ercole, F.; Krstina, J.; Jeffery, J.; Le, T. P. T.; Mayadunne, R. T. A.; Meijs, G. F.; Moad, C. L.; Moad, G.; Rizzardo, E.; Thang, S. H. *Macromolecules* 1998, 31, 5559-5562.
- (30) Smulders, W.; Gilbert, R. G.; Monteiro, M. J. *Macromolecules* 2003, 36, 4309-4318.
- (31) Le, T. P.; Moad, G.; Rizzardo, E.; Thang, S. H. In *PCT Int Appl*, 1998.
- (32) Tonge, M. P.; McLeary, J. B.; Vosloo, J. J.; Sanderson, R. D. *Macromolecular Symposia* 2003, 193, 289-304.
- (33) Barner, L.; Quinn, J. F.; Barner-Kowollik, C.; Vana, P.; Davis, T. P. *European Polymer Journal* 2003, 39, 449-459.
- (34) Perrier, S.; Davis, T. P.; Carmichael, A. J.; Haddleton, D. M. *European Polymer Journal* 2003, 39, 417-422.
- (35) Severac, R.; Lacroix-Desmazes, P.; Boutevin, B. *Polymer International* 2002, 51, 1117-1122.



## ***Chapter 2: Historical and theoretical background***

---

- (36) Prescott, S. W.; Ballard, M. J.; Rizzardo, E.; Gilbert, R. G. *Macromolecules* 2002, 35, 5417-5425.
- (37) Bouhadir, G.; Legrand, N.; Quiclet-Sire, B.; Zard, S. Z. *Tetrahedron Letters* 1999, 40, 277-280.
- (38) Quiclet-Sire, B.; Wilczewska, A.; Zard, S. Z. *Tetrahedron Letters* 2000, 41, 5673-5677.
- (39) Thang, S. H.; Chong, Y. K. B.; Mayadunne, R. T. A.; Moad, G.; Rizzardo, E. *Tetrahedron Letters* 1999, 40, 2435-2438.
- (40) Degani, I.; Fochi, R.; Gatti, A.; Regondi, V. *Synthesis* 1986, 894-899.
- (41) Stenzel, M. H.; Davis, T. P. *Journal of Polymer Science: Part A: Polymer Chemistry* 2002, 40, 4498-4512.
- (42) You, Y.-Z.; Chun-Yan, H.; Bai, R.-K.; Pan, C.-Y.; Wang, J. *Macromolecular Chemistry and Physics* 2002, 203, 477-483.
- (43) Mayadunne, R. T. A.; Rizzardo, E.; Chiefari, J.; Krstina, J.; Moad, G.; Postma, A.; Thang, S. H. *Macromolecules* 2000, 33, 243-245.
- (44) You, Y.-Z.; Bai, R.-K.; Pan, C.-Y. *Macromolecular Chemistry and Physics* 2001, 202, 1980-1985.
- (45) Chong, Y. K. B.; Krstina, J.; Le, T. P. T.; Moad, G.; Postma, A.; Rizzardo, E.; Thang, S. H. *Macromolecules* 2003, 36, 2256-2272.
- (46) Chiefari, J.; Chong, Y. K. B.; Ercole, F.; Krstina, J.; Jeffery, J.; Le, T. P. T.; Mayadunne, R. T. A.; Meijs, G. F.; Moad, C. L.; Moad, G.; Rizzardo, E.; Thang, S. H. *Macromolecules* 1998, 31, 5559-5562.
- (47) Chiefari, J.; Mayadunne, R. T. A.; Moad, C. L.; Moad, G.; Rizzardo, E.; Postma, A.; Skidmore, M. A.; Thang, S. H. *Macromolecules* 2003, 36, 2273-2282.
- (48) Colombani, D. *Progress in Polymer Science* 1999, 24, 425-480.
- (49) Chong, B. Y. K.; Le, T. P. T.; Moad, G.; Rizzardo, E.; Thang, S. H. *Macromolecules* 1999, 32, 2071-2074.
- (50) Vana, P.; Davis, T. P.; Barner-Kowollik, C. *Macromolecular Theory and Simulations* 2002, 11, 823-835.
- (51) Calitz, F. M.; Tonge, M. P.; Sanderson, R. D. *Macromolecules* 2003, 36, 5-8.
- (52) Mayadunne, R. T. A.; Rizzardo, E.; Chiefari, J.; Chong, Y. K.; Moad, G.; Thang, S. H. *Macromolecules* 1999, 32, 6877-6980.

## ***Chapter 2: Historical and theoretical background***

---

- (53) Mayadunne, R. T. A.; Rizzardo, E.; Chiefari, J.; Krstina, J.; Moad, G.; Postma, A.; Thang, S. H. *Macromolecules* 2000, 33, 243-245.
- (54) Monteiro, M. J.; Hodgson, M.; de Brouwer, H. *Journal of Polymer Science: Part A: Polymer Chemistry* 2000, 38, 3864-3874.
- (55) Uzulina, I.; Kanagasabapathy, S.; Claverie, J. *Macromolecular Symposia* 2000, 150, 33-38.
- (56) Monteiro, M. J.; de Barbeyrac, J. *Macromolecules* 2001, 34, 4416-4423.
- (57) Tsavalas, J. G.; Schork, F. J.; Brouwer, H.; Monteiro, M. J. *Macromolecules* 2001, 34, 3938-3946.
- (58) Gilbert, R. G. *Emulsion Polymerization: A Mechanistic Approach*; Academic Press, 1995, Sydney, Australia.
- (59) Bechthold, N.; Landfester, K. *Macromolecules* 2000, 33, 4682-4689.
- (60) Vana, P.; Quinn, J. F.; Davis, T. P.; Barner-Kowollik, C. *Australian Journal of Chemistry* 2002, 55, 425-431.
- (61) Barner-Kowollik, C.; Quinn, J. F.; Morsley, D. R.; Davis, T. J. *Poly Sci., Part A: Polymer Chemistry* 2001, 39, 1353.
- (62) Barner-Kowollik, C.; Quinn, J. F.; Nguyen, T. L. U.; Heuts, J. P. A.; Davis, T. P. *Macromolecules* 2001, 34, 7849.
- (63) de Brouwer, H.; Schellekens, M. A. J.; Klumperman, B.; Monteiro, M. J.; German, A. L. J. *Polymer Science, Part A: Polymer Chemistry Review* 2000, 38, 3596.
- (64) Kwak, Y.; Goto, A.; Tsujii, Y.; Murata, Y.; Komatsu, K.; Fukuda, T. *Macromolecules* 2002, 35, 3026-3029.
- (65) Calitz, F. M.; McLeary, J. B.; McKenzie, J. M.; Tonge, M. P.; Klumperman, B.; Sanderson, R.D. *Macromolecules* 2003, 36, 9687-9690.
- (66) McLeary, J. B.; Calitz, F. M.; McKenzie, J. M.; Tonge, M. P.; Sanderson, R. D.; Klumperman, B. *Macromolecules* 2004, 37, 2383-2394.
- (67) Wang, Q.; Fu, S.; Yu, T. *Progress in Polymer Science* 1994, 19, 703.
- (68) Aizpurua, I.; Amalvy, J. I.; Barandiaran, M. J. *Colloids and Surfaces A: Physicochemical and Engineering Aspects* 2000, 166, 59-66.
- (69) Harkins, W. D. *Journal of American Chemical Society* 1947, 69, 1428.
- (70) Capek, I.; Chern, C. *Advances in Polymer Science* 2001, 155, 102-124.
- (71) Asua, J. M. *Progress in Polymer Science* 2002, 27, 1283-1346.
- (72) Chang, H.; Lin, Y.; Chern, C.; Lin, S. *Langmuir* 1998, 14, 6632-6638.

## ***Chapter 2: Historical and theoretical background***

---

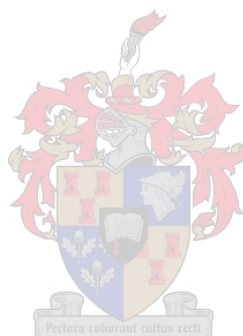
---

- (73) Blythe, P. J.; Sudol, E. D.; El-Aasser, M. S. *Journal of Polymer Science: Part A: Polymer Chemistry* 1997, 35, 807-811.
- (74) Capek, I.; Chudej, J.; Janickova, S. *Journal of Polymer Science: Part A: Polymer Chemistry* 2003, 41, 804-820.
- (75) Landfester, K.; Bechthold, N.; Forster, S.; Antonietti, M. *Macromolecular Rapid Communications* 1999, 20, 81-84.
- (76) Cunningham, M.F. *Progress in Polymer Science* 2002, 27, 1039-1067.
- (77) Landfester, K. *Macromolecules* 1999, 32, 2679-2683.
- (78) Antonietti, M.; Landfester, K. *Progress in Polymer Science* 2002, 27, 689-757.
- (79) Lim, M.-S.; Chen, H. *Journal of Polymer Science: Part A: Polymer Chemistry* 2000, 38, 1818-1827.
- (80) Charmot, D.; Corpart, P.; Adam, H.; Zard, S. Z.; Biadatti, B. G. *Macromolecular Symposia* 2000, 150, 23-32.
- (81) Percec, V.; Barboiu, B.; Neumann, A.; Ronda, J. C.; Zhao, M. *Macromolecules* 1996, 29, 3665-3668.
- (82) Luo, Y.; Tsavalas, J. G.; Schork, F. J. *Macromolecules* 2001, 34, 5501-5507.
- (83) Guyot, A.; Tauer, K. In *Reactions and synthesis in surfactant systems*; J, T., Ed.; Marcel Dekker: New York, 2001; pp 547-575.
- (84) Unzue, M. J.; Schoonbrood, H. A. S.; Asua, J. M.; Gon, A. M.; Sherrington, D. C.; Stahler, K.; Goebel, K.; Tauer, K.; Sjoberg, M.; Holmberg, K. *Journal of Applied Polymer Science* 1997, 66, 1803-1820.
- (85) Guyot, A.; Graillat, C.; Favero, C. *C.R. Chimie* 2003, 6, 1319-1327.

## **Chapter 3: Synthesis, characterization and homogeneous polymerization of polymerizable surfactants using the RAFT process**

### **Abstract**

This Chapter describes the synthetic pathways that were used for the preparation of surfmers, RAFT agent and oligosurfmers. It also includes the characterization of these compounds.



### **3.1: Introduction**

The term surfmer refers to a broad class of surface active compounds derived from a polymerizable moiety and a surfactant. The class consists of the H- and T-types of surfmers as described in Chapter 2. Synthesis of the T-type surfmers can be carried out in a single step by choosing a monomer with polar or ionic functionality as well as a reactive group to attach the hydrophobic tail.<sup>1</sup> Synthesis of the H-type surfmers can be carried out via a polymerizable intermediate in two steps.<sup>2</sup> The first step involves attaching the polymerizable group to the hydrophobic part of the surfmer, forming a polymerizable intermediate which can be regarded as a monomer. Purification of the intermediate is required at this point as the later purification of amphiphilic compounds can be problematic. The second step involves attaching a hydrophilic head to the polymerizable intermediate. It is important to note that by attaching the polymerizable group first, before the hydrophilic head, the problems associated with surface active compounds which can require several synthetic and separation steps are eliminated. Surface active compounds are difficult to purify as they interact readily with polar and non-polar surfaces and are soluble in both types of solvent.<sup>2</sup> Another important consideration is that mild reaction or separation conditions are preferred in order to prevent polymerization. In most cases, polymerization inhibitors are used to prevent polymerization during the synthesis of surfmers.<sup>1</sup>

In this Chapter, the synthesis of two H-type surfmers with different head groups, but with the same polymerizable group (i.e. methacrylate), is described. Characterization of these surfmers was carried out using the following techniques and instruments: Nuclear Magnetic Resonance spectroscopy (NMR) using a Varian VXR 300 MHz spectrometer; Infra-red spectroscopy (IR), using a FT-IR NEXUS instrument; and Electro-Spray-Mass Spectrometry (ESMS), using a Waters API Q-TOF Ultima instrument.

## 3.2: Synthesis of sulfate surfmer: Sodium 11-methacryloyloxyundecan-1-yl sulfate (SS)

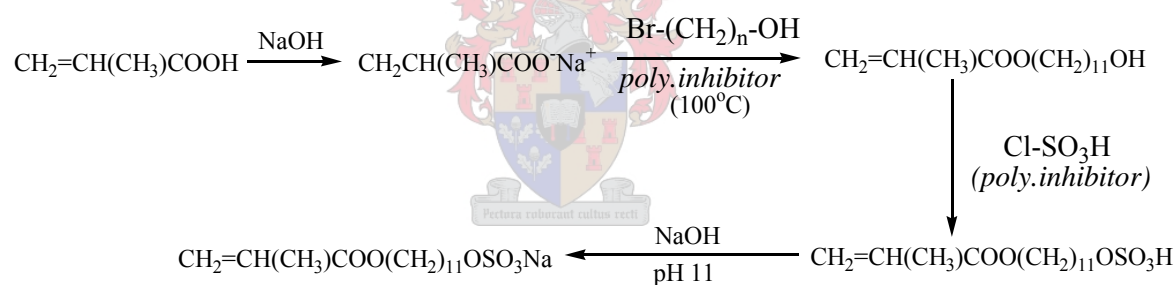
### Materials

The following reagents were used:

sodium hydroxide 97% (Associated Chemical Enterprises Pty (Ltd), methacrylic acid 99% (Aldrich), 11-bromo undecan-1-ol 99% (Fluka Chemie AG), n-tetra butyl-ammonium bromide (99% Aldrich), 1,4-dihydroxybenzol 99% (Merck-Schuchardt), chlorosulfonic acid 98% (Fluka Chemie AG), triethyl amine solution (35% ethanol) (Fluka), and triethylamine 99% (Aldrich).

### 3.2.1: Experimental

Sodium 11-methacryloyloxyundecan-1-yl sulfate, hereafter referred to as sulfate surfmer or SS, was synthesized according to the method of Unzue *et al.*<sup>2</sup> The reactions, which follow a nucleophilic elimination (S<sub>N</sub>2) mechanism, are presented in the Scheme below:

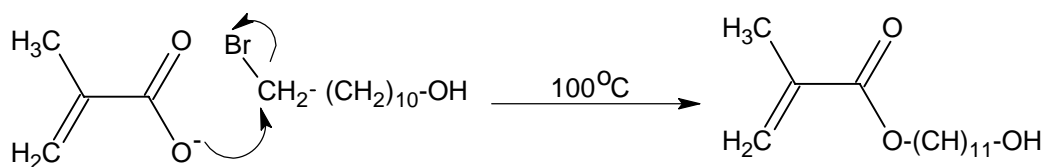


**Scheme 3.1: Reaction pathway and conditions for the synthesis of sodium 11-methacryloyloxyundecan-1-yl sulfate (SS)**

#### 3.2.1.1: Sodium methacrylate salt formation

Sodium hydroxide (56.9 g; 1.422 mol) was dissolved in 100 ml of de-ionized water and placed in a round-bottomed flask. The solution was kept in an ice bath for 15 minutes, and then methacrylic acid (121.8 g; 1.416 mol) was added drop-wise, under stirring. After 45 minutes, 150 ml of acetone was added to precipitate the sodium salt. The latter was then filtered and dried under vacuum. A white powder (73.58 g) was obtained in 96% yield. No impurities were detected by <sup>1</sup>HNMR spectroscopy [  $\delta$  (ppm) 1.9 (CH<sub>3</sub>);  $\delta$  (ppm) 5.4 & 5.7 (=CH<sub>2</sub>)].

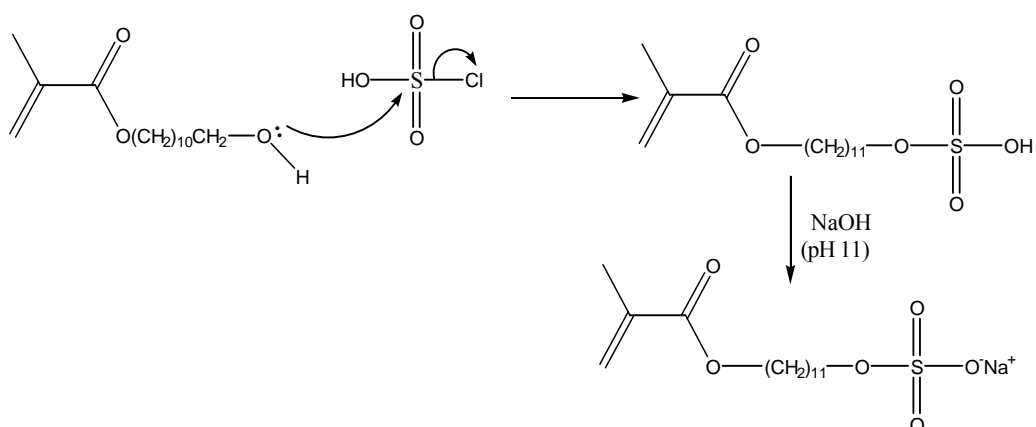
**3.2.1.2: Synthesis of 11-methacryloyloxyundecan-1-ol**



**Scheme 3.2: Reaction mechanism for the synthesis of 11-methacryloyloxyundecan-1-ol**

Sodium methacrylate (18.0 g; 0.165 mol), 11-bromoundecan-1-ol (7.5 g; 0.0277 mol), n-tetrabutylammonium bromide (2.77 g; 0.00801 mol), which acts as the phase transfer catalyst, and 1,4-dihydrobenzol (0.015 g; 0.0680 mol), a polymerization inhibitor, were dissolved in a mixture of de-ionized water (40 ml) and chloroform (25 ml) in a round-bottomed flask fitted with a condenser. The reaction mixture was refluxed at 100°C with vigorous stirring, using a magnetic stirrer, for three days. At this point, the chloroform layer was washed with a 2% sodium hydroxide solution (4 x 250 ml), followed by distilled water (4 x 250 ml). The organic layer was dried over magnesium sulfate and the solvent was evaporated. A yellowish viscous liquid (5.8 g) 81% yield was obtained. Purity was estimated from <sup>1</sup>H NMR spectroscopy to be above 90%. <sup>1</sup>H NMR chemical shifts;  $\delta$  (ppm) 1.3 (7CH<sub>2</sub>),  $\delta$  (ppm) 1.6 & 1.7 (2x  $\beta$ -CH<sub>2</sub>),  $\delta$  (ppm) 2.0 (CH<sub>3</sub>),  $\delta$  (ppm) 3.6 & 4.2 (2x  $\alpha$ -CH<sub>2</sub>),  $\delta$  (ppm) 5.6 & 6.1 (=CH<sub>2</sub>).

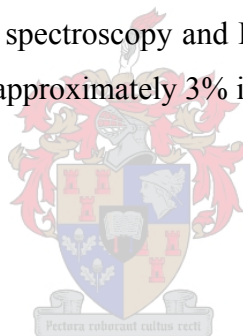
**3.2.1.3: Synthesis of sodium 11-methacryloyloxyundecan-1-yl sulfate**



**Scheme 3.3: Reaction mechanism for the synthesis of sodium 11-methacryloyloxyundecan-1-yl sulfate**

### **Chapter 3: Synthesis of surfmers, the RAFT agent and oligosurfmers**

Chlorosulfonic acid (2.5 g; 0.0214 mol) was placed in a three-necked round-bottomed flask that was fitted with a mechanical stirrer, dropping funnel and a nitrogen inlet. 11-Methacryloyloxybromoundecan-1-ol (5.5 g; 0.0214 mol) was added drop-wise over one hour with vigorous stirring. The reaction mixture was purged with nitrogen gas and stirred for four hours. The product, a brown viscous liquid, was then added drop-wise, using a dropping funnel, to triethylamine (2.25 g; 0.0223 mol), with vigorous stirring while the reaction vessel was cooled in ice. A hydroscopic, gelatinous, yellowish precipitate was formed. The ammonium counter ion was removed from the quaternary ammonium surfmer by adjusting the pH to 11 using a solution of 0.943 M sodium hydroxide. The electrode of the pH meter was dipped into the surfmer solution whilst adding the sodium hydroxide. The sodium salt was obtained after evaporation of triethylamine and water using a rotary evaporator, keeping the temperature below 50°C. The salt was recrystallized using ethyl acetate, yielding a white powder (6.97 g), in 90.55% yield. The product was characterized using <sup>1</sup>H NMR spectroscopy, IR spectroscopy and ESMS spectrometry. Results from ESMS indicated the presence of approximately 3% impurities.





### 3.2.2: Characterization of sodium 11-methacryloyloxyundecan-1-yl sulfate

#### 3.2.2.1: $^1\text{H}$ NMR spectroscopy of sodium 11-methacryloyloxyundecan-1-yl sulfate

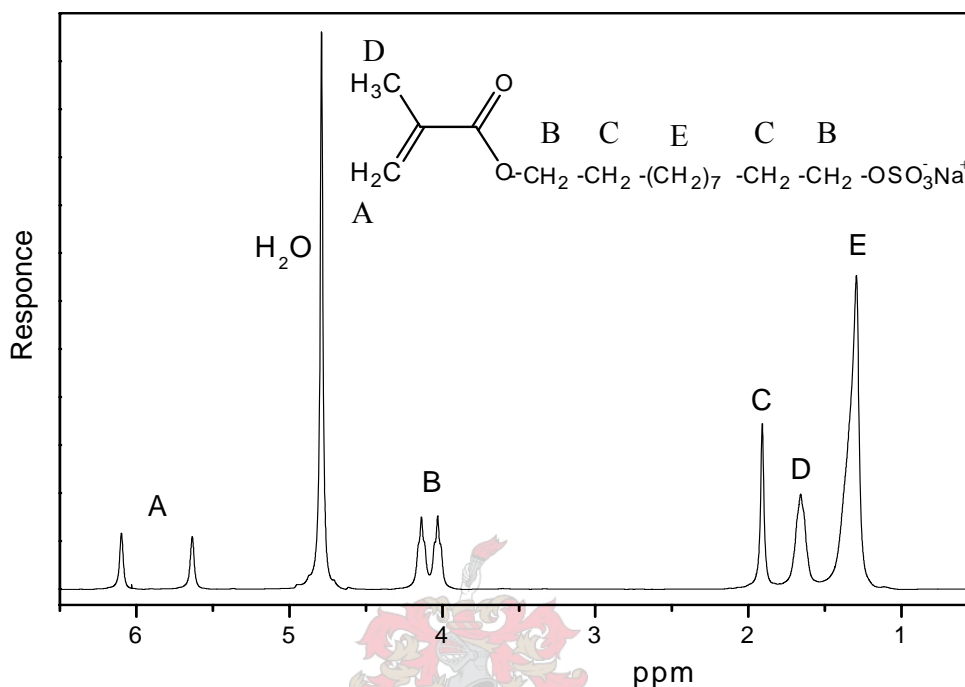
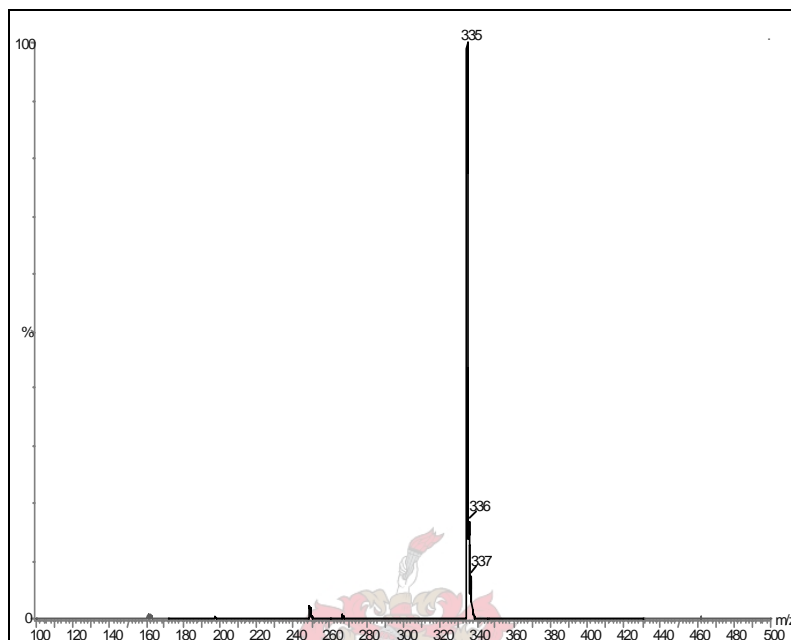


Fig 3.1:  $^1\text{H}$  NMR spectrum of sodium 11-methacryloyloxyundecan-1-yl sulfate ( $\text{D}_2\text{O}$  solvent)

The chemical shifts were as follows;  $\delta$  (ppm) 6.1 (1H),  $\delta$  (ppm) 5.7 (1H),  $\delta$  (ppm) 4.0 to 4.2 (4H),  $\delta$  (ppm) 2.9 (3H),  $\delta$  (ppm) 1.7 (4H),  $\delta$  (ppm) 1.3 (2 $\text{CH}_2$ ).

**3.2.2.2: Electro spray-mass spectroscopy (ES/MS) of sodium 11-methacryloyloxyundecan-1-yl sulfate**

Empirical formula:  $C_{15}H_{27}O_6S = 335.18$  (MS in the negative mode)



**Fig 3.2: ESMS spectrum of sodium 11-methacryloyloxyundecan-1-yl sulfate**

ESMS spectroscopy showed a base peak molecular weight 335.18, which is equivalent to the molecular weight of the anionic species of the surfmer.

**3.2.2.3: Infra-red (IR) spectroscopy of sodium 11-methacryloyloxyundecan-1-yl sulfate**

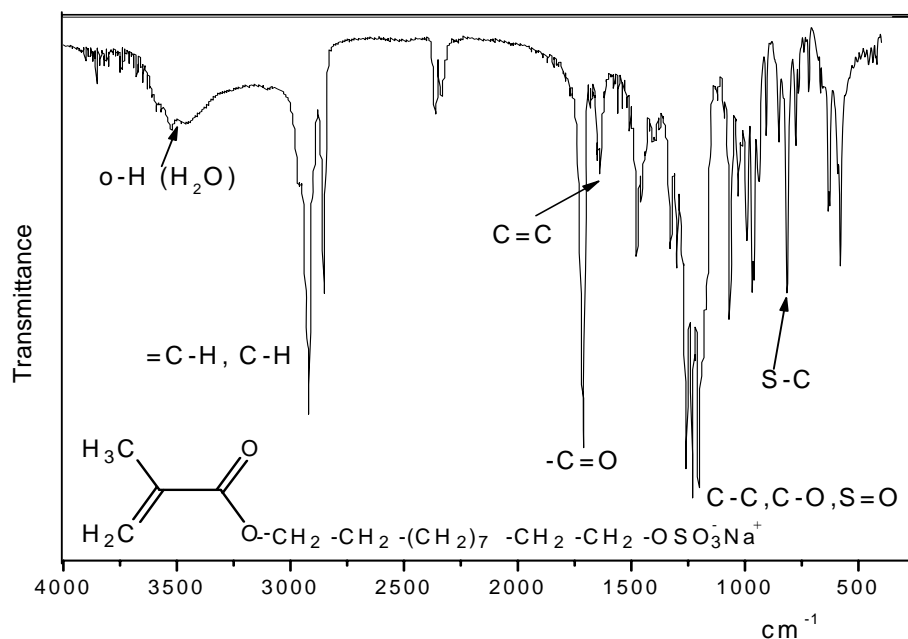
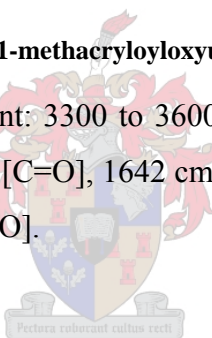


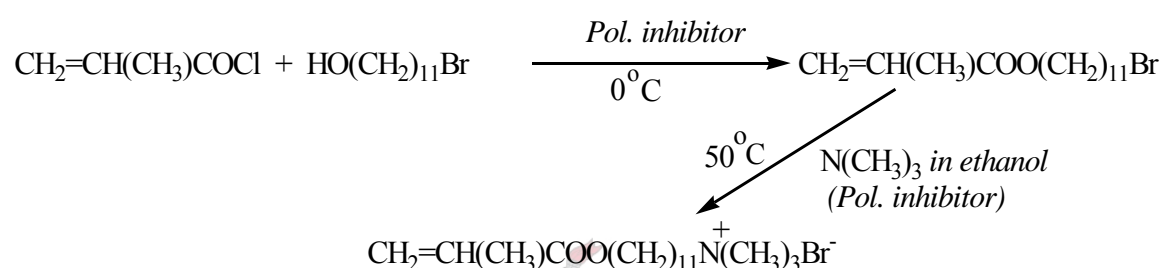
**Fig 3.3: Infra-red spectrum of sodium 11-methacryloyloxyundecan-1-yl sulfate**

Wave numbers and their assignment: 3300 to 3600  $\text{cm}^{-1}$  [O-H  $\text{cm}^{-1}$  ( $\text{H}_2\text{O}$ )], 2810 to 3045  $\text{cm}^{-1}$  [=C-H, C-H], 1726  $\text{cm}^{-1}$  [C=O], 1642  $\text{cm}^{-1}$  [C=C], 1147 to 1381  $\text{cm}^{-1}$  [C-C, S=O], 818  $\text{cm}^{-1}$  [S-C], 626  $\text{cm}^{-1}$  [S-O].



### 3.3: Synthesis of the ammonium surfmer: Synthesis of 11-methacryloyloxyundecan-1-yl trimethyl ammonium bromide (AS)

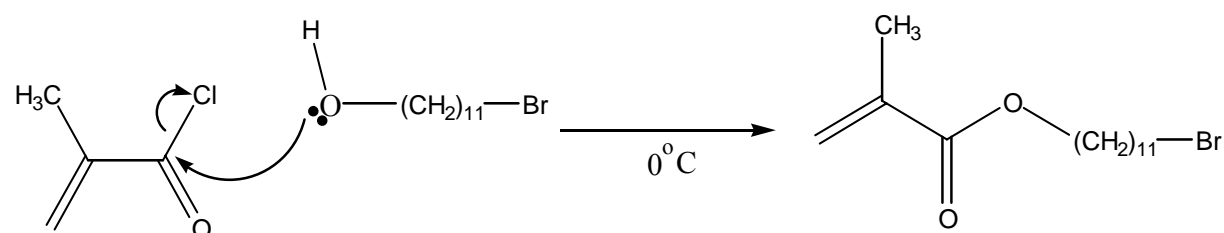
Synthesis of 11-methacryloyloxyundecan-1-yl trimethyl ammonium bromide, hereafter referred to as the ammonium surfmer or AS, was carried out according to the method of Joynes and Sherrington.<sup>3</sup> They synthesized and characterized a number of quaternary ammonium surfmers and prepared homopolymers as well as copolymers from them. Synthesis of the ammonium surfmer was carried out according to Scheme 3.4:



**Scheme 3.4: Reaction pathway and conditions for the synthesis of sodium 11-methacryloyloxyundecan-1-yl trimethyl ammonium bromide**

#### 3.3.1: Experimental

##### 3.3.1.1: Synthesis of 11-methacryloyloxyundecan-1-yl bromide

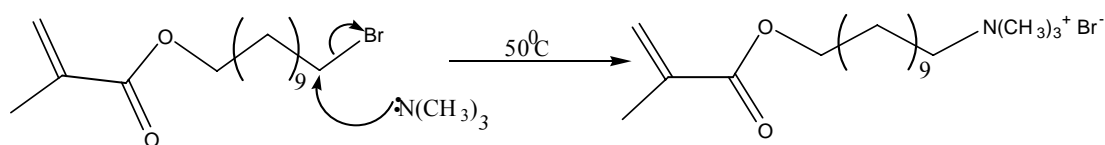


**Scheme 3.5: Reaction mechanism for the synthesis of 11-methacryloyloxyundecan-1-yl bromide**

11-Bromoundecan-1-ol (20.0 g; 0.0796 mol) was dissolved in diethyl ether (60 ml) then dried over magnesium sulfate for 12 hours in a round-bottomed flask fitted with a pressure equalizing dropping funnel with a drying tube. The flask was immersed in an ice bath and the contents stirred for 15 minutes. Firstly, sodium carbonate (17.0 g; 0.1604 mol) was added to the stirring solution and then methacryloyl chloride (16.6 g;

0.1592 mol) was added drop-wise over 30 minutes. The ether solution was washed with a 4% sodium hydrogen carbonate solution (4 x 50 ml) to remove unreacted methacryloyl chloride by first hydrolyzing it to methacrylic acid. The product was a yellow liquid (19.8 g, 99% yield), the purity of which was estimated from  $^1\text{H}$  NMR spectroscopy to be above 95%. The  $^1\text{H}$  NMR chemical shifts were as follows:  $\delta$  (ppm) 1.3 (7CH<sub>2</sub>),  $\delta$  (ppm) 1.6 & 1.7 (2x  $\beta$ -CH<sub>2</sub>),  $\delta$  (ppm) 2.0 (CH<sub>3</sub>),  $\delta$  (ppm) 3.4 & 4.2 (2x  $\alpha$ -CH<sub>2</sub>),  $\delta$  (ppm) 5.5 & 6.1 (=CH<sub>2</sub>).

**3.3.1.2: Synthesis of 11-methacryloyloxyundecan-1-yl trimethyl ammonium bromide**



**Scheme 3.6: Reaction mechanism for the synthesis of 11-methacryloyloxyundecan-1-yl trimethyl ammonium bromide**

11-Bromoundecyl-2-methylmethacrylate (18 g; 0.07165 mol) and a small amount of hydroquinone (0.0075 g;  $6.81 \times 10^{-5}$  mol) polymerization inhibitor were placed in a pressure reactor and trimethyl amine, 33% in ethanol (15.2 g; 0.0846 mol) were added. The pressure reactor was heated using an oil bath set at 50°C, for twelve hours. The reactor was then cooled using nitrogen gas to reduce the pressure inside and the contents were poured in to a 500 ml beaker. The surfmer was precipitated out using 60 ml diethyl ether. The product was washed 4 times with 40 ml of diethyl ether and filtered to yield a solid, which became sticky on contact with air due to water absorption. Finally, the AS surfmer was re-crystallized from ethyl acetate, filtered and then stored in a desiccator. The yield of the product was 17.59 g, (82.2% yield). Results from ESMS indicated that impurities comprised about 8%.

### 3.3.2: Characterization of 11-methacryloyloxyundecan-1-yl trimethyl ammonium bromide

#### 3.3.2.1: $^1\text{H}$ NMR spectroscopy of 11-methacryloyloxyundecan-1-yl trimethyl ammonium bromide

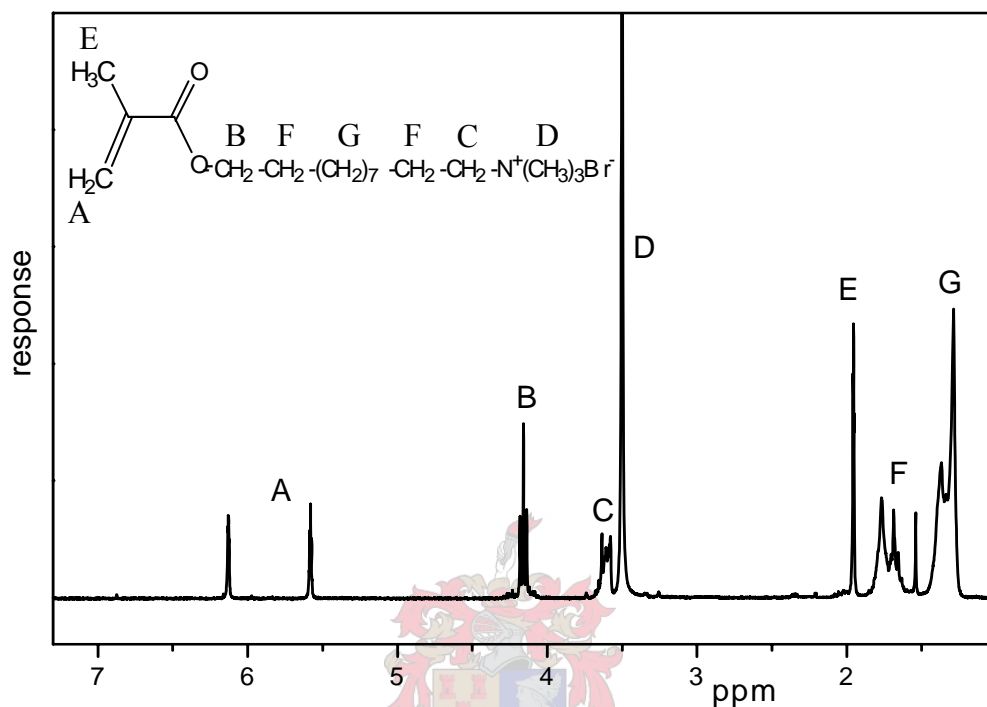
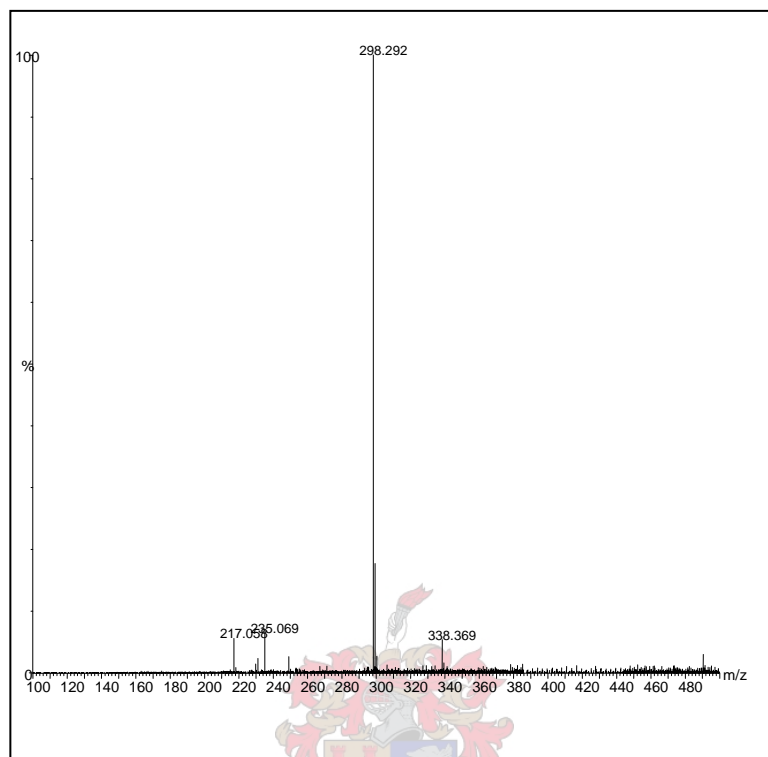


Fig 3.4:  $^1\text{H}$  NMR spectrum of 11-methacryloyloxyundecan-1-yl trimethyl ammonium bromide ( $\text{CDCl}_3$  solvent)

The chemical shifts were as follows:  $\delta$  (ppm) 5.5 & 6.19 (2H),  $\delta$  (ppm) 4.2 & 3.6 (2  $\alpha$ - $\text{CH}_2$ ),  $\delta$  (ppm) 3.5 (3  $\text{CH}_3$ ),  $\delta$  (ppm) 1.9 ( $\text{CH}_3$ ),  $\delta$  (ppm) 1.6 to 1.8 (2  $\beta$ - $\text{CH}_2$ ),  $\delta$  (ppm) 1.3 to 1.4 (7 $\text{CH}_2$ ).

**3.3.2.2: ES/MS spectroscopy of 11-methacryloyloxyundecan-1-yl trimethyl ammonium bromide**

Empirical formulae:  $C_{18}H_{36}O_2N = 298.29$  (MS in the positive mode)



**Fig 3.5: ES/MS of 11-methacryloyloxyundecan-1-yl trimethyl ammonium bromide**

ES/MS of 11-trimethylammonium-bromide undecyl-2-methylacrylate, shown in Fig 3.5 has the base peak at molecular weight 298.29 which is the equivalent to the empirical Mw of the cation species of the surfmer. The ES/MS was carried out in the positive mode.

**3.3.2.3: IR spectroscopy of 11-methacryloyloxyundecan-1-yl trimethyl ammonium bromide**

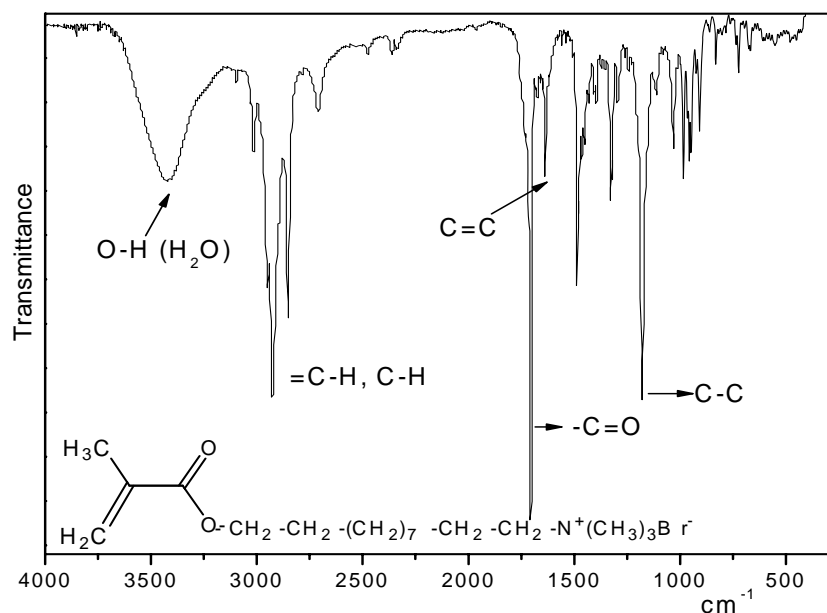


**Fig 3.6: Infra-red spectrum of 11-methacryloyloxyundecan-1-yl trimethyl ammonium bromide**

Wave numbers and their assignment: 3155-3650 [O-H (H<sub>2</sub>O)], 2770-3058 [=C-H, C-H (stretch)], 1697 [C=O], 1629 [C=C], 1176 [C-C], 1312 [C-N].

**3.3.3: Discussion: Surfmer synthesis (SS and AS)**

<sup>1</sup>H NMR spectroscopy, IR spectroscopy and ES/MS were used to characterize the surfmers (SS and AS) synthesized as described in Sections 3.1 and 3.2. <sup>1</sup>H NMR spectroscopy showed the presence of all the functional groups expected in the spectra for both surfmers. The characteristic absorption peaks for different chemical bonds (such as C=O, C=C, C-H and =C-H and other specific bonds for each surfmer) were seen in the infra-red spectra of the two surfmers. The molecular weights of the surfmers were determined by ES/MS spectroscopy. Results confirmed that the surfmers had been successfully synthesized. The ES/MS spectra of the sulfate surfmer showed that there were relatively low levels of impurities in the product (3%) compared to ammonium surfmer (8%), as determined from the ES/MS spectrum of AM surfmer which had numerous peaks due to impurities. The yields were considered acceptable for these materials.



### 3.4: Critical micelle concentration (CMC) of surfmers and surfactants

CMC measurements are affected by the temperature at which they are measured as well as the method used (refer to Chapter 2 Section 2.4.1). Moreover, the presence of impurities such as metal salts<sup>4</sup> and temperature<sup>5</sup> affect the measured CMC values. For completeness, the CMC of classical surfactants, specifically SDS 90% (Saarchem) and CTAB 99% (Acros), were also measured using the same method and conditions.

#### 3.4.1: Experimental

Solutions of surfmers (SS & AS) and surfactants (SDS & CTAB) of varying concentrations, ranging from 0 to 0.05 M, were prepared using distilled de-ionized water. The conductivities of the samples were measured using a Cyber Scan CON500 conductivity meter at 22.3°C. The CMCs were determined by extrapolation methods from the graphs of log molar conductivity against concentration.

#### 3.4.2: Results

##### 3.4.2.1: CMC of SDS and SS

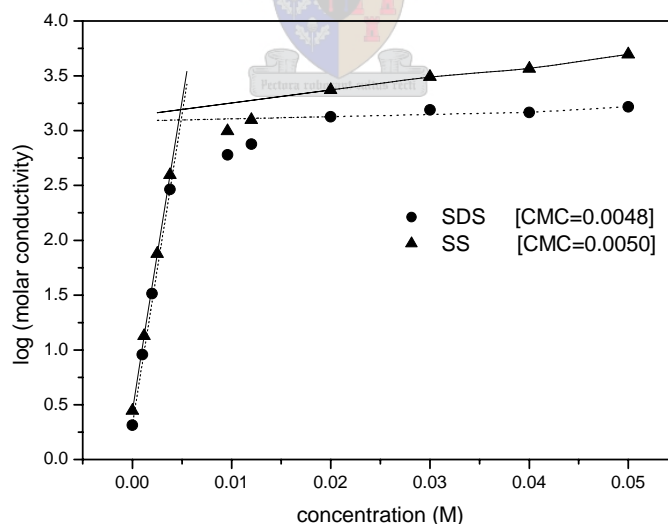
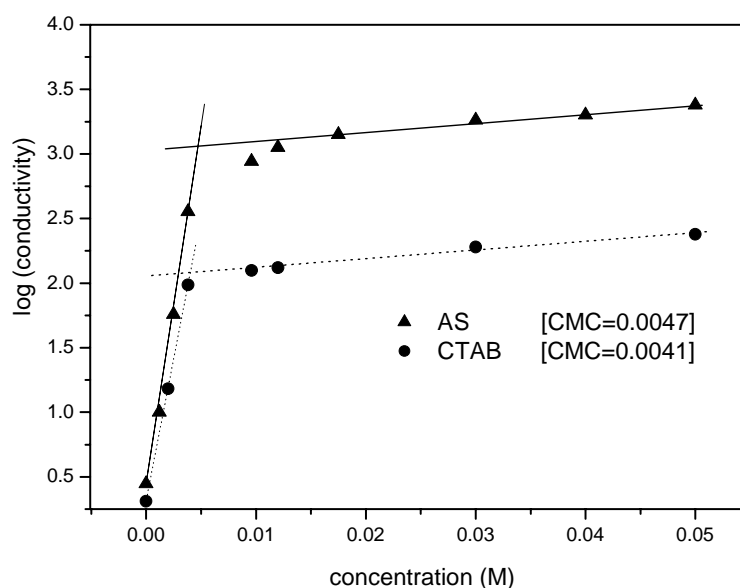


Fig 3.7: A plot of logarithm of conductivity against concentration (M) for the determination of critical micelle concentration of sulfate surfmer (SS) and sodium dodecyl sulfate (SDS)

**3.4.2.2: CMC of CTAB and AS**



**Fig 3.8:** A plot of logarithm of conductivity against concentration (M) for the determination of critical micelle concentration of ammonium surfmer (AS) and CTAB

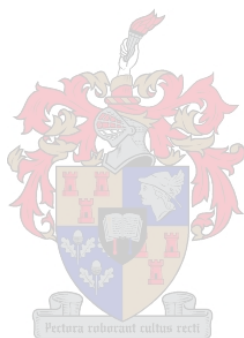
**Table 3.1:** The CMC values of SDS, SS, CTAB and AS, as determined by the conductivity method

Surfmer/ surfactant	CMC (M)
Sodium lauryl sulfate (SDS)	0.0048
Sulfate surfmer (SS)	0.0050
Cetyl trimethylammonium bromide (CTAB)	0.0041
Ammonium surfmer (AM)	0.0047

The literature value given for 91% SDS is 0.004 (tensiometry) and that of 53% SS is 0.007 (tensiometry).<sup>2</sup> The high value of the latter may be attributed to the presence of some inorganic salts in the compound. These inorganic salts originate from the addition of sodium carbonate in order to form the sodium salt of the SS surfmer. In the present study, the precipitation step using inorganic salts was avoided by first precipitating the surfmer using triethylamine and then bringing the pH of the solution to 11 using NaOH solution to precipitate the surfmer. The value of the CMC obtained thus was lower than that recorded in the literature. The CMC of the AS surfmer has not been reported in literature and that of highly pure CTAB is reported as 0.002 M.<sup>6</sup>

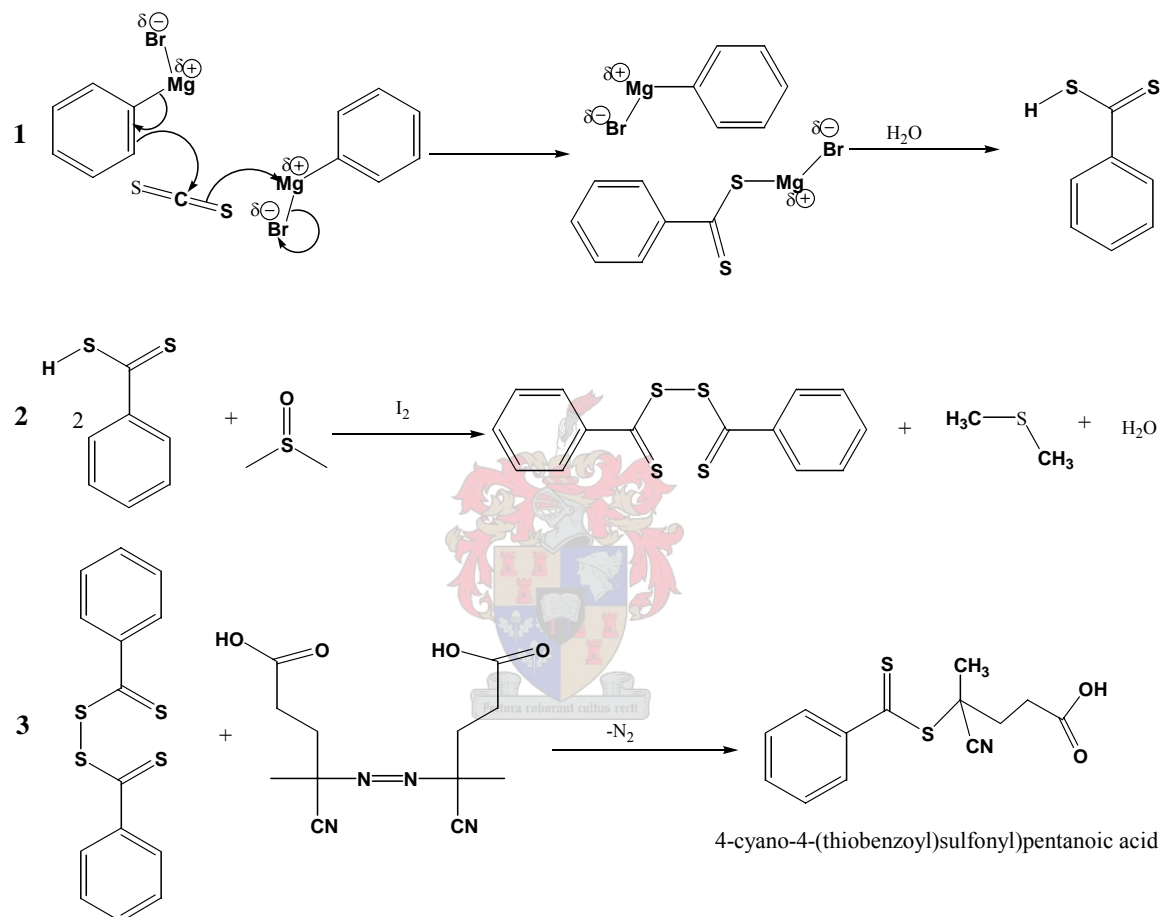
### *Chapter 3: Synthesis of surfmers, the RAFT agent and oligosurfmers*

The table above shows that the CMCs of the surfmers are higher than those of classical surfactants. One of the reasons might be that the hydrophobic tail of surfmers has a degree of solubility in water due to the presence of the ester group at the tail end. This means that more of the surfmer is required to reach CMC.



### 3.5: Synthesis of the RAFT agent 4-cyano-4-(thiobenzoyl) sulfonyl pentanoic acid (CVADTB)

The RAFT agent 4-cyano-4-(thiobenzoyl) sulfonyl pentanoic acid was synthesized by the method of Le *et al.*<sup>7</sup> Thang *et al.*<sup>8</sup> proposed a free radical mechanism for the reaction between the azo compound and the disulfide (Scheme 3.7). Synthesis was carried out according to Scheme 3.7:



**Scheme 3.7: Reaction pathway used for the synthesis of 4-cyano-4-(thiobenzoyl) sulfonyl pentanoic acid**

## **Reagents**

Distilled and dried (molecular sieves) tetrahydrofuran: dried magnesium turnings (98%), Aldrich; iodine (99%), Aldrich; bromo-benzene (99%), Aldrich; carbon disulphide (99.9%), Aldrich; 33% HCl, dimethyl sulfoxide (99.7%), Fluka; ethyl acetate 99%; 4,4' azo-bis-(4-cyanovaleric acid) (75%), Aldrich.

## **3.5.1: Experimental**

### **3.5.1.1: Preparation of the Grignard reagent.**

The reaction was carried out in a 250 ml, 3-necked, round-bottomed flask fitted with two dropping funnels and a condenser fitted with a calcium chloride drying tube. THF (60 g; 0.84 mol) was placed in one dropping funnel while bromobenzene (12.56 g; 0.08 mol) was placed in the other. Magnesium turnings (2 g; 0.08 mol) were placed in a reaction vessel together with a crystal of iodine. A little dry THF was added, enough to cover the magnesium turnings. The bromobenzene was slowly added to the system. The disappearance of iodine colour signified the start of the reaction. All the bromobenzene was then added drop-wise. The reaction temperature was kept below 40°C, using an ice bath. The remainder of the THF was then added and the reaction vessel was left to cool by itself for 30 minutes. The contents were brown in colour.

### **3.5.1.2: Preparation of dithiobenzoic acid**

Carbon disulphide (6.1 g; 0.08 mol) was placed in one of the above mentioned dripping funnels and slowly added to the reaction vessel containing the Grignard reagent. The reaction temperature was kept below 40°C by cooling the reaction vessel in an ice bath. During addition of carbon disulphide, the colour of the reaction changed from brown to red. After the reaction was complete, 20 ml of water was added (until no more heat of reaction was released) to neutralize the Grignard reagent, followed by acidification using approximately 35 ml 33% HCl to give a pink/purple coloured product. The dithiobenzoic acid was extracted from the mixture using diethyl ether and the water phase was washed twice using 50 ml of diethyl ether. The ether extracts were combined and dried using magnesium sulfate, for four hours. The ether layer was decanted and the solvent removed by rotary evaporation, yielding 11.21 g (91% yield) of dithiobenzoic acid

**3.5.1.3: Preparation of bis (thiocarbonyl) disulfide**

A catalytic amount of iodine (two crystals) and excess DMSO (12.50 g; 0.16 mol) were added to the dithiobenzoic acid (12.32 g, 0.079 mol) in 80 ml of absolute ethanol (i.e. twice the molar ratio of DMSO to the dithiobenzoic acid). The excess DMSO favours a rapid reaction. The reaction was carried out for 24 hours at room temperature to yield crystals of bis (thiocarbonyl) disulphide. The reaction vessel was then cooled overnight to allow further crystallization. The crystals were filtered and dried, yielding 10.73 g (89%) crude product. The purity of the product was estimated from <sup>1</sup>H NMR spectroscopy to be 97%. <sup>1</sup>H NMR spectral data (CDCl<sub>3</sub>); δ (ppm) 7.46, m, 4H, H<sub>meta</sub>; δ (ppm) 7.6, 2H, H<sub>para</sub>; δ (ppm) 8.21, 4H, H<sub>ortho</sub>.

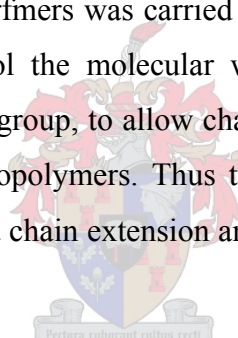
**3.5.1.4: Preparation of the RAFT agent 4-cyano-4-(thiobenzoyl) sulfonyl pentanoic acid**

Bis (thiocarbonyl) disulfide (18.57 g; 0.06 mol) and 4, 4' azo-bis-(4-cyanovaleric acid) (16.96 g; 0.06 mol) were refluxed in ethyl acetate at 85°C for 8 hours, under nitrogen, in a free radical reaction. The solvent was then removed by rotary evaporation and the crude product was purified by column chromatography over silica, using an eluent system comprised of ethyl acetate, hexane and heptane in the ratio 6:2:2. The yield was 13.1 g (78%). <sup>1</sup>H NMR spectroscopy was used to characterize the RAFT agent 4-cyano-4-(thiobenzoyl) sulfonyl pentanoic acid. The percentage purity was estimated to be >94%. The chemical shifts were as follows: <sup>1</sup>H NMR spectroscopy (CDCl<sub>3</sub>) δ (ppm) 1.88 (s, 3H); 2.35 to 2.80 (m, 4H); 7.33 (m, 2H); 7.50 (m, 1H) and 7.83 (m, 2H). The chemical shifts for the product 4-cyano-4-(thiobenzoyl) sulfonyl pentanoic acid were the same as those reported in literature.<sup>8</sup>

## **3.6: Synthesis and characterization of oligosurfmers**

### **3.6.1: General**

In light of recent progress in controlled radical polymerization in miniemulsion and emulsion polymerization stabilized by block<sup>9</sup> and graft copolymers<sup>10</sup>, it seemed likely that oligosurfmers may be successfully applied for controlled radical polymerization in emulsion. Secondary nucleation (refer to Chapter 2, Section 2.3.2.5) in the system is likely to be limited by the fact the oligosurfmers will form the first block of the block copolymer in the emulsion system leaving very little surfactant available in the aqueous phase to support secondary particles. Polymeric surfactants have been used to stabilize polymer latexes.<sup>11</sup> The homopolymers of surfmers are often referred to as polyelectrolytes and they are expected to be water soluble, just like their monomers.<sup>11</sup> In this study, oligosurfmers were used in the miniemulsion polymerization of styrene and MMA. Synthesis of oligosurfmers was carried out in homogenous media using a RAFT agent in order to control the molecular weight. Most of the chains were expected to have the RAFT end group, to allow chain extension during miniemulsion polymerization forming block copolymers. Thus the oligosurfmer would act as the first block for polymerization via chain extension and no secondary particle formation was expected.

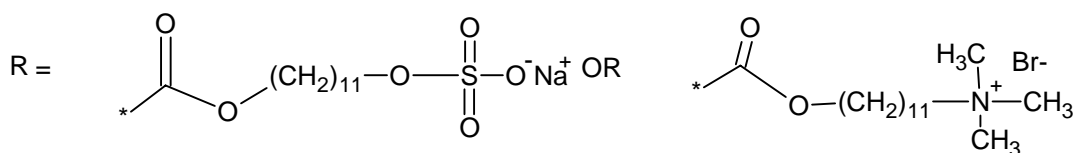
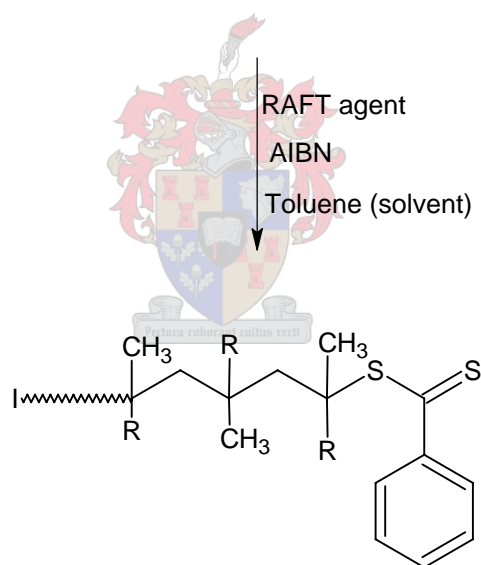
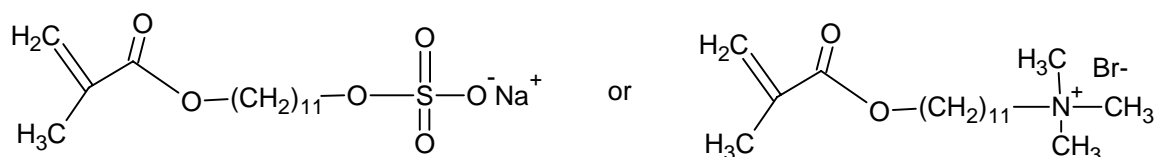


### **3.6.2: Experimental**

The selected surfmer, initiator [ $\alpha$ ,  $\alpha'$  azoisobutyronitrile (AIBN)] and RAFT agent were dissolved in toluene (50 ml). The oil bath was set at 75°C and the reaction was carried out for ten hours under a continuous nitrogen purge. The polymer was precipitated out using diethyl ether and washed 3 times with 30 ml of diethyl ether.

**Table 3.2: Reagents and quantities used for the synthesis of SS and AS oligosurfmers**

	SS oligomer synthesis	AM oligomer synthesis
SS surfmer	2.58 g ( $7.2 \times 10^{-3}$ mol)	-
AM surfmer	-	2.58 g ( $6.8 \times 10^{-3}$ mol)
RAFT agent	0.06 g ( $2.2 \times 10^{-4}$ mol)	0.06 g ( $2.2 \times 10^{-4}$ mol)
Initiator (AIBN)	0.0244 g ( $1.5 \times 10^{-4}$ mol)	0.0244 g ( $1.5 \times 10^{-4}$ mol)



**Scheme 3.8: Synthesis of oligosurfmers in solution**



### 3.6.3: Characterization of oligosurfmers

$^1\text{H}$  NMR spectroscopy was used to follow whether the oligomerization reaction was complete by observing the disappearance of the double bonds of the surfmer. The  $^1\text{H}$  NMR spectra showed that the vinyl protons were no longer present after polymerization of the surfmers SS and AM. However, it could not be determined whether control over the molar mass distribution was achieved. The RAFT moiety could not be observed directly in the  $^1\text{H}$  NMR spectra due to dilution effects. Upon enlarging the spectra, however, peaks due to the aromatic ring of the RAFT moiety were indeed observed, indicating the presence of the RAFT agent in the oligosurfmers. The oligosurfmers retained the pink color of RAFT agent, i.e. after washing and drying.

#### 3.6.3.1: Characterization of SS oligomer (SSO) by $^1\text{H}$ NMR spectroscopy

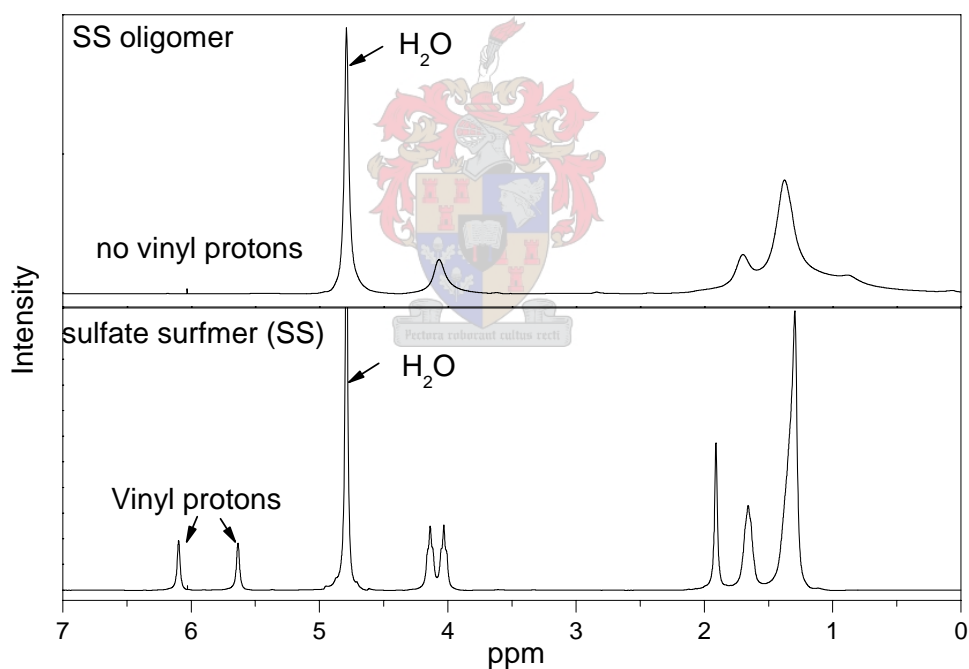
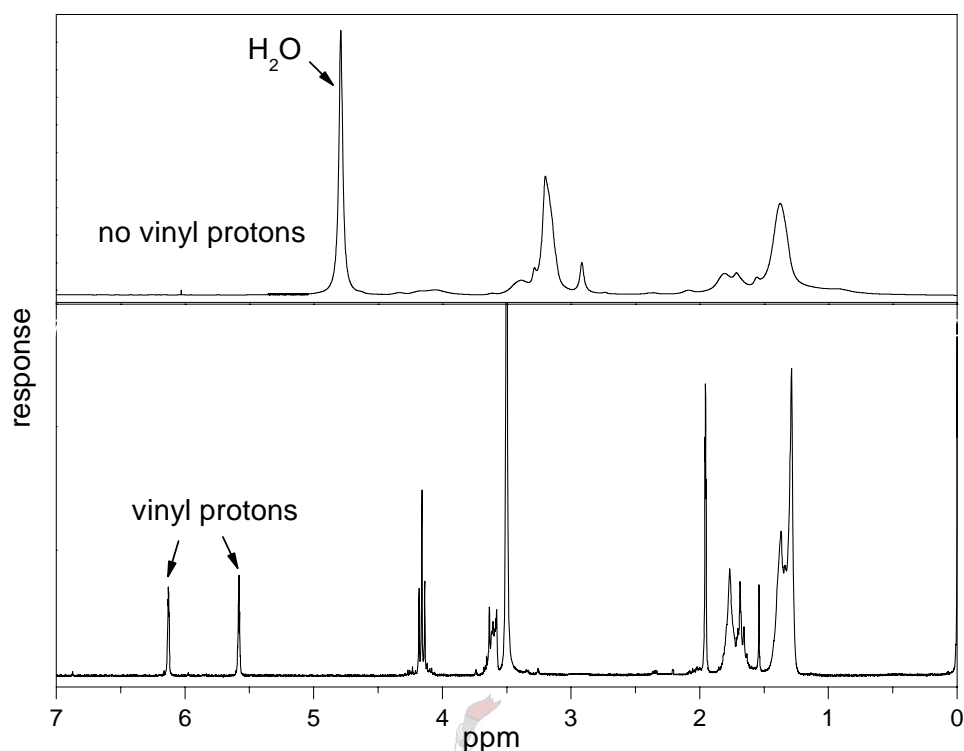


Fig 3.9:  $^1\text{H}$  NMR spectra of SS oligosurfmer and the surfmer, showing the changes after polymerization of the sulfate surfmer ( $\text{D}_2\text{O}$  solvent)

**3.6.3.2: Characterization of AS oligomer (ASO) by  $^1\text{H}$  NMR spectroscopy**



**Fig 3.10:**  $^1\text{H}$  NMR spectra of AS oligosurfmer and the AS surfmer showing the changes after homopolymerization of the ammonium surfmer (Solvents:  $\text{D}_2\text{O}$  [ASO],  $(\text{CD}_3)_2\text{SO}$  [AS])

The proton NMR spectra of the oligosurfmers (Figs 3.10 and 3.11) showed that the surfmers could be polymerized to form the oligosurfmers. These oligosurfmers are polyelectrolytes due to the ionic charges originating from the surfactant moiety. Like all polyelectrolytes, these oligosurfmers dissolve in polar solvents, mainly water, and they emulsify. However the degree of polymerization could not be evaluated from molecular weight determination techniques as the oligomers required aqueous GPC conditions. This facility was unavailable.

**3.6.3.3: Characterization of oligosurfmers (SSO & ASO) by UV spectroscopy**

UV spectroscopy is a method that is used to determine the absorption wavelength ( $\lambda_{\max}$ ) of UV-absorbing species. In this work, the oligosurfmers were expected to absorb at 320 nm, where the RAFT agent absorbs. The UV spectra of the oligosurfmers, surfmers and the RAFT agent are presented in Figs 3.11 and 3.12.

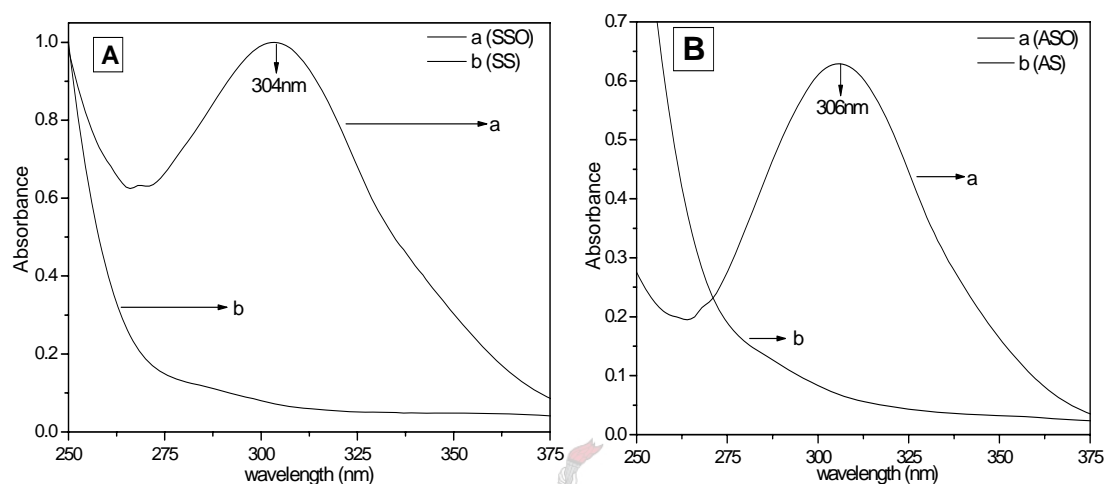


**Fig 3.11: UV/VIS spectra: (A) sulfate oligomer (SSO) and sulfate surfmer (SS); (B) ammonium oligomer (ASO) and ammonium surfmer (AS) [Water was used as solvent (UV-cutoff 180 nm)]**

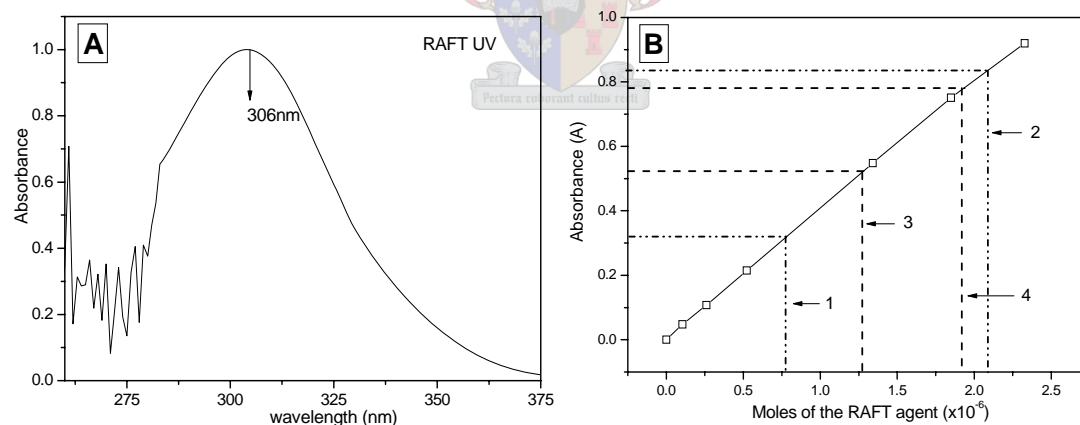


**Fig 3.12: (A) UV/VIS spectra of the RAFT agent [Toluene was used as solvent (UV-cutoff 285 nm)] and (B) calibration curve for the determination of  $M_n$  of oligosurfmers. [The dotted lines (labeled 1 to 4) are extrapolation lines (see Table 3.3)]**

UV-analysis of the oligosurfmers (Figs 3.11A & B) showed that the oligosurfmers were RAFT terminated, as they showed a strong absorption peak in the region where the RAFT agent absorbs (Fig 3.12 A). The strong absorption peak was absent in the surfmers, thus only the oligomers had the RAFT end group.

A calibration curve was used to determine the equivalent amount of the RAFT moieties in the oligosurfmers. Various concentrations of the RAFT agent were prepared and their UV absorptions measured. A plot of absorbance versus amount, in moles, of the RAFT agent was constructed (Fig 4.12 B). Two samples of different known masses per each oligosurfmer were dissolved in water and their absorbencies were measured. The corresponding equivalent amount of RAFT agent in the oligosurfmers was determined from the calibration curve and averaged (see Table 3.3).

**Table 3.3: UV data for the determination of the  $M_n$  of the oligosurfmers as well as the predicted  $M_n$  (from equation 3.1)**

Sample number (see Fig 3.12B)	Oligomer	Mass of oligomer	Absorbance	Equivalent Amount of RAFT $\text{mol} \times 10^{-6}$	Experimental $M_n$	Average $M_n$	Theoretical $M_n$
1	SSO	0.006	0.320	0.774	7750	7580	12000
2	SSO	0.016	0.836	2.088	7400		
3	ASO	0.012	0.523	1.272	9040	9170	12000
4	ASO	0.020	0.781	1.929	9290		

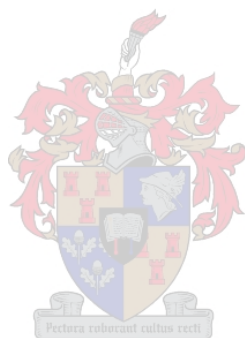
The predicted  $M_n$  was calculated using the Equation below:

$$\overline{M}_{n,theory} = \frac{X * [\text{monomer}] * M_{W_{monomer}}}{[\text{RAFT}]} + M_{W_{RAFT}} \quad 3.1$$

where  $\overline{M}_{n,theory}$  is the theoretical number average molecular weight,  $X$  is the % conversion,  $[\text{monomer}]$  is the number of moles of monomer consumed,  $[\text{RAFT}]$  is the number of moles of the RAFT agent used,  $M_{W_{monomer}}$  and  $M_{W_{RAFT}}$  are the molecular weights of the monomer and RAFT agent respectively. The assumption, for the calculation of theoretical  $M_n$ , was that the conversion of the surfmer was 100% and initiator derived chains were not taken into consideration. The experimental  $M_n$  were lower than the theoretical  $M_n$  values in both cases (i.e. SS and AS oligomers). The assumption, for the calculation of experimental  $M_n$ , was that all the chains have the

### Chapter 3: Synthesis of surfmers, the RAFT agent and oligosurfmers

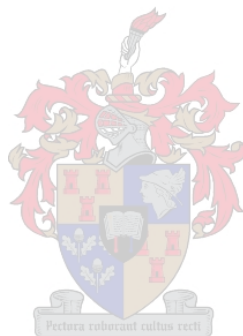
RAFT end-group. If some of the chains do not have the RAFT end-group, the results presented are an overestimation. The lower experimental  $M_n$  values can also be attributed to the fact that the initiator derived chains that terminate were not accounted for during calculation. It has been observed in RAFT reactions that, at high monomer conversion (where there is little conversion of monomer), the  $M_n$  does not increase linearly with conversion but decreases due to the contribution of chains originating from initiator decomposition.<sup>12</sup>



### **3.7: Conclusions**

The polymerizable surfactants (SS and AS) were successfully prepared and polymerized by the RAFT process. This was confirmed by the characterization techniques used. The purity of the compounds was checked by NMR (and ES/MS for surfmers) and the levels of impurities were low in all the synthesized compounds. ES/MS showed that the ammonium surfmer had relatively more impurities than the sulfate surfmer. UV analysis of the oligosurfmers showed that the oligosurfmers have the terminal RAFT moiety. Furthermore, the experimental  $M_n$  values obtained by the UV method were lower than the theoretical  $M_n$  values.

Further characterization of the oligosurfmers is required to determine the molar mass and molar mass distribution so as to ascertain whether the RAFT process was indeed effective in controlling the molar mass of these surface active monomers.



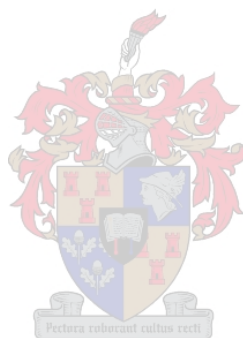
### **3.8: References**

- (1) Guyot, A.; Graillat, C.; Favero, C. *C.R Chimie* 2003, 6, 1319-1327.
- (2) Unzue, M. J.; Schoonbrood, H. A. S.; Asua, J. M.; Gon, A. M.; Sherrington, D. C.; Stahler, K.; Goebel, K.; Tauer, K.; Sjoberg, M.; Holmberg, K. *Journal of Applied Polymer Science* 1997, 66, 1803–1820.
- (3) Joynes, D.; Sherrington, D. C. *Polymer* 1996, 37, 1453-1462.
- (4) Tominaga, T.; Nishinaka, M. *Journal of Molecular liquids* 1995, 65/66, 333-334.
- (5) Zielinski, R.; Ikeda, S.; Nomura, H.; Kato, S. *Journal of Colloid and Interface Science* 1989, 129, 175-184.
- (6) Firouzabadi, H.; Iran, N. *Green Chemistry* 2001, 3, 131-132.
- (7) Le, T. P.; Moad, G.; Rizzardo, E.; Thang, S. H. *PCT Int Appl wo98/01478*, 1998.
- (8) Thang, S. H.; Chong, Y. K. B.; Mayadunne, R. T. A.; Moad, G.; Rizzardo, E. *Tetrahedron Letters* 1999, 40, 2435-2438.
- (9) Lim, M.-S.; Chen, H. *Journal of Polymer Science: Part A: Polymer Chemistry* 2000, 38, 1818-1827.
- (10) Esquena, J.; Dominguez, F. J.; Solants, C.; Levecke, B.; Booten, K.; Tadros, T. F. *Langmuir* 2003, 19, 10463-10647.
- (11) Guyot, A.; Tauer, K. In *Reactions and synthesis in surfactant systems*; J, T., Ed.; Marcel Dekker: New York, 2001; pp 547-575.
- (12) Tsavalas, J. G.; Schork, F. J.; Brouwer, H.; Monteiro, M. J. *Macromolecules* 2001, 34, 3938-3946.
- (10) Tsavalas, J. G.; Schork, F. J.; Brouwer, H.; Monteiro, M. J. *Macromolecules* 2001, 34, 3938-3946
- (11) Tominaga, T; Nishinaka, M. *Journal of Molecular liquids* 1995, 65/66, 333-334
- (12) Zielinski, R.; Ikeda, S.; Nomura, H.; Kato, S. *Journal of Colloid and Interface Science* 1989, 129, 175-184

## **Chapter 4: RAFT mediated miniemulsion polymerization of styrene and MMA**

### **Abstract**

A comparative study of surfmer stabilized and classical surfactant stabilized RAFT miniemulsion polymerization reactions is presented. The efficiency of surfmers in terms of rates of reaction and their effect on particle size is evaluated. The effect of the emulsifier head-group in terms of the type of monomer and emulsifier type is also evaluated. The effect, in terms of rates, molecular and molecular weight distribution, of using oligosurfmers as emulsifiers in RAFT mediated miniemulsion polymerization reaction is also addressed.





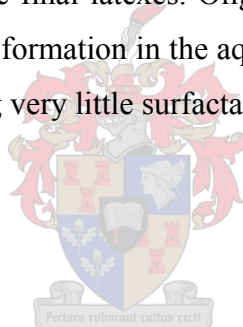
### 4.1: Introduction

Surfmers were used as emulsifiers in RAFT miniemulsion polymerization with an aim of comparing the resultant reaction rates, molar mass distributions, and latex particle sizes to those obtained using classical surfactants. A focus point in free radical polymerization is to be able to control the molar mass distribution in aqueous dispersed polymerizations, achieved by using transfer agents. RAFT agents have been successfully used in miniemulsion when classical surfactants were used as emulsifiers.<sup>1-4</sup> When surfmers are used as emulsifiers in either emulsion or miniemulsion, they are expected to copolymerize with the main monomer (styrene and MMA in this study) so that they become grafted at the particle surface through chemical bonding.<sup>5-10</sup> The surfmer moiety on the surface of the particle is partitioned between the particle surface and the water phase. Oligosurfmers were used in RAFT miniemulsion polymerization in order to investigate their influence on rates of reaction, molar mass distributions and particle sizes of the final latexes. Oligosurfmers terminated with a transfer agent may reduce secondary particle formation in the aqueous phase because they can act as a center for particle nucleation, leaving very little surfactant to support secondary particles.<sup>11</sup>

### 4.2: Experimental

#### 4.2.1: Reagents

In all miniemulsion polymerization reactions, the monomers were first washed with 0.3 M KOH to remove stabilizers/inhibitors and then distilled under reduced pressure. They were kept under refrigeration for later use. The water used in all reactions was distilled de-ionized water. The chemicals: 90% sodium lauryl sulfate (SDS), Aldrich Chemicals; 99% n-hexadecane, ACROS; azo bis(isobutyronitrile) (AIBN), Riedel de Haen; and 99% cetyl trimethylammonium bromide (CTAB), ACROS; were used as received. The sulfate surfmer (SS) and sulfate oligosurfmer (SSO), ammonium surfmer (AS) and ammonium oligosurfmer (ASO) were synthesized as described in Chapter 3.



### 4.2.2: Analysis

Molecular weights were determined using Size Exclusion Chromatography (SEC). The SEC instrument consisted of a Waters 717plus Auto-sampler, Waters 600E System Controller (run by Millennium<sup>32</sup> V3.05 software) and a Waters 610 fluid unit. A Waters 410 differential refractometer was used at 35°C as detector. Tetrahydrofuran (THF, HPLC grade) sparged with IR-grade helium was used as eluent at a flow rate of 1 mL. min<sup>-1</sup>. The column oven was kept at 30°C and the injection volume was 100  $\mu$ m. Two PLgel 5  $\mu$ m Mixed-C columns and a pre-column (PLgel 5  $\mu$ m Guard) were used. Calibration was done using narrow polystyrene standards ranging from 800 to 2x10<sup>6</sup> g.mol<sup>-1</sup>. All molecular masses were reported as polystyrene equivalents.

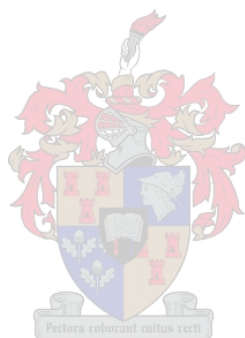
### 4.2.3: General procedure

Two phases were prepared separately i.e. the oil phase and the water phase; the oil phase was prepared by dissolving the RAFT agent (CVADTB), (0.125 g; 4.48x10<sup>-4</sup> mol), AIBN (0.051 g; 1.78x10<sup>-4</sup> mol), n-hexadecane (0.433 g; 1.90x10<sup>-3</sup> mol) in 10.054 g of monomer styrene in a 250 ml Erlenmeyer flask and stirring using a magnetic stirrer until all the chemicals had dissolved. The water phase was prepared by dissolving the surfactant/oligosurfmer of interest in a 250 ml long form beaker using distilled de-ionized water (40.12 g). The latter phase was stirred using a magnetic stirrer until all the surfactant/surfmer has dissolved. The oil phase was then gradually poured into the beaker containing the water phase whilst stirring. Stirring was continued for one hour to form a pre-emulsion. The pre-emulsion was then sonicated for 10 minutes in a water-jacketed vessel to minimize heating of the pre-emulsion. A minimum of heating is required to prevent the initiator from decomposing, i.e. preventing premature polymerization. The temperature cut off was set at 50°C and the amplitude was set at 80%. The sonicator was a sonics Vibra Cell Autotune Series high intensity ultrasonic processor 750VCX. The average energy was 95 KJ.

*(N.B: The masses given above are for the reaction labeled 1 and serve as an example of the recipe used in all the miniemulsion polymerization reactions,)*

#### **4.2.4: Polymerization**

The resulting miniemulsions were polymerized in 250 ml three-necked, round-bottomed flask, fitted with a condenser, stopper and a gas-inlet valve. Nitrogen gas was passed through the pre-emulsions for 5 minutes to remove oxygen before heating the reaction vessel to the reaction temperature. All reactions were conducted under nitrogen gas and samples were withdrawn at specific time intervals via a septum, until the reaction reached its final conversion. Conversions were calculated gravimetrically.



### 4.3: RAFT mediated miniemulsion polymerization of styrene

**Table 4.1: The quantities of reagents and reaction temperature used in the miniemulsion polymerizations of styrene**

Reaction	Surfactant	Temperature (°C)	Surfactant (moles x 10 <sup>-3</sup> )	DDI water (moles)	AIBN (moles x10 <sup>-3</sup> )	RAFT (moles x10 <sup>-4</sup> )	n-hexadecane (moles x10 <sup>-3</sup> )	Styrene (moles x10 <sup>-2</sup> )
1	SDS	85	3.471	2.229	3.124	4.495	1.919	9.645
2	SDS	75	3.512	2.222	3.100	4.484	1.909	9.597
3	CTAB	85	3.457	2.223	3.215	4.509	1.900	9.626
4	CTAB	75	3.468	2.224	3.154	4.498	1.910	9.635
5	SS	85	3.465	2.234	3.142	4.487	1.941	9.626
6	SS	75	3.481	2.223	3.100	4.513	1.917	9.607
7	AS	85	3.451	2.239	3.118	4.495	1.899	9.702
8	AS	75	3.440	2.224	3.179	4.498	1.905	9.655

#### 4.3.1: SDS and CTAB in RAFT mediated miniemulsion polymerization of styrene

Classical surfactants SDS and CTAB were used in control (reference) reactions in the RAFT mediated miniemulsion polymerization of styrene and MMA. According to literature, the effectiveness of the two classical surfactants SDS and CTAB in the miniemulsion polymerization of styrene is similar in terms of rates of reaction as well as final latex particle size.<sup>12,14</sup>

### 4.3.1.1: Rates of reactions

The rate of reaction was similar in both SDS and CTAB stabilized miniemulsions (Fig 4.1) at the two reaction temperatures (85 & 75°C) employed.

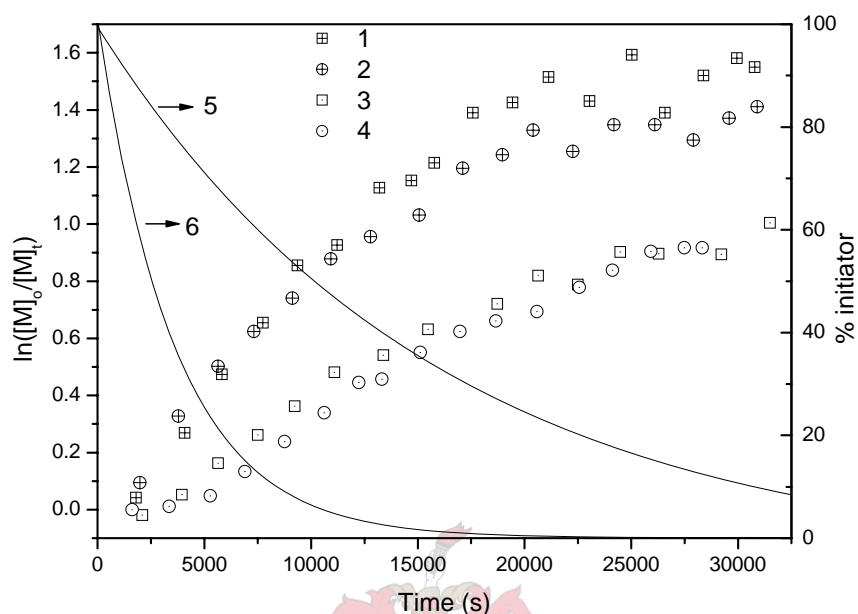


**Fig 4.1: 1st order rate kinetics for SDS and CTAB stabilized miniemulsion polymerization of styrene: 1 = SDS (85°C); 2 = CTAB (85°C); 3 = SDS (75°C); 4 = CTAB (75°C); 5 and 6 are initiator decay curves at 75°C and 85°C respectively**

The rate of reactions could be varied by increasing the surfactant concentration, which results in much smaller monomer droplets, hence faster rates of reaction.<sup>14</sup> The efficiency of stabilization depended largely on the properties of the surfactant.<sup>20</sup> It will however be seen later in this work that efficiency also depends on the type of monomer used.

4.3.1.2: Molecular weight distributions as determined by SEC

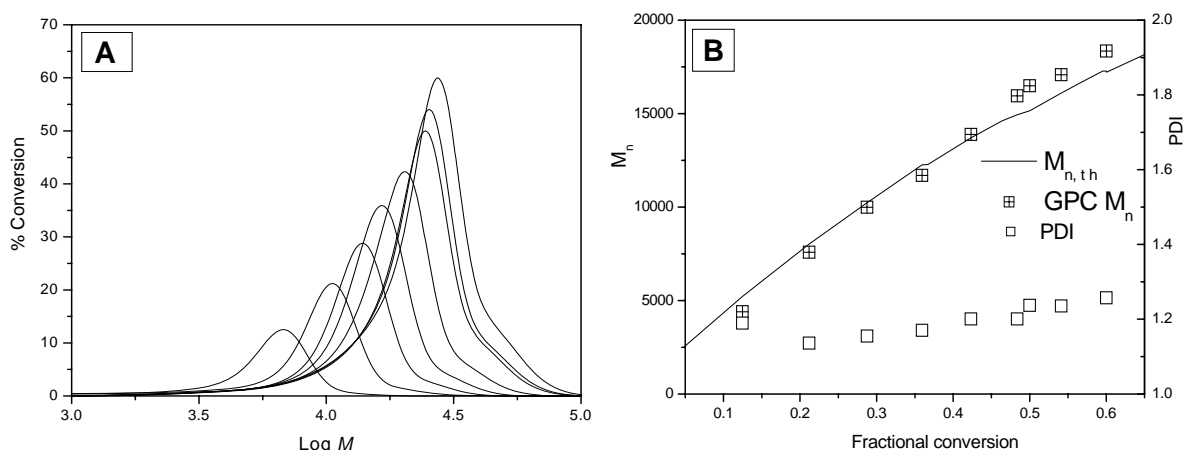


Fig 4.2: SDS stabilized RAFT mediated miniemulsion polymerization of styrene (reaction 2): A = molecular weight distribution for SDS stabilized reaction at 75°C and B = evolution of  $M_n$  and PDI for RAFT mediated miniemulsion polymerizations of styrene at 75°C

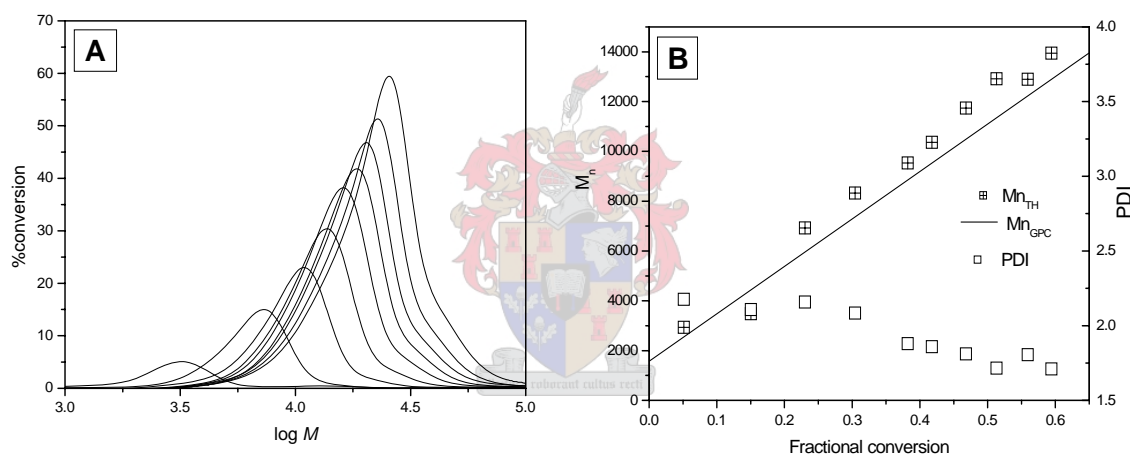


Fig 4.3: CTAB stabilized RAFT mediated miniemulsion polymerization of styrene (reaction 4): A = molecular weight distribution for CTAB stabilized reaction at 75°C and B = evolution of  $M_n$  and PDI for RAFT mediated miniemulsion polymerizations of styrene at 75°

The molecular weight increased with conversion (Figs 4.2A and 4.3A, reactions 2 and 4 respectively) showing that the polymerization reactions were controlled, as expected for a living/controlled system. The molecular weight distribution showed a shoulder at high molecular weight, possibly because styrene propagating radicals normally undergo termination by coupling.<sup>13</sup> Termination by coupling leads mostly to higher molecular weight polymer chains. The polydispersities for the SDS stabilized RAFT miniemulsion polymerizations of styrene (Fig 4.2B) increased slightly with conversion. This was attributed to termination of the growing chains in the system resulting in an increase in polydispersity

with conversion. Theoretically, in RAFT living systems, polydispersity should decrease with conversion ending close to unity upon full conversion if termination is negligible (i.e., if the number of initiator derived chains is small compared to the number of dormant chains).<sup>29</sup> However, Fig 4.3B (CTAB stabilized miniemulsion) shows a decrease in polydispersity with conversion. Aqueous phase polymerization results in high polydispersities since there is likely to be no control in the aqueous phase. The reduction in polydispersity could be due to the fact that as the monomer in the aqueous phase gets depleted, there was a reduction in the rate of uncontrolled polymerization. Hence polydispersity was expected to decrease with conversion because polymerization would be solely via a controlled mechanism. The polydispersity of the CTAB stabilized miniemulsion is above 1.5 whereas that of the SDS stabilized miniemulsion is below 1.2. The high polydispersity in CTAB could be attributed to poor emulsification, resulting in homogeneous nucleation, which resulted in high polydispersity polymers. Homogeneous nucleation also leads to high polydispersities. Figs 4.2B and 4.3B show that the experimental and theoretical  $M_n$  values are similar at lower conversion although at higher conversion there is some deviation. The theoretical/predicted  $M_n$  was calculated using Equation 2.15 (Chapter 2). An increase in  $M_n$  with conversion showed that there was control over molar mass during the entire reaction.<sup>14</sup> The higher values of experimental  $M_n$  at higher conversion could be due to underestimation of the theoretical  $M_n$ .<sup>15</sup> In theory, the initiator derived chains would cause the theoretical  $M_n$  to decrease from linearity at higher conversion. The theoretical  $M_n$  curves shown in Figs 4.2B and 4.3B indicate this behavior but the SEC  $M_n$  does not follow the behavior. Thus, it is concluded that the initiator derived chains were not significantly affecting detected chain populations in the reactions, leading to a linear increase in GPC even at high conversions

**4.3.2: SS and AS in RAFT miniemulsion polymerization of styrene**

Fig 4.4 compares the rates of reaction in surfmer stabilized RAFT mediated miniemulsion polymerizations of styrene.

**4.3.2.1: Rates of reaction in styrene polymerization**

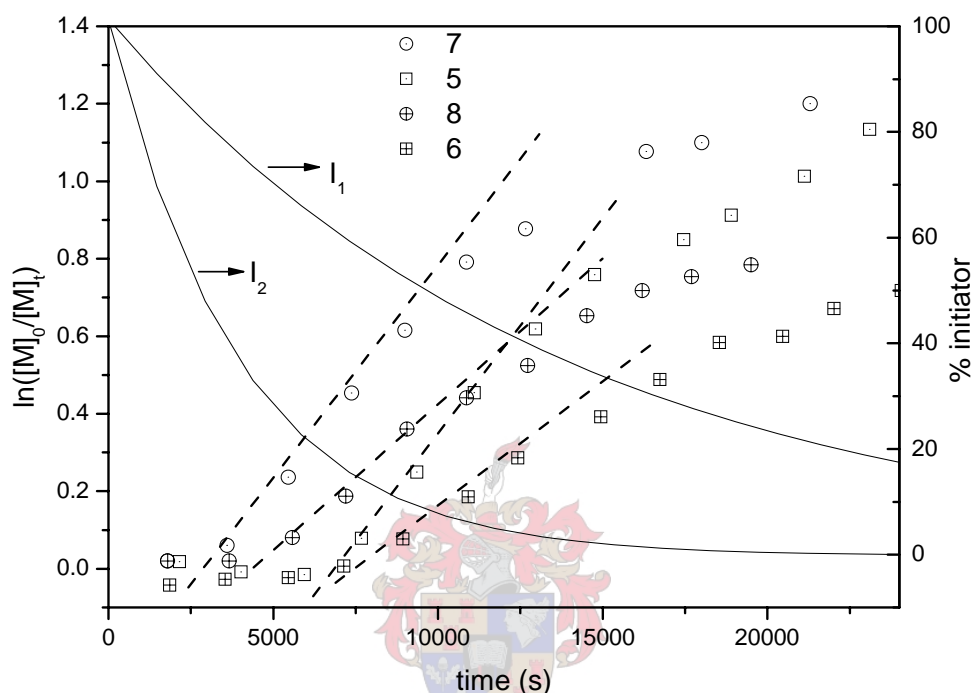


**Fig 4.4:** 1st order rate kinetics for SS and AS stabilized miniemulsion polymerization of styrene: 7 = AS (85°C); 5 = SS (85°C); 8 = AS (75°C); 6 = SS (75°C). I<sub>1</sub> and I<sub>2</sub> are initiator decay curves at 75°C and 85°C, respectively. [The dotted lines on the rate curves are a guide to the eye]

The rates of reaction were similar for both the AS and SS stabilized miniemulsion polymerization of styrene. By examining the graphs of reactions conducted at the same temperatures, it is seen that the rate curves were approximately parallel, i.e. the reaction curves labeled 7&8 are parallel as are 5&6. The rate of reaction is given by the gradient of the curve; it is similar for complementary reactions. The SS stabilized miniemulsion polymerization reactions were characterized by longer inductive effects, which might be due to some residual inhibitors in the SS surfmer. In the synthesis of sulfate surfmer, a substantial amount of inhibitor was added in the reaction that was carried out at 100°C (see Section 3.1.1.2) and this may have resulted in SS having more residual inhibitor than AS. This was observed in the kinetic rate plots



### 4.3.2.2: Surfmer conversion in RAFT miniemulsion polymerization

The consumption of surfmers during miniemulsion polymerization was followed by  $^1\text{H}$  NMR spectroscopy.

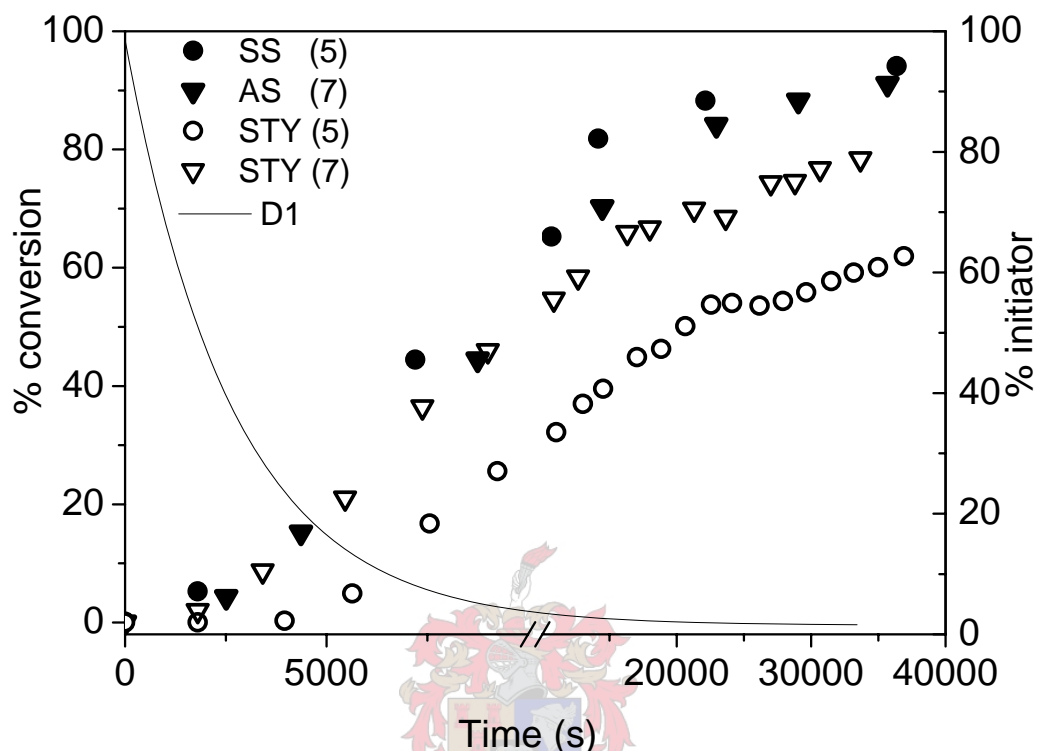


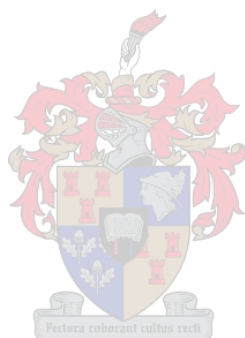
Fig 4.5: Conversion time graphs of SS & styrene (reaction 5, 85°C) and AS & styrene (reaction 7, 85°C) in RAFT miniemulsion polymerization of styrene. The solid line ( $I_2$ ) is the initiator decay curve at 85°C

The surfmer conversion curves above showed that after about four hours of reaction most of the surfmer had reacted. Fig 4.5 shows that the SS and AS surfmers had similar rates of reaction. This could be due to the fact that the two surfmers are both derived from methacrylic monomer and hence are likely to have the same  $k_p$  values. Typical  $k_p$  values (at 50°C) for methacrylates, for example methyl, ethyl and n-butyl methacrylate, are 649, 723, and 794  $\text{L}\cdot\text{mol}^{-1}\cdot\text{s}^{-1}$ .<sup>30</sup> The SS stabilized RAFT mediated miniemulsion polymerization reactions in Figure 4.5 (reactions 5) show a longer period in which the styrene was not consumed, potentially due to the preferential polymerization of the SS monomer. The preferential polymerization of the SS in styrene polymerization may lead to formation of polysurfmers in

## ***Chapter 4: RAFT mediated miniemulsion polymerization***

---

the aqueous phase and the droplet/particle stabilization mechanism is likely to deviate from that of classical surfactant to that of polymeric surfactants.



**4.3.2.3: Molecular weight distribution in RAFT mediated miniemulsion polymerization of styrene**

The SEC curves in Figs 4.5 A through D show the difference between the AS and SS stabilized miniemulsion polymers in terms of the molecular weight distributions.

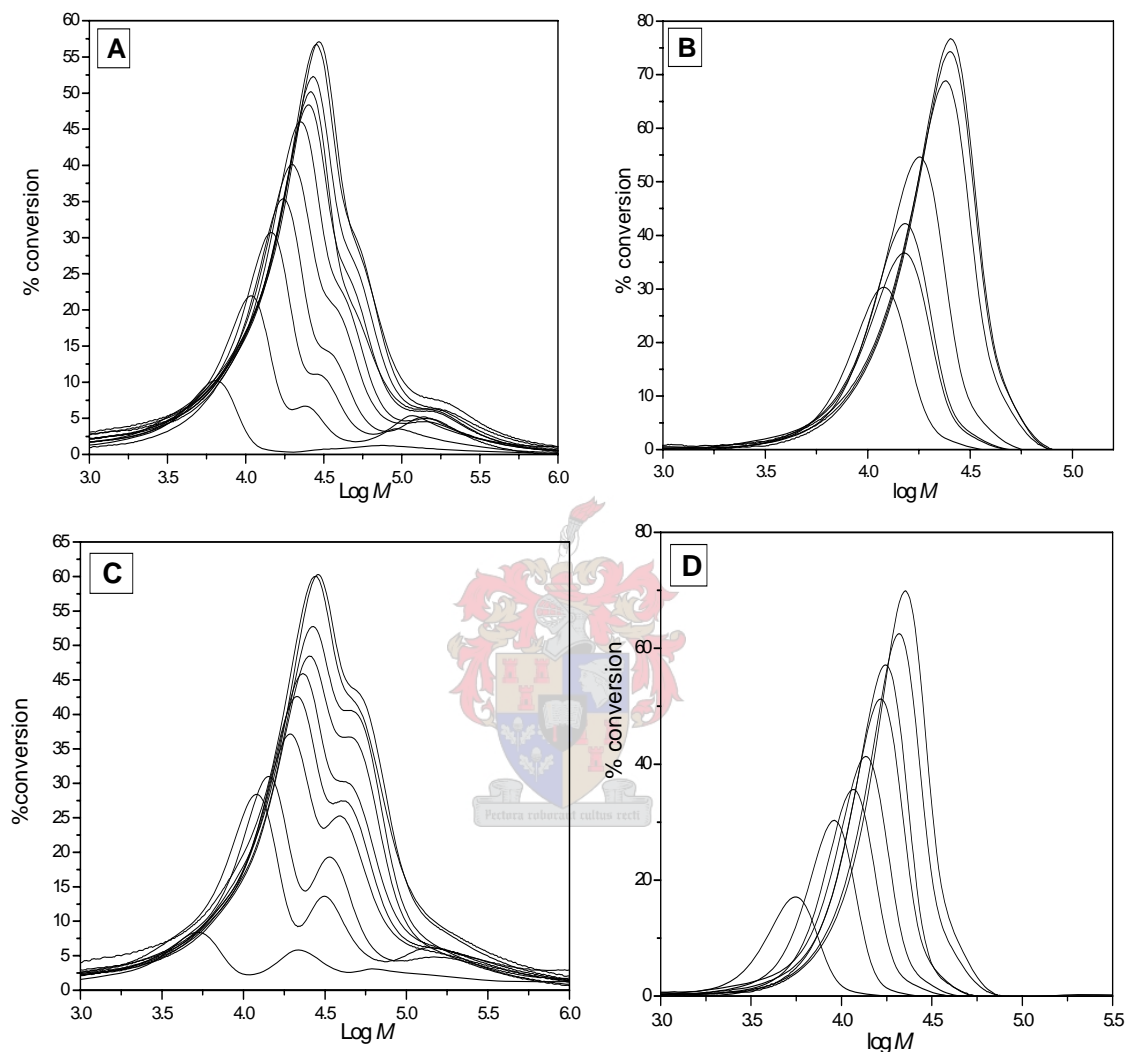


**Fig 4.6: Molecular weight distributions for SS and AS surfmer stabilized RAFT miniemulsion polymerization of styrene: A = SS at 85°C; B = AS at 85°C; C = SS at 75°C and D = AS at 75°C**

In all the curves the molecular weight increased with conversion, indicating that the reactions were controlled. However, the molecular weight distributions for SS stabilized RAFT miniemulsion polymerization of styrene show a tri-modal distribution for both the reactions carried out at 85°C and 75°C. On the other hand, the molecular weight distributions for AS stabilized RAFT miniemulsion polymerizations show a unimodal distribution for the two reactions carried out at 85°C and 75°C. Although the overall reaction kinetics appear similar, the mechanism of polymerization in these systems might be different. The explanation is not

simple as there is need for further characterization of the polymers in order to draw solid conclusions. (This characterization will be discussed later in the Chapter). Explanations can be based on reactivity ratios, solubility and partitioning of the surfmer between the oil and water phases. The mechanism of nucleation is also very important. Guyot *et al* found that the solubility of maleic anhydride derived surfmers in the aqueous phase was high compared to that of most conventional surfactants and it is likely that these surfmers promote aqueous phase polymerization.<sup>7</sup> However, the molecular weight distributions in Figure 3B suggest three different growing radical populations which could indicate that polymer particles were formed via different nucleation mechanisms as well as containing polymer with different comonomer (SS) content.

### **4.3.2.4: UV-RI analysis of the SS reaction at 85°C**

The presence of RAFT end groups can be examined using dual detectors for SEC. UV and RI detectors were used to determine whether the polymer chains have the RAFT end group. The UV detector was set at 320 nm as the dithioester of the RAFT agent absorbs strongly at this wavelength (see Chapter 3, Section 3.6.3.3) The UV detector is sensitive to chains with the RAFT end group and the RI is a mass sensitive detector (every chain is detected). Overlay comparisons of the two signals can tell whether all the chains have the RAFT terminal moiety or whether some of the chains do not have the RAFT end group. One of the factors affecting the UV signal is the dilution effect due to an increase in molecular weight, which results in a weaker signal at high molecular weight. At lower molecular weight the UV signal observed is very strong due to the fact that the chains are much smaller, resulting in a high concentration of RAFT agent per mass of chain.

In Fig 4.6 A through D the UV-RI overlays show that not all the chains have the terminal RAFT moiety. Explanations can include the possibility that two mechanisms of nucleation are occurring, namely homogenous and droplet nucleation. It is possible that there is a substantial amount of free SS (compared to the case of SDS, CTAB and AS) in the aqueous phase of a miniemulsion stabilized by the respective emulsifiers, resulting in homogeneous nucleation in SS stabilized miniemulsion polymerization.

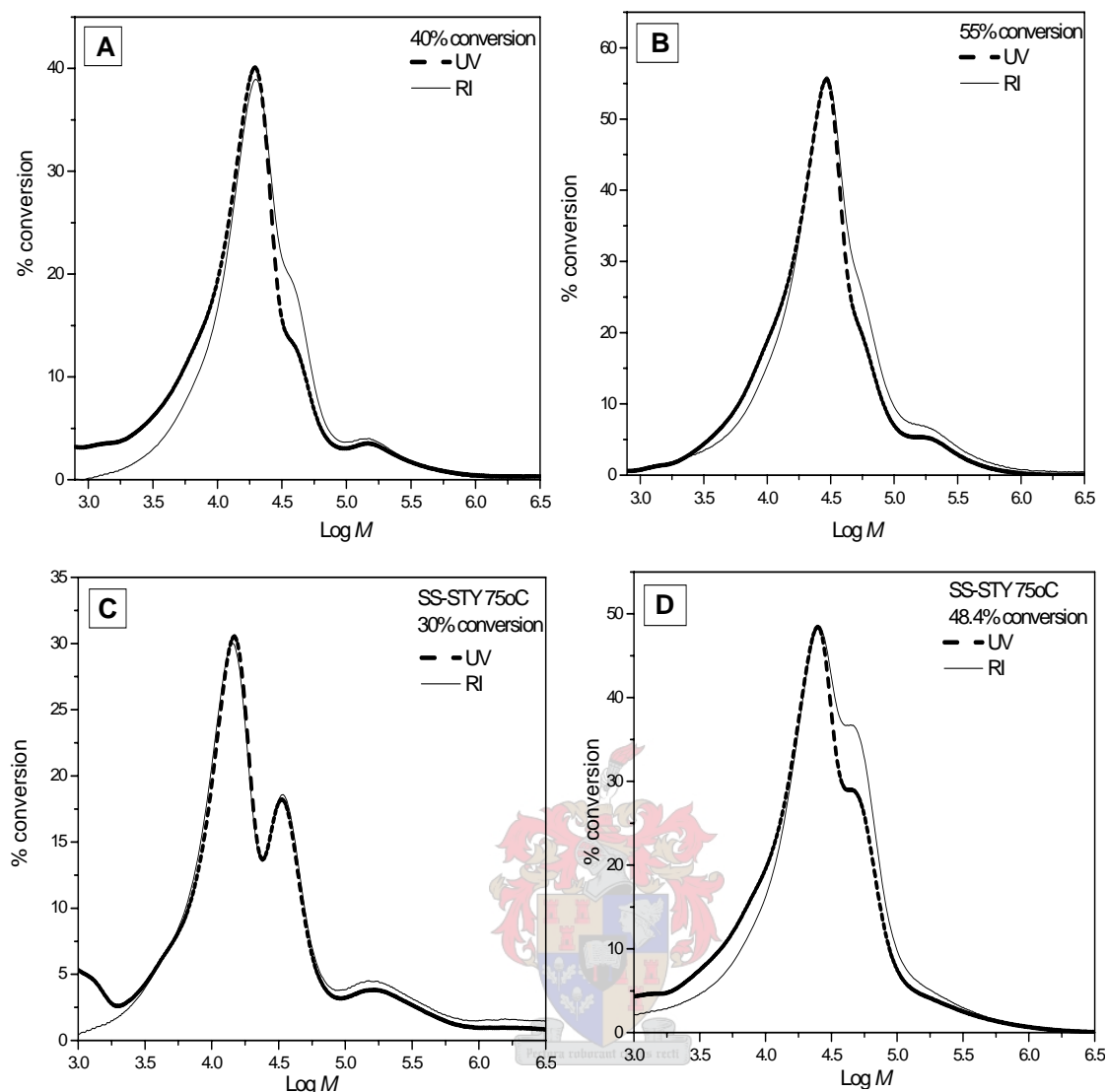


**Fig 4.7: UV-RI overlays: A, B and C, D are for the SS stabilized RAFT mediated miniemulsion polymerization of styrene at 85°C and 75°C respectively**

The solubility of SDS is 0.1M at 20°C<sup>24</sup> and that of CTAB is 0.008 M.<sup>25</sup> This means that the sulfate head group lends the long chain hydrocarbon more water solubility than the ammonium head group. The sulfate head group can be more easily hydrated than the ammonium head group because it is more polar and has a high charge density. Therefore we expect the solubility of SS to be higher than that of AS (sulfate head group versus ammonium head group), hence more aqueous phase polymerization could probably occur in SS stabilized miniemulsion polymerization than in AS stabilized miniemulsion polymerization. Polymer chains formed in the aqueous phase are likely to be less controlled because of the limited solubility of the RAFT agent in the aqueous phase.<sup>5</sup> The presence of SS and lack of control in the aqueous phase may result in homopolymerization of the SS and formation of high molecular weight polymer in the aqueous phase, respectively. Thus the higher distribution in

## Chapter 4: RAFT mediated miniemulsion polymerization

the molecular weight distribution curves (Fig 4.6) may be attributed to homopolymerization of SS and uncontrolled polymerization of styrene occurring in the aqueous phase. The middle molecular weight distribution could probably be due to random copolymers whereas the lower distribution could be due to homopolystyrene. There is a noticeable difference between the reactions carried out at 85°C and 75°C. At 75°C the rate of reaction is very slow and it is expected that both homogeneous and droplet nucleation should be affected. However, the middle distribution seems to be very prominent at 75°C and this can be explained in terms of the reactivity of the methacrylate group of the surfmer which is very reactive.<sup>8</sup>

In Fig 4.7 the UV-RI overlays for the AS mediated polymerizations are presented and it is clear that they match closely. This means that most of the chains have the terminal RAFT moiety. In contrast to the SS stabilized polymers, the AS stabilized miniemulsions behaved in a similar fashion to those stabilized by a classical surfactant i.e. a single molecular weight distribution was observed.

The difference between AS and SS can be explained in terms of the amount of free surfmer in the aqueous phase. Due to the high CMC of SS (see Chapter 3, Section 3.4.2), it is most probable that it is more water soluble than AS. The solubility suggests that the aqueous phase concentration of SS is much higher and that there is substantial free SS in the aqueous phase to support secondary particle formation and/or formation of SS homopolymer (polysurfmer) in the aqueous phase compared to AS stabilized reactions. The polysurfmer may collapse forming new particles. Homopolymerization of the SS in the aqueous phase is likely to occur given that the leaving group of the RAFT agent, which is water soluble, may diffuse into the aqueous phase leading to a substantial amount of aqueous phase radicals. In the case of AS stabilized miniemulsion polymerization, the oppositely charged surfmer molecules may prohibit the RAFT leaving group from escaping into the aqueous phase.

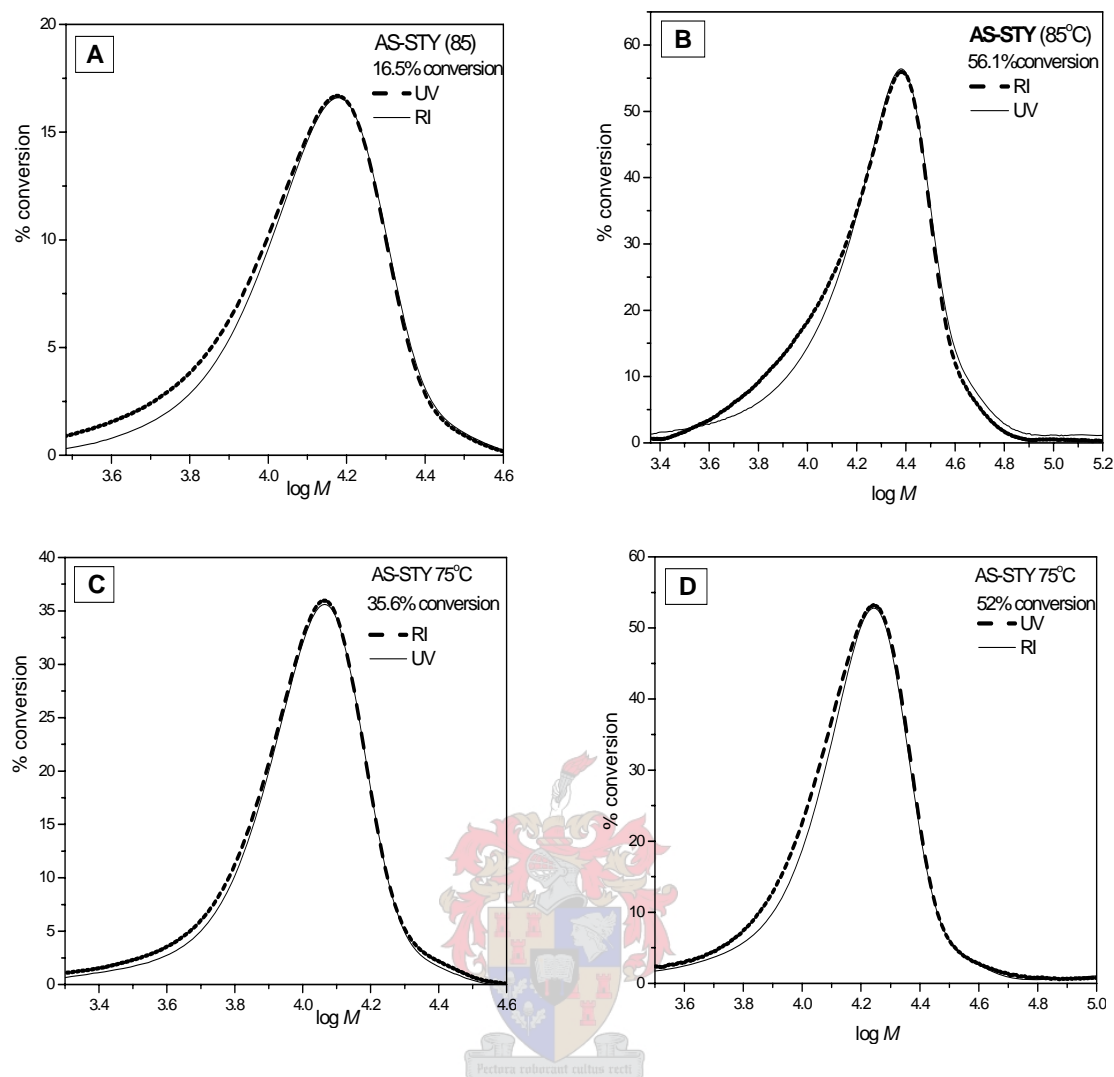


**Fig 4.8: UV-RI overlays: A, B and C, D are for the AS stabilized RAFT mediated miniemulsion polymerization of styrene at 85°C and 75°C, respectively. [Two plots per reaction for different conversions have been provided]**

The amount of free surfactant in the system depends on how effective the surfmer/surfactant is in droplet surface coverage and thus depends on the surface activity of the surfmer/surfactant. The sulfate head group lends better surface activity to the surfmer than the ammonium head group; hence better emulsification of monomer droplets is achieved. It implies that more free SS surfmer than AS could be in the aqueous phase since equimolar quantities were used and miniemulsion preparation conditions were the same. Thus, more uncontrolled aqueous phase polymerization and homopolymerization of the surfmer is more probable in SS stabilized miniemulsion polymerization than in AS stabilized miniemulsion polymerization.

### 4.3.3: SDS and SS in RAFT mediated miniemulsion polymerization of styrene

#### 4.3.3.1: Rates of reactions

A comparison of anionic emulsifiers, non-polymerizable surfactant (SDS) and SS surfmer was made. Fig 4.8 shows that the rates of reaction are similar in SDS and SS miniemulsion polymerization at the two reaction temperatures. Previous work by Guoyot<sup>7</sup> showed that the T-type surfmers (maleic anhydride derived surfmers) were less effective than classical surfactants in terms of the rates of reaction in miniemulsion polymerization of MMA.

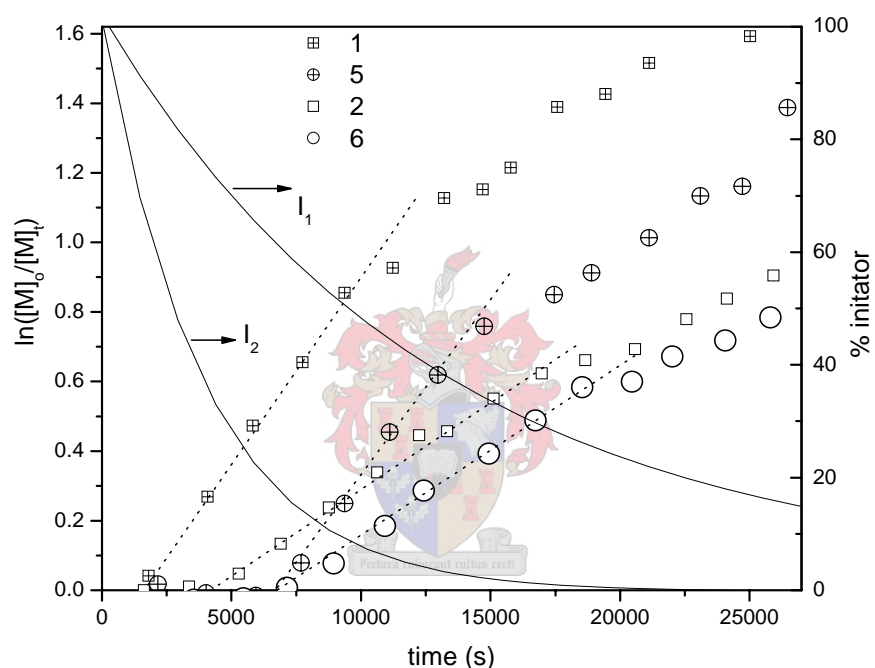


Fig 4.9: 1st order rate kinetics for SDS and SS stabilized miniemulsion polymerization of styrene: 1= SDS (85°C); 5 = SS (85°C); 2 = SDS (75°C) and 6 = SS (75°C). I<sub>1</sub> and I<sub>2</sub> are initiator decay curves at 75°C and 85°C respectively. [The dotted lines are a guide to the eye]

The SS miniemulsion polymerization reactions show a longer inductive effect, potentially due to residual inhibitors. The final monomer conversion was higher in SDS than SS stabilized miniemulsions at the respective temperatures due to the induction period.



### 4.3.3.2: Molecular weight distribution in styrene RAFT miniemulsion polymerization (SDS vs. SS)

The SDS stabilized RAFT miniemulsion polymerization of styrene at 85°C gave controlled molecular weight distribution curves (See Fig 4.9).

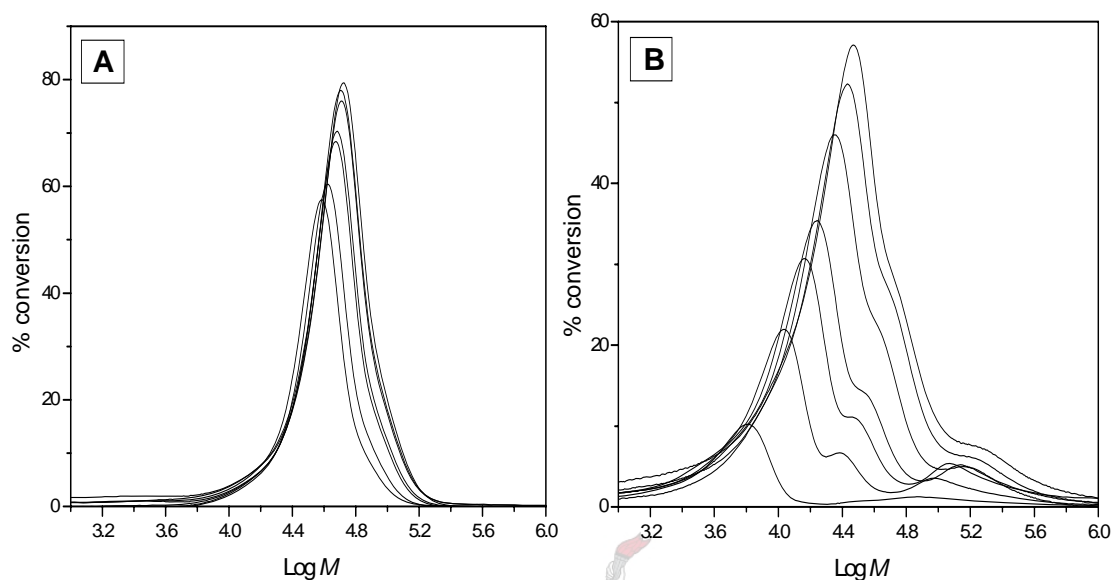


**Fig 4.10: Molecular weight distributions for SDS and SS surfmer stabilized RAFT miniemulsion polymerizations of styrene: A = SDS at 85°C and B = SS at 85°C**

Higher molecular weight polymer and lower polydispersities were obtained in SDS than in SS stabilized miniemulsion polymerizations. The polydispersities in SDS stabilized reactions were less than 1.25. The molecular weight distribution was more complex in SS stabilized miniemulsion polymerization and the base line was poor, making the determination of polydispersities difficult. However, there was an increase in molecular weight with conversion in the SS stabilized miniemulsion for the low molecular weight distribution, which is a characteristic of controlled free radical polymerization.

### 4.3.4: CTAB and AM in RAFT mediated miniemulsion polymerization of styrene

#### 4.3.4.1: Rates of reactions

The rate of reaction in AS stabilized miniemulsion polymerization is similar to that of CTAB stabilized miniemulsion polymerization (Fig 4.10).

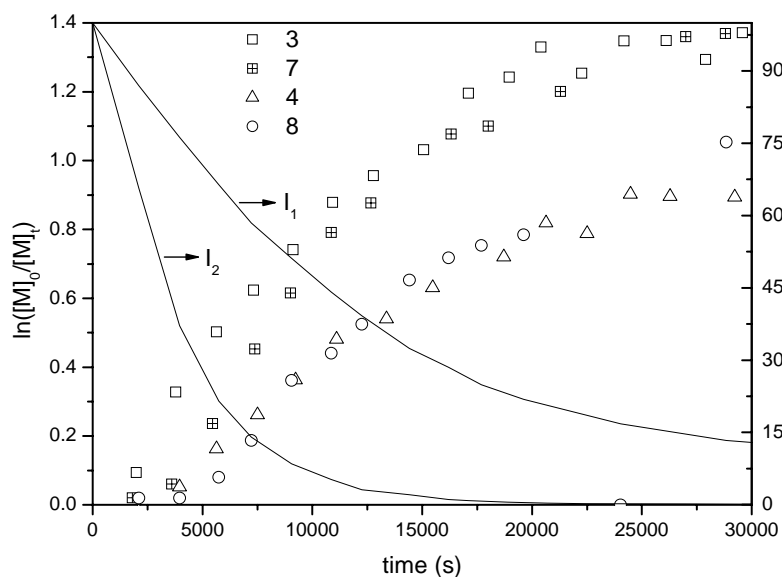


**Fig 4.11:** 1st order rate kinetics for CTAB and AS stabilized miniemulsion polymerization of styrene: 3 = CTAB (85°C); 7 = AS (85°C); 4 = CTAB (75°C) and 8 = AS (75°C).  $I_1$  and  $I_2$  are initiator decay curves at 75°C and 85°C respectively.

The AS stabilized miniemulsion polymerization reactions show a longer induction period than the corresponding CTAB stabilized miniemulsion polymerization reactions and this can be attributed to residual inhibitors present in the AS. For the reactions conducted at 75°C (Fig 4.10) the effects of residual inhibitors are masked and the two reactions have similar reaction rates.

#### 4.3.4.2: Molecular weight distribution in RAFT mediated miniemulsion polymerization of styrene (CTAB vs AS)

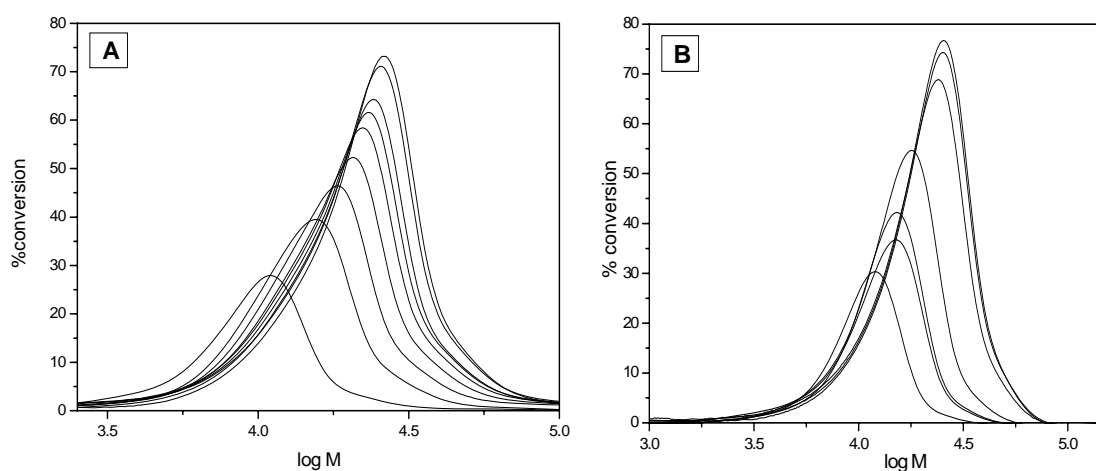


**Fig 4.12:** Molecular weight distribution for CTAB and AS stabilized RAFT mediated miniemulsion polymerization of styrene: A = CTAB at 85°C and B = AS at 85°C

The molecular weight distributions (Fig 4.11 A and B) are similar. Unlike SS, AS gave well controlled molecular weight distributions without multiple distributions.

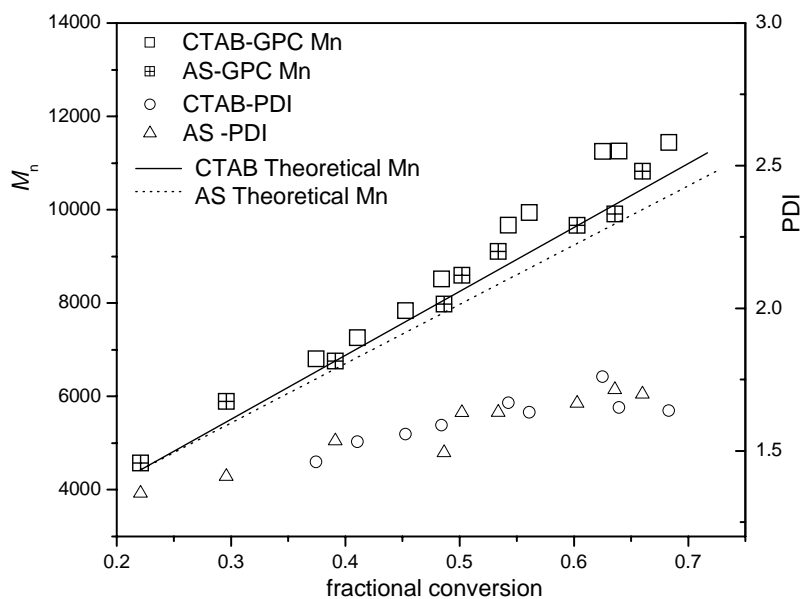


**Fig 4.13: Evolution of  $M_n$  and PDI for RAFT mediated miniemulsion polymerizations of styrene at 75°C with quaternary ammonium surfactants**

From Fig 4.12 it is observed that the experimental  $M_n$  values for both CTAB and AS stabilized miniemulsion polymerizations of styrene are higher than their theoretically predicted  $M_n$  values (using Equation 2.15). The experimental  $M_n$  values for the CTAB system are slightly higher than the experimental  $M_n$  values for the AS system and this was also the trend observed in their theoretically predicted  $M_n$  values. The deviation of GPC  $M_n$  from theoretical  $M_n$  could be attributed to the high molecular shoulder observed in the molecular weight distribution (Figs 4.11 A and B). The shoulder was due to termination by coupling, resulting in higher molecular weight polymer chains.<sup>13</sup> In general, there is a possibility of overestimation and underestimation in the theoretical  $M_n$  determined by Equation 2.14. Overestimation normally occurs when initiator derived chains are neglected and underestimation is a function of the efficiency factor ( $f$ ; a measure of radicals that will form chains).<sup>15, 16</sup> The efficiency factor ( $f$ ) is a function of both the initiator efficiency and the radical entry efficiency.<sup>15</sup>

## 4.4: MMA RAFT mediated miniemulsion polymerization reactions

Table 4.2: Reagents and reaction conditions used in miniemulsion polymerizations of MMA

Reaction	Surfactant	Temperature (°C)	Surfactant (moles x10 <sup>-3</sup> )	DDI water (moles)	AIBN (moles x10 <sup>-3</sup> )	RAFT (moles x10 <sup>-4</sup> )	n-hexadecane (moles x10 <sup>-3</sup> )	MMA (moles x10 <sup>-2</sup> )
9	SDS	80	3.478	2.223	3.185	4.484	1.941	9.988
10	SDS	75	3.475	2.224	3.234	4.491	1.939	9.998
11	CTAB	80	3.460	2.223	3.118	4.501	1.921	10.018
12	CTAB	75	3.476	2.223	3.106	4.516	1.922	10.048
13	SS	80	3.470	2.223	3.173	4.513	1.941	10.008
14	SS	75	3.487	2.229	3.130	4.495	1.941	9.998
15	AS	80	3.445	2.224	3.106	4.491	1.904	10.028
16	AS	75	3.458	2.222	3.136	4.480	1.907	9.998

#### 4.4.1: SDS and CTAB in RAFT mediated miniemulsion polymerization of MMA

##### 4.4.1.1: Rates of reaction

The SDS stabilized miniemulsion polymerization rates of reaction are faster than the CTAB stabilized reaction rates at the two reaction temperatures used (75°C and 80°C). The final monomer conversion was also higher in the SDS stabilized polymerization reaction than in the CTAB stabilized reaction.

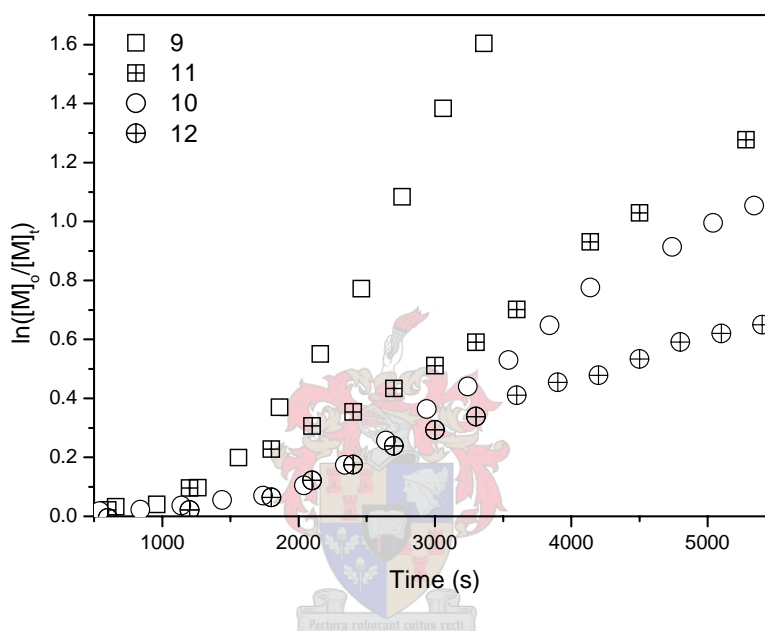


**Fig 4.14: 1st order rate kinetics for SDS and CTAB stabilized miniemulsion polymerization of MMA: 9 = SDS (80°C); 11 = CTAB (80°C); 10 = SDS (75°C) and 12 = CTAB (75°C)]**

The difference between the classical surfactants SDS and CTAB in terms of the rates of reactions is more profound in MMA RAFT mediated miniemulsion polymerization than in styrene polymerization (see Fig 4.1 for rate plots for styrene). This means that the efficiency of the anionic and cationic surfactants differs in the stabilization of a more water soluble monomer, as observed in Fig 4.14. Since the rate of polymerization roughly depends on the number of initial droplets that have reached steady state (neglecting secondary particle formation),<sup>18,14</sup> we can say that the SDS stabilized miniemulsion consists of smaller kinetically stabilized monomer droplets than the CTAB stabilized miniemulsion. Particle size data (Table 4.6 in Section 4.7.1.2) illustrate that the particle size of SDS stabilized latexes (prepared at two different temperatures) were smaller than the corresponding CTAB latexes. Small monomer droplets depend on a dense surfactant layer to stay stable whereas large droplets are stable at less dense surfactant layers.<sup>14,20</sup> This implies that CTAB miniemulsions

reach their pseudo steady state at relatively large monomer droplets, where the overall energy consideration favours droplet stability and pseudo equilibrium is established.<sup>14</sup> We can also postulate that since MMA is more soluble in water, it requires a better emulsifier to effectively form kinetically stable monomer droplets than styrene. Thus, if the efficiency of the surfactant in surface coverage of the droplet is low, the droplets will grow by coalescence until they are kinetically stable. The ability to prevent coalescence is a function of the charge density on the hydrophilic head group.<sup>20</sup> SDS has a smaller head group than CTAB and thus has a higher charge density than CTAB. This means that SDS is a better stabilizer against coalescence than CTAB in MMA miniemulsion. The rate curve (9) in Fig 4.14 shows the gel effect at higher conversion, due to the Trommsdorff effect.<sup>31,32</sup> It is possible to observe the Trommsdorff effect in RAFT systems and still get control over molecular weight. This is so because, in principle, diffusion coefficient is higher than chain transfer coefficient by orders of magnitude and rate of diffusion can decrease as conversion increases leading to reduction in termination but rate of chain transfer will still be fast enough to give controlled molecular weight. The net result would be an increase in the average number of radicals per particle ( $\bar{n}$ ), meaning that there would be a deviation from zero-one behavior in the system.<sup>31</sup>

### 4.4.1.2: Molecular weight distribution in MMA RAFT mediated miniemulsion polymerization

The molecular weight distribution curves for reactions 9 & 11 show that the two reactions stabilized by the anionic (SDS) and cationic (CTAB) surfactants were unimodal. The molecular weights increased with conversion.

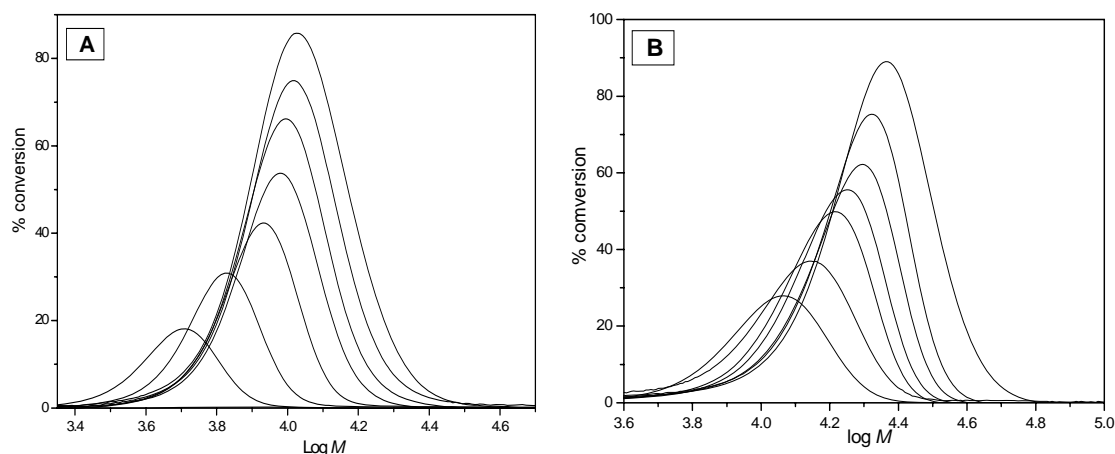
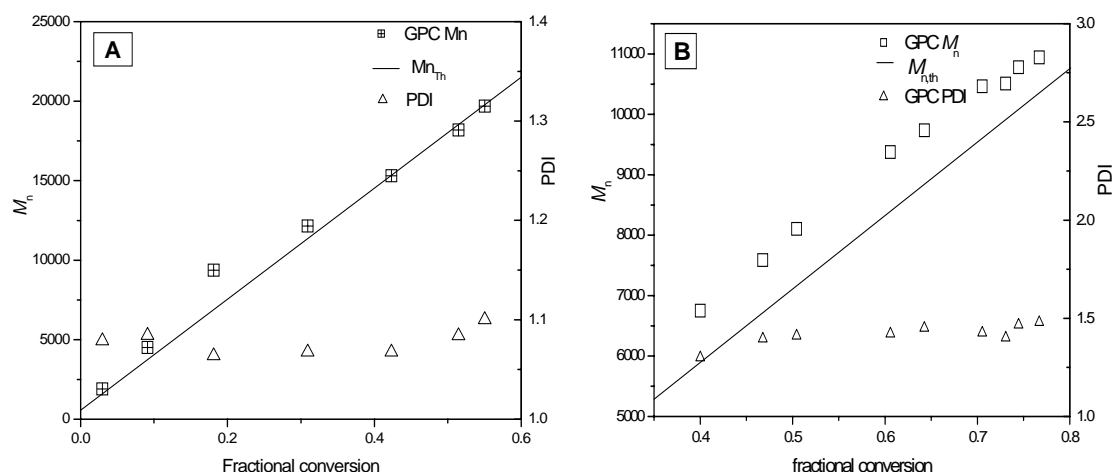


Fig 4.15: Molecular weight distribution for SDS and CTAB stabilized RAFT mediated miniemulsion polymerization of MMA: A = SDS at 80°C and B = CTAB at 80°C



**Fig 4.16: Evolution of  $M_n$  and PDI for RAFT miniemulsion polymerizations of MMA: A = SDS and B = CTAB, reactions conducted at 80°C**

The SDS stabilized miniemulsion polymerization yielded a polymer with lower polydispersity than a CTAB stabilized miniemulsion polymer. As illustrated in Figs. 4.16A and B, the polydispersity in the SDS stabilized miniemulsion was below 1.1 throughout the reaction, whereas the polydispersity of the CTAB stabilized miniemulsion was close to 1.5. The  $M_n$  in SDS and CTAB stabilized miniemulsions increased with conversion. However, the  $M_n$  of the CTAB stabilized polymerization was above the theoretical plot throughout the reaction whereas the  $M_n$  of the SDS stabilized miniemulsion followed the theoretical curve at high monomer conversion. De Brouwer *et al*<sup>15</sup> explained the deviation of GPC  $M_n$  from theoretically predicted  $M_n$  in terms of the calibration standards used for GPC in determining the molecular weight of PMMA. The calibration standards used in the present study were polystyrene standards. Corrections were therefore made using Mark Houwink constants, but such corrections are not reliable for low molecular mass polymers.<sup>15</sup> The deviation could also be due to underestimation of the theoretical  $M_n$ . Moreover, the PDI of 1,5 indicates that the uncontrolled MMA polymerization probably occurs in the water phase and can lead to secondary particles with a low RAFT concentration.

## 4.4.2: SS and AS in RAFT miniemulsion polymerization of MMA

### 4.4.2.1: Rates of reactions

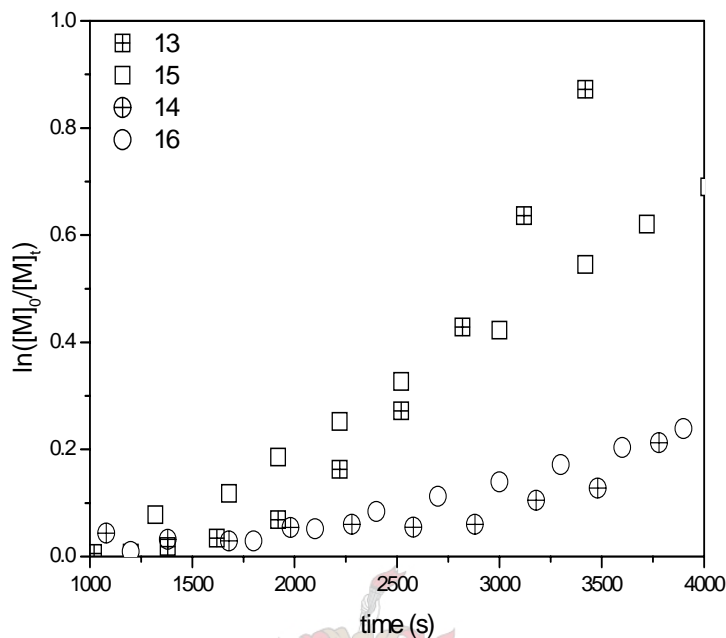


**Fig 4.17:** 1st order rate kinetics for SS and AS stabilized RAFT mediated miniemulsion polymerization of MMA: 13= SS (80°C); 15 = AS (80°C); 14 = SS (75°C) and 16 = AS (75°C)

The rates of reaction in surfmer stabilized miniemulsion polymerization of MMA (Fig 4.17) followed the trend for classical surfactants. The rates of reaction were higher for the sulfate surfmer than the ammonium surfmer. Similarly, the rates of reaction were higher in the SDS stabilized RAFT mediated miniemulsion polymerization of MMA than in the CTAB case (Fig 4.14). Gel formation<sup>31,32</sup> was observed in reaction 13 stabilized by SS, and was previously observed in reaction 9 stabilized by SDS. The SS surfmer gave higher rates of reactions than did the AS surfmer at respective temperatures. The final conversion was also higher in the SS stabilized miniemulsion polymerization than in the AS stabilized one. Again this showed the advantage of the sulfate head group in stabilizing a more water soluble monomer (MMA). The copolymerization of MMA and the surfmers is less selective than in the case of styrene. The probability of ionic groups being buried inside the particle as polymerization proceeds is increased as their distribution in the chains is more random and



the number of sulfate moieties available on the surface of the droplet will decrease.<sup>51</sup> This may lead to destabilization and possibly coalescence of particles during the reaction as well as after polymerization leading to large latex particle size.

### 4.4.2.2: Molecular weight distribution in RAFT mediated miniemulsion polymerization of MMA

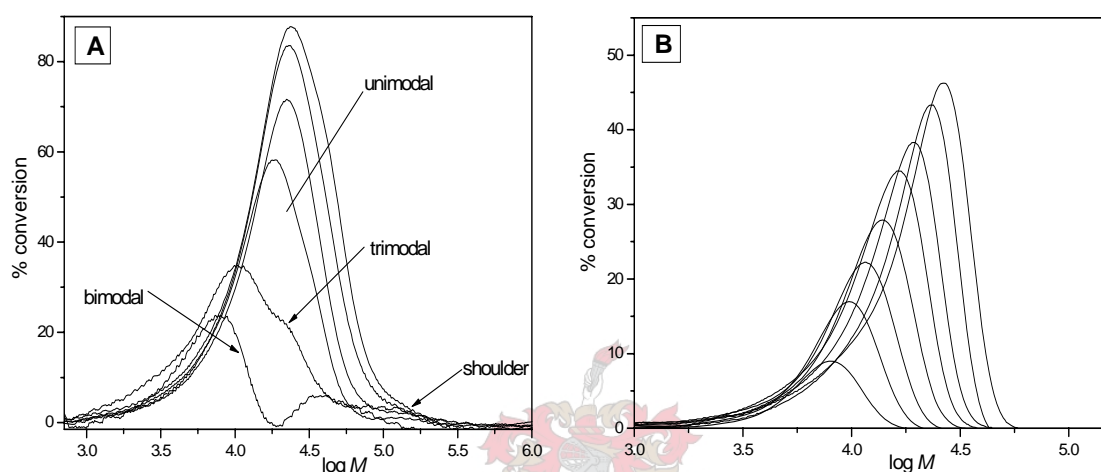


**Fig 4.18: Molecular weight distributions for SS and AS surfmer stabilized RAFT mediated miniemulsion polymerizations of MMA: A = SS at 80°C and B = AS at 80°C**

The molecular weight distribution curves for the SS stabilized miniemulsion polymerization of MMA (Fig 4.18A above) commenced with a bimodal distribution at low conversions. However, as conversion increased, a trimodal distribution (labeled in Fig 4.18A) was observed which was later buried under the lower distribution, giving an apparent unimodal distribution with a higher molecular weight shoulder (labeled in Fig 4.18A) at higher molecular weight. This was also found for the styrene system stabilized by SS, the only difference being that in the styrene-SS system the trimodal distribution is well pronounced at all conversions (reaction 5). One of the reasons why the trimodal distribution in the MMA-SS miniemulsion polymerization is less pronounced than in the case of styrene-SS could be the fact that the SS surfmer is based on a methacrylic monomer and therefore copolymerization is not monomer selective, as the two monomers (MMA and SS) are likely to have similar reactivities. The higher molecular weight shoulder is probably due to aqueous phase polymerization. The third molecular weight distribution in the styrene system, at very high molecular weight, may also be attributed to aqueous phase polymerization (secondary particle formation) which results in high molecular weight chains.

A single molecular weight distribution (with a severe low molecular weight tailing) was observed for AS (Fig 4.18B above) in contrast to a mixed modal distribution observed in the SS stabilized RAFT miniemulsion polymerization of MMA (reaction 5). As in styrene polymerization, AS behaved like a classical surfactant. Again the author proposes two mechanisms of nucleation (homogeneous and droplet nucleation) in the SS stabilized RAFT miniemulsion polymerization of MMA resulting in a bimodal molecular weight distribution. The molecular weight distribution at low molecular weight (for SS stabilized miniemulsion, Fig 4.18 A) showed that the molecular weight increased with conversion, suggesting that the mechanism of nucleation for the particle containing this polymer was droplet nucleation since the RAFT agent is soluble in this oil phase. The second distribution for the bi and trimodal peaks (at high molecular weight, Fig 4.18A) showed no control and thus the mechanism of nucleation was likely to be homogeneous nucleation. Uncontrolled polymerization in the aqueous phase results in higher molecular weight than polymerization in the oil phase. The fact that the end group may be attached to a water soluble oligomer makes transport between particles more likely, leading to the possibility of a certain degree of control in the aqueous-phase nucleated particles.

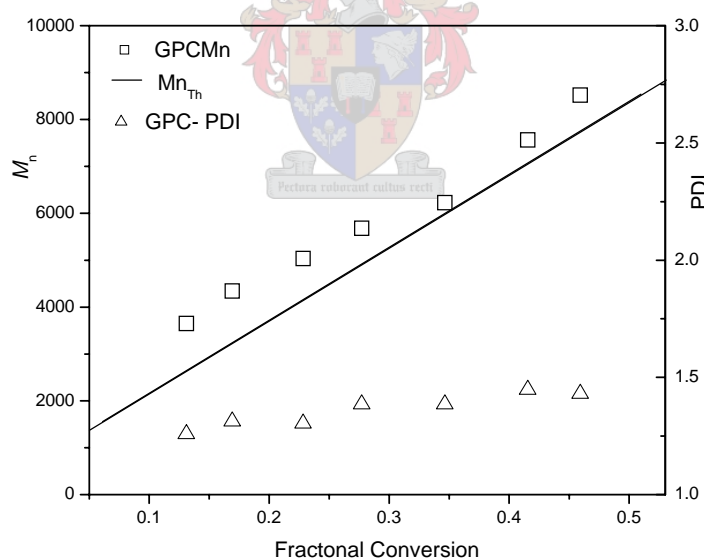


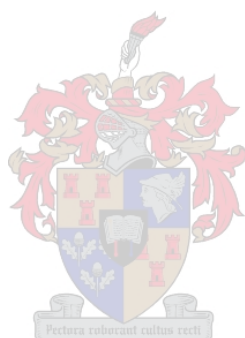
**Fig 4.19: Evolution of  $M_n$  and PDI for RAFT miniemulsion polymerizations of MMA, using AS at 80°C**

The number average molecular weight (Fig 4.19) increased fairly linearly with increasing conversion, which is characteristic of a controlled system. The polydispersity increased slightly with conversion. For controlled free radical polymerization, polydispersity should decrease with conversion as most of the chains will be growing via the RAFT mechanism.<sup>16</sup>

## ***Chapter 4: RAFT mediated miniemulsion polymerization***

---

The slight increase in polydispersity is due to secondary particle formation (observed as severe tailing in Fig 4.18B) which become more effective as monomer is depleted.



4.4.2.3: UV-RI analysis of the SS and AS stabilized reactions at 80°C

Fig 4.20A and B show the UV-RI overlays for the SS stabilized miniemulsion polymerization of MMA at two different conversions.

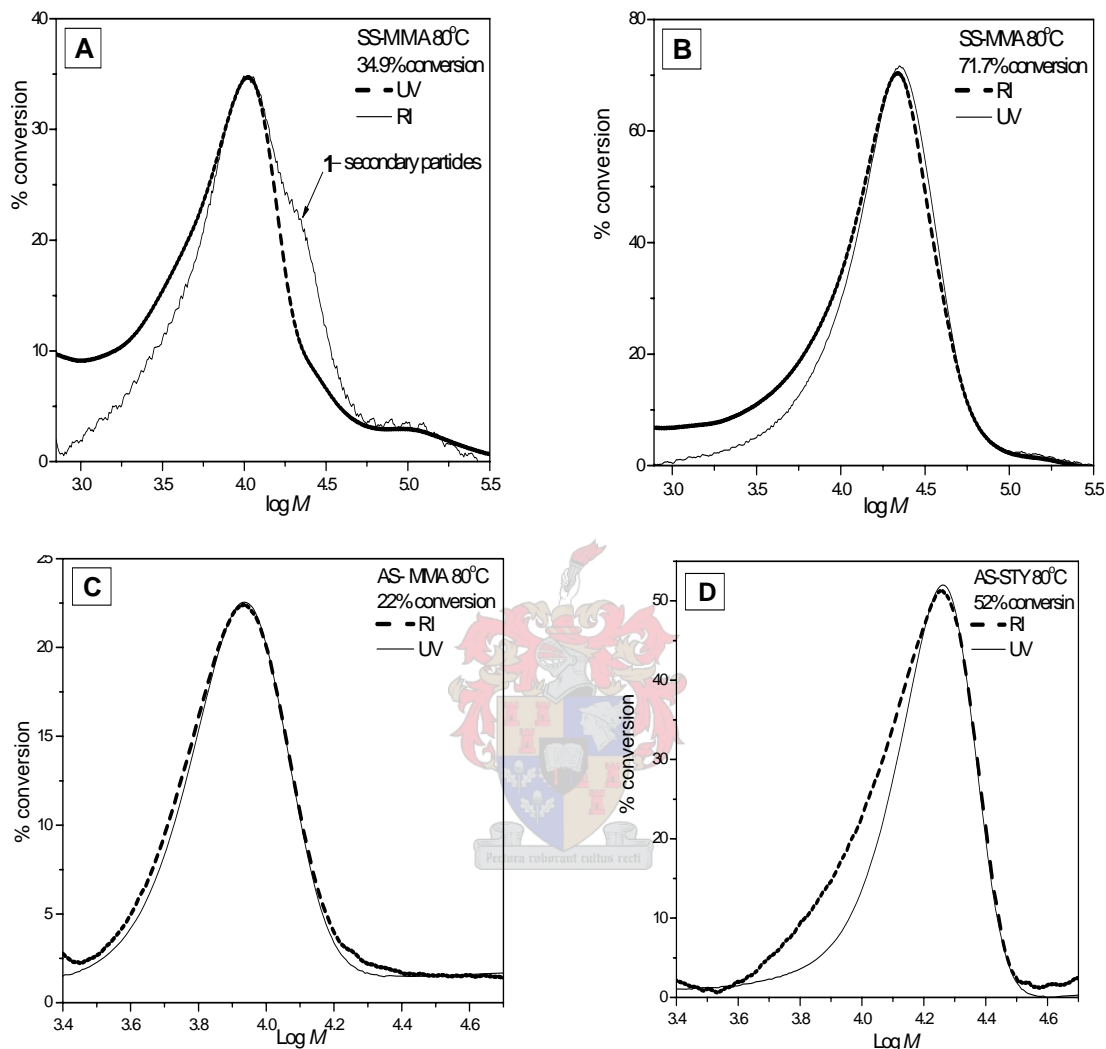


Fig 4.20: UV-RI overlays: A, B and C, D for SS and AS stabilized RAFT miniemulsion polymerization of MMA at 80°C, respectively. [Two plots were provide per reaction at different conversions]

The UV wavelength of 320 nm was used for detection of chains with the RAFT end group. At 34.9% conversion (Fig 4.20A) some of the chains did not have the terminal RAFT moiety, as illustrated by a lower UV signal at the middle distribution labeled **I** in Fig 4.20A. As the percentage conversion increased, the peak labeled **I** was buried under the peak which was at lower molecular weight, as seen in Fig 4.20B. Thus the bi-modality was obscured with conversion. At 71.7% conversion, most of the chains had the RAFT terminal moiety as the UV and RI overlay showed an improved fit.

Figs 4.20C and D show that most of the chains have the RAFT terminal moiety at both 22 and 52% conversion. The UV signal at 52% conversion was very intense at low molecular weight due to lower molecular weight chains terminated with the RAFT moiety.

### 4.4.3: SDS and SS in MMA RAFT miniemulsion polymerization

#### 4.4.3.1: Rates of reaction

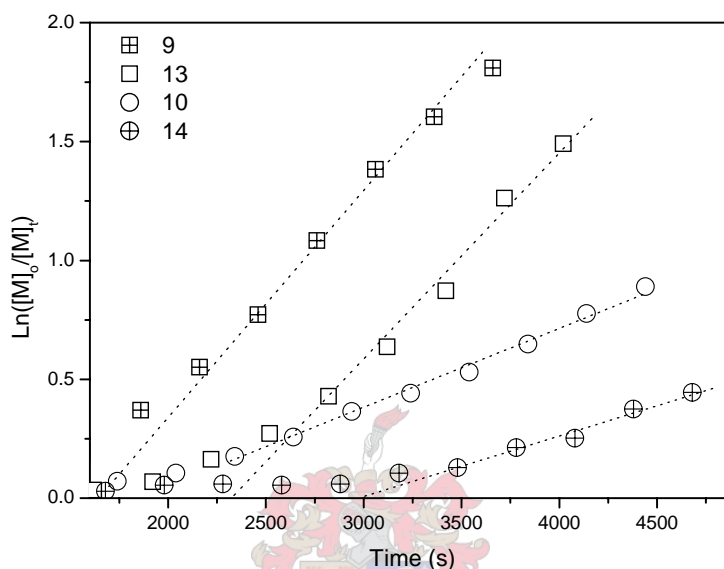


**Fig 4.21:** 1st order rate kinetics for SDS and SS stabilized miniemulsion polymerization of MMA: 9= SDS (80°C); 13 = SS (80°C); 10 = SDS (75°C) and 14 = SS (75°C). [The dotted lines are a guide to the eye]

The reaction rate curves for both SDS and SS have similar shapes, and are also similar at the two temperatures used (80°C and 75°C). However, the SS stabilized miniemulsion reactions showed longer induction periods due to residual polymerization inhibitors in SS. Although the sulfate surfmer showed some bimodality, the behavior of the two surfactants (SDS and SS) in MMA was the same. The final MMA monomer conversion was also similar; again the sulfate head surfactant and surfmer (SDS and SS) had similar efficiencies and gave higher rates of reaction than their cationic counterparts (CTAB and AS); see Figs 4.14 and 4.17.

4.4.3.2: Molecular weight distributions as determined by SEC

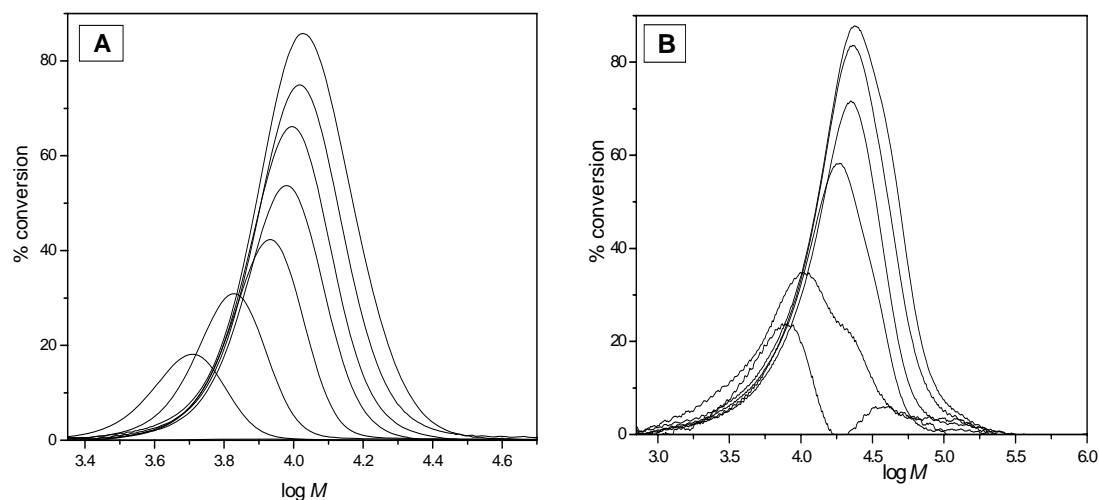
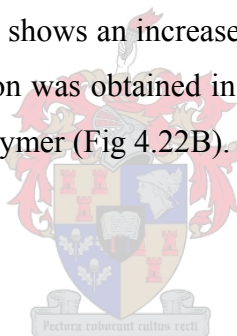


Fig 4.22: Molecular weight distributions for SDS and SS surfmer stabilized RAFT miniemulsion polymerization of MMA: A = SDS at 80°C and B = SS at 80°C

The molecular weight distribution for SDS stabilized RAFT mediated miniemulsion polymerization of MMA (Fig 4.22A) shows an increase in molecular weight with conversion. A single molecular weight distribution was obtained in the SDS stabilized system in contrast to the SS stabilized miniemulsion polymer (Fig 4.22B).



#### 4.4.4: CTAB and AM in RAFT miniemulsion polymerization of MMA

##### 4.4.4.1: Rates of reaction

Faster rates of reaction were found in the CTAB stabilized RAFT miniemulsion polymerizations of MMA than those of AS. As shown in Fig 4.23, the reactions conducted using the classical surfactant (CTAB) had higher rates of reactions when compared to the corresponding AS reactions at the two reaction temperatures.

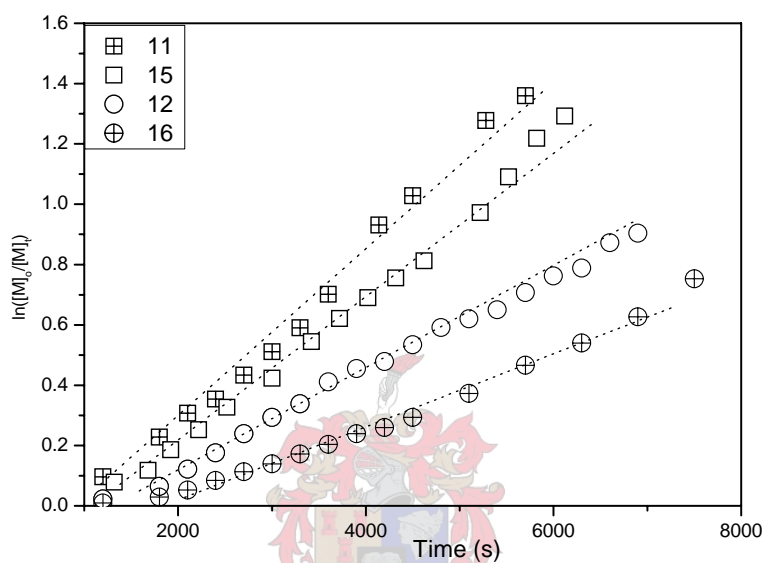


Fig 4.23: 1st order rate kinetics for CTAB and AS stabilized miniemulsion polymerization of MMA: 11 = CTAB (80°C); 15 = AS (80°C); 12 = CTAB (75°C) and 16 = AS (75°C). [The dotted lines are a guide to the eye]

The higher rates in the CTAB stabilized miniemulsion reactions can be explained in terms of the emulsification efficiency of the surfactant. The classical surfactant (CTAB) has a longer hydrophobic tail than AS and the hydrophobic tail of the AS is partially polar due to the presence of the ester group. This means that in terms of emulsification efficiency, CTAB is a better emulsifier. AS is expected to be more water soluble than CTAB and have a higher CMC value than CTAB. The results suggest that AS is less effective in the stabilization of a more water soluble monomer such as MMA, since for styrene the rates of reaction were similar to that of the CTAB stabilized reaction and the particle size was also approximately the same (see Section 4.7.1.1, Table 4.4). The final particle size was larger in the AS than the CTAB stabilized miniemulsion polymerization of MMA (see Section 4.7.1.2, Table 4.6) therefore the initial monomer droplets will be relatively larger in AS stabilized MMA miniemulsion than in CTAB stabilized MMA miniemulsion. The rate of polymerization depends on the number of initial monomer droplets, suggesting that the AS stabilized

miniemulsion starts from large monomer droplets. In MMA RAFT miniemulsion polymerizations, surfmers gave larger particle sizes than classical surfactants in the RAFT mediated miniemulsion polymerization of MMA (see Section 4.7.1.2, Table 4.6).

### 4.4.4.2: Molecular weight distribution in RAFT mediated miniemulsion polymerization of MMA

The CTAB and AS stabilized RAFT mediated miniemulsions of MMA gave increasing molecular weight distribution curves. The AS behaved in a similar fashion to the classical surfactant.

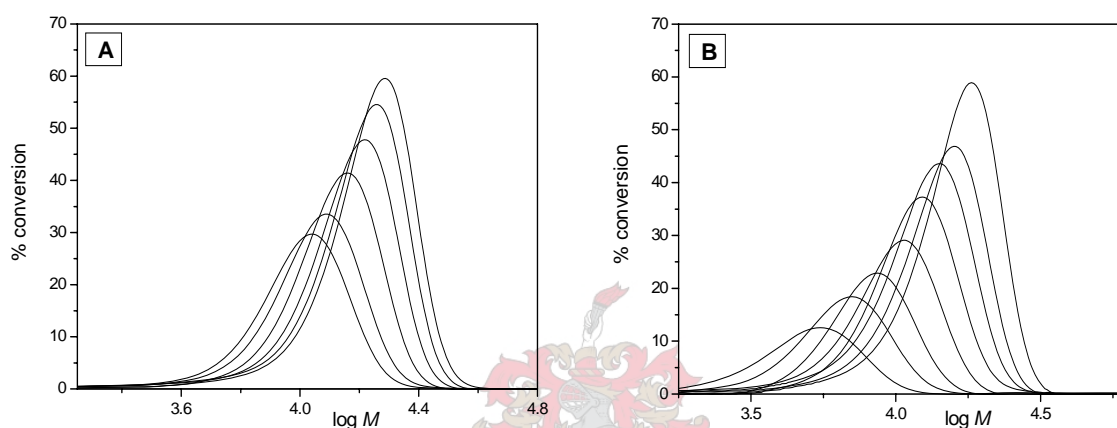


**Fig 4.24: Molecular weight distribution for CTAB and AS surfmer stabilized RAFT miniemulsion polymerization of MMA: A = CTAB at 75°C and B = AS at 75°C**

The similar behaviour of AS to classical surfactants is postulated to be due to its lower solubility in the aqueous phase compared to SS. This has an effect of leaving minimal free surfmer in the aqueous phase, and hence less homogeneous nucleation or homopolymerization of the surfmer in the aqueous phase, as postulated for the SS system.



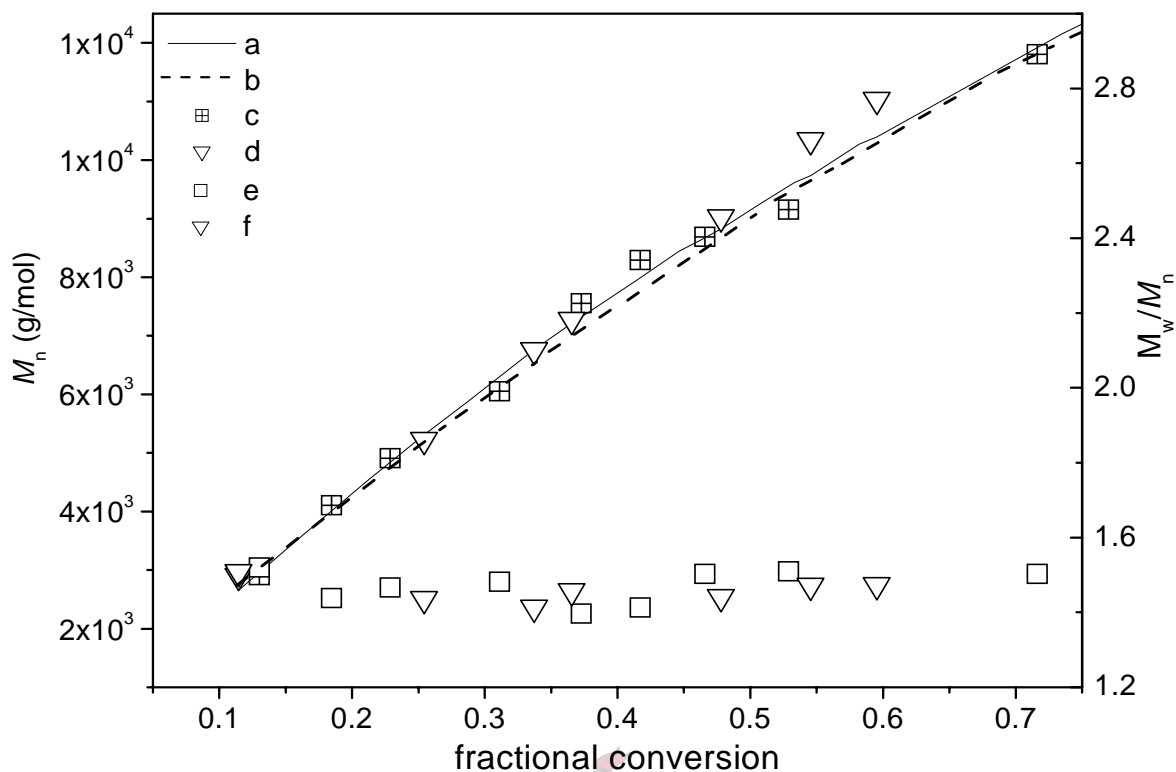


Fig 4.25: Evolution of  $M_n$  and PDI for RAFT miniemulsion polymerizations of MMA at 75°C: (a) and (b) are the theoretical  $M_n$  values for CTAB and AS stabilized miniemulsions, reactions 12 and 16 respectively; (c) and (e) GPC  $M_n$  and PDI respectively for AS stabilized miniemulsions (reaction 16); finally (d) and (f) GPC  $M_n$  and PDI respectively for CTAB stabilized miniemulsion polymerization (reaction 12)

From Fig 4.24 it can be seen that the increase in  $M_n$  with conversion is relatively similar for the CTAB and AS stabilized miniemulsion polymerizations of MMA. However the predicted  $M_n$  for the AS stabilized miniemulsion gave a plot which fitted the GPC  $M_n$ , whilst the predicted  $M_n$  for the CTAB system was slightly lower than the GPC  $M_n$  at higher conversion. The deviation can be explained in terms of under-estimation of the theoretical  $M_n$ . The PDIs are also similar in the two systems; they remained relatively constant with increasing conversion, which is again a characteristic of a controlled polymerization.

## **4.5: Analysis of copolymers of styrene and surfmers (2D-chromatography)**

An investigation was carried out to determine the chemical composition of the styrene-surfmer random copolymers using chromatographic methods at the critical conditions for styrene. No attempt was made to analyze MMA copolymers because for this there was a need to first determine suitable conditions for separation and the scope of the current project did not allow for this investigation to be expanded at this time. The development of chromatographic conditions for methacrylic comonomers may however form part of future studies.

### **4.5.1: Introduction**

Copolymers are complex multi-component materials with a molar mass distribution (MMD) as well as a chemical composition distribution (CCD). The determination of CCD is essential in the characterization of copolymers, and yet a difficult task. For the past 20 years the use of high-performance liquid chromatography (HPLC) has been a tool of choice for unravelling the molecular heterogeneity of complex polymers.<sup>26</sup> In liquid adsorption chromatography (LAC) copolymers can be separated according to the CCD, regardless of the MMD, by using an appropriate combination of good and poor solvents as the eluent. In LAC, precipitation should not occur on the stationary phase: separation should exclusively be due to adsorptive interactions.

In this study, the choice of a suitable chromatographic system is difficult due to the opposing chemical nature of the two monomers. A system used for the analysis of amphiphilic block copolymers of poly(ethyleneglycol-styrene) and first published by Baran *et al*<sup>297</sup> was investigated for this project. The system consisted of a reverse phase column (Nucleosil C18) and a mixture of THF and water (10% vol) as the mobile phase. The critical point of adsorption of polystyrene is met under in these conditions, allowing us to separate diblock copolymer only according to the molar mass of the other block.

### 4.5.2: Experimental conditions

#### Equipment and materials for 2D experiments

A modular chromatographic system comprising two chromatographs connected via one electrically driven eight-port injection valve (Valco) and two storage loops was used.

For the first dimension a Waters 2690 Alliance separation module equipped with a Supelco Nucleosil C18 100 Å, 5mm average particle size, 250 x 4.6 mm column, was used. The mobile phase was tetrahydrofuran: water (90:10) and the temperature was 30°C.

For the second dimension a Waters 515 HPLC pump was used. The column was a PSS SDV linearM high-speed, 5µm average particle size, 50 × 20(ID) mm (Polymer Standards Service) and the mobile phase THF at a flow rate of 4 mL/min. The detector was an evaporative light scattering detector (ELSD) PL-ELS 1000 from Polymer Laboratories and the calibration was based on linear monodisperse polystyrene standards (EasiVial PS from Polymer Laboratories). The operation of the coupled injection valves was controlled by PSS Win GPC7, which was also used for data collection and processing (software obtained from Polymer Standards Service, Mainz, Germany).

### 4.5.3: Results

Copolymers of SS-styrene (reaction 5) and AS-styrene (reaction 7) were soluble in the eluent system and were analysed in LAC mode according to the experimental conditions described above. Chromatographic traces of SS-styrene and AS-styrene were determined. PS had an elution volume between 2.5 and 2.7 mL, independent of its molar mass.

#### 4.5.3.1: LCCC of SS-styrene

SS-styrene was separated into two different compounds, as shown in Fig 4.26. The first one, at 1.6 mL, was expected to be the copolymer and the second one, at 2.5 mL, was homopolystyrene that was formed during the reaction. Further 2D chromatography analysis of this sample is expected to give information on the molar mass distribution of each of these components.

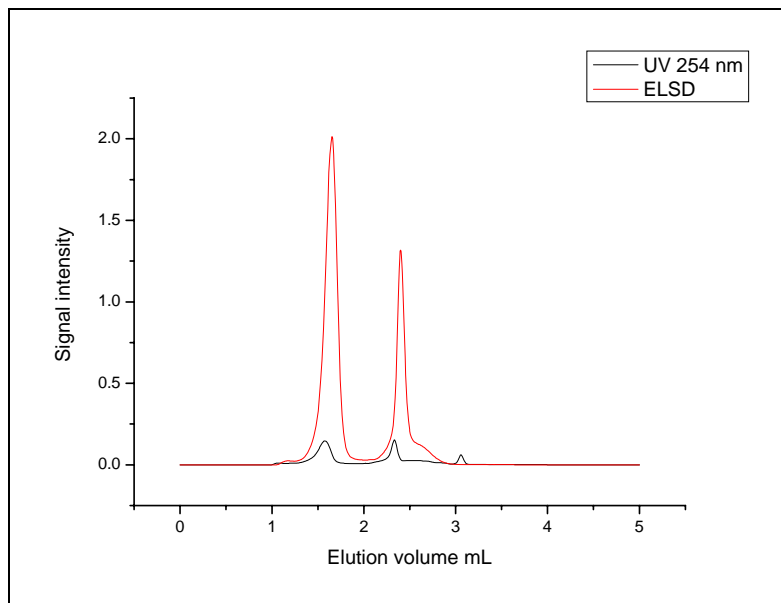


Fig 4.26: Liquid adsorption chromatogram (1st dimension) for SS-styrene copolymer, reaction 5

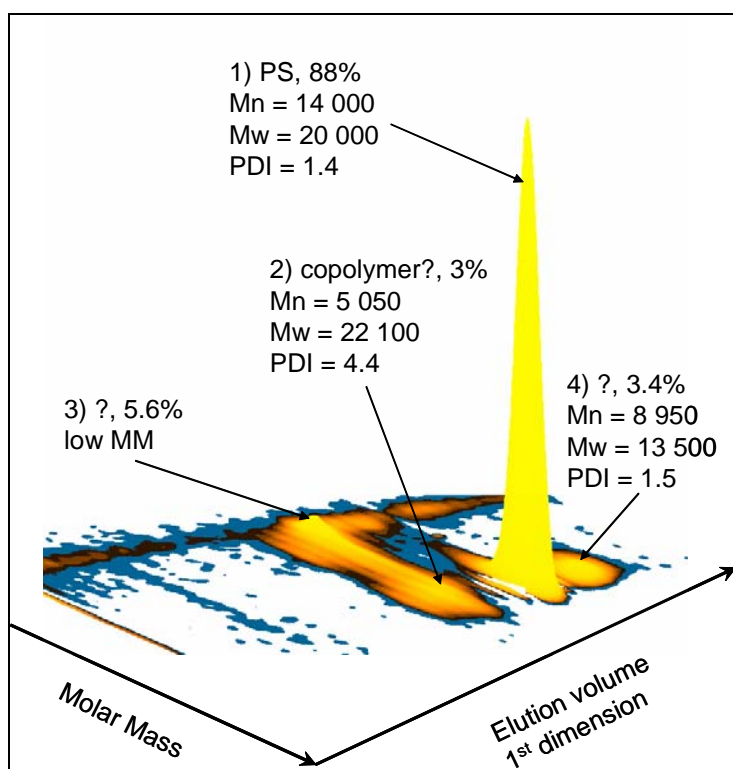


Fig 4.27: 3-D chromatogram for SS-styrene copolymer reaction 5

The 2-D chromatography experiment on the SS-styrene sample, performed with LAC as the first dimension and high speed SEC as the second dimension, gave the unexpected results, as

shown in the 3D presentation above (Fig 4.27). The copolymer may elute as the polystyrene peak in the second dimension.

(Plans are currently underway to investigate 2D analysis using a different stationary phase in the second dimension, to enable the use of a mixture of THF and water that will ensure total solubility of the sample in the SEC column. In this experiment the eluent in the SEC dimension is THF, and the stationary phase used cannot tolerate water.)

### 4.5.3.2: LCCC of AS-styrene

The chromatogram of AS-styrene shows only one component, eluting at 2.5 mL, indicating that it is only polystyrene or its copolymer.

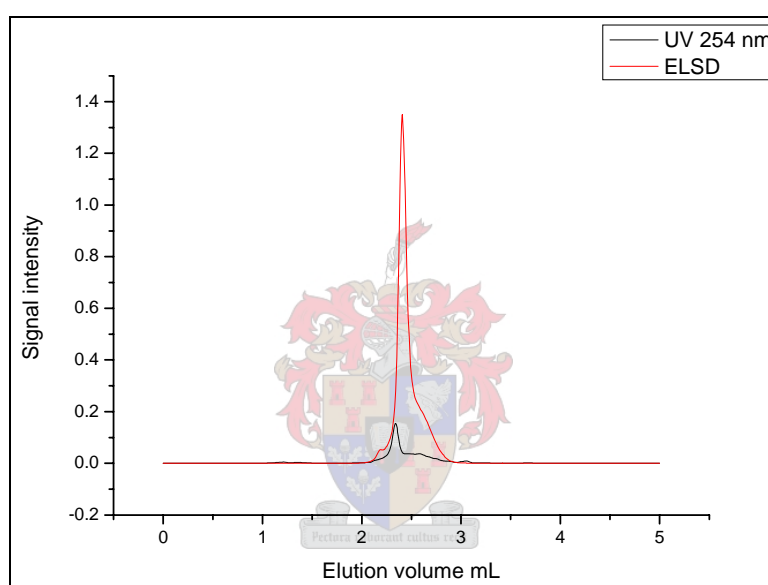


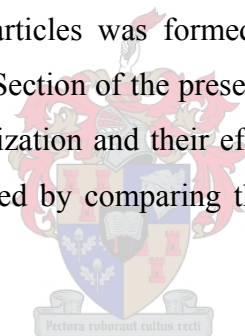
**Fig 4.28: Liquid adsorption chromatogram (1st dimension) for AS-styrene copolymer, reaction 7**

The results above are misleading, as they suggest that no copolymerization occurred. This is in contrast with the results from  $^1\text{H}$  NMR spectroscopy, which showed that the surfmers are indeed reactive, and thus either the surfmers are incorporated into the polymers or polymerize to form homopolymers.  $^1\text{H}$  NMR spectroscopy results are more acceptable as the technique is more sensitive. The reason for no separation in the LAC for AS-styrene could be the fact that the solvent system was poor for the polymer in question and random copolymers do not separate, only block copolymers. Further investigation is required, by combining HPLC results with an IR spectrum. Analysis of copolymers with PMMA will require further research as suitable conditions for LAC still need to be determined.

## **4.6: The use of oligosurfmers in RAFT mediated miniemulsion polymerization of styrene and MMA**

*N.B: RAFT agent (CVADTB) was added to these miniemulsion polymerization reactions stabilized by oligosurfmers with RAFT end groups.*

The oligosurfmers of the ionic surfmers are water soluble and act as polyelectrolytes in aqueous solutions. The oligosurfmers were prepared as described in Chapter 3, Section 3.6. Oligosurfmers have emulsifying capabilities and thus can be used as emulsifiers in both emulsion and miniemulsion polymerization. The use of polymeric emulsifiers can alleviate the problems associated with classical surfactants (see Chapter 2, Section 2.4.3) as they can be coagulated from aqueous solutions by adding a non-solvent. The size of the oligomer determines the droplet size. Lim *et al*<sup>23</sup> used poly (methyl methacrylate-*b*-(diethyl amino) ethyl methacrylate diblock copolymer as surfactant and hexadecane as hydrophobe for miniemulsion stabilization and found that a significant fraction of particles was formed by micellar nucleation at high surfactant concentration. In this Section of the present study, oligosurfmers were used in RAFT miniemulsion polymerization and their efficiency as emulsifiers in relation to their monomers were evaluated by comparing the rates of reaction and the final particle size.



### **4.6.1: Procedure**

The oligosurfmers (SSO and ASO, prepared as described in Chapter 3, Section 3.6.2) were used as emulsifiers in the RAFT mediated polymerization of styrene and MMA. Thus the standard recipe for miniemulsion described in Section 4.2 was applied. Only the mass of the oligomer was varied; all other variables (initiator, temperature, monomer, time of sonication and amount RAFT agent) were kept constant.

**Table 4.3: The masses of reagents and reaction temperatures used in miniemulsion polymerizations of styrene and MMA**

Reaction	Oligomer	Temperature (°C)	Oligomer (g)	DDI water (g)	AIBN (g)	RAFT (g)	n-Hexa-decane (g)	Monomer (g)
17	SSO	(85)	1.501	40.04	0.052	0.125	0.439	10.00 (STY)
18	SSO	(80)	1.505	40.03	0.053	0.125	0.430	10.01 (MMA)
19	ASO	(85)	1.013	40.07	0.051	0.125	0.432	10.02 (STY)
20	ASO	(85)	1.510	40.09	0.050	0.125	0.432	10.01 (STY)
21	ASO	(80)	1.012	40.02	0.051	0.125	0.432	10.04 (MMA)
22	ASO	(80)	1.501	40.018	0.053	0.125	0.434	10.01 (MMA)
23	SSO	(85)	1.023	40.010	0.051	0.126	0.431	10.03 (STY)
24	SSO	(80)	1.010	40.013	0.051	0.125	0.432	10.09 (MMA)

### 4.6.2: Sulfate surfmer oligomer (SSO) in RAFT miniemulsion of styrene and MMA

#### 4.6.2.1: Rates of reactions

The shapes of the rate curves of the reactions for the SSO stabilized miniemulsion polymerization of styrene and MMA resemble those of their respective SS stabilized miniemulsions.

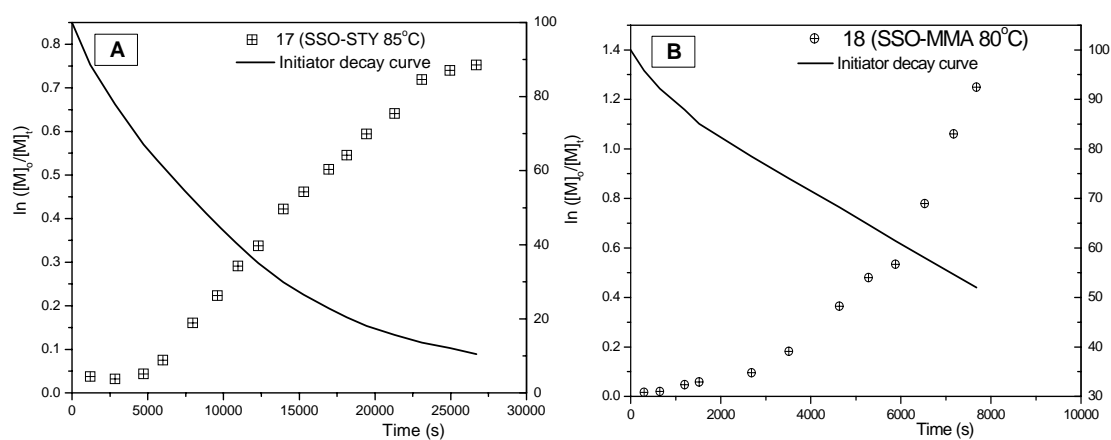


**Fig 4.29: 1st order rate kinetics for SSO stabilized miniemulsion polymerization of: A = styrene at 85°C and B = MMA at 80°C**

## Chapter 4: RAFT mediated miniemulsion polymerization

The gel effect was also observed in the SSO stabilized miniemulsion polymerization of MMA (observed initially in the SS stabilized miniemulsion polymerization of MMA; see Section 4.4.2.1). This is common in MMA miniemulsion polymerization. The rate of reaction was slower in the SSO stabilized RAFT mediated miniemulsion polymerization compared to the rate of reactions recorded for its monomer (SS). The final monomer conversion was lower in the oligomer stabilized miniemulsion polymerization. This can be attributed to the fact that, in styrene-methacrylate copolymerization kinetics, methacrylates lead to more rapid rates of polymerization of styrene. Therefore, since oligosurfmers are not reactive, they do not influence the rate of styrene polymerization, hence this may explain the slower rate of reaction observed in SSO stabilized miniemulsion polymerization of styrene than in SS stabilized miniemulsion polymerization system. The final particle sizes of the latexes were larger when compared to particle size of the latexes obtained with the SS, hence slow rates of reaction could also be due to poor emulsification of the oligosurfmers which could result in polymerization starting from large monomer droplets.

### 4.6.2.2: Molecular weight distribution in RAFT mediated miniemulsion polymerization of styrene and MMA with SSO as the emulsifier

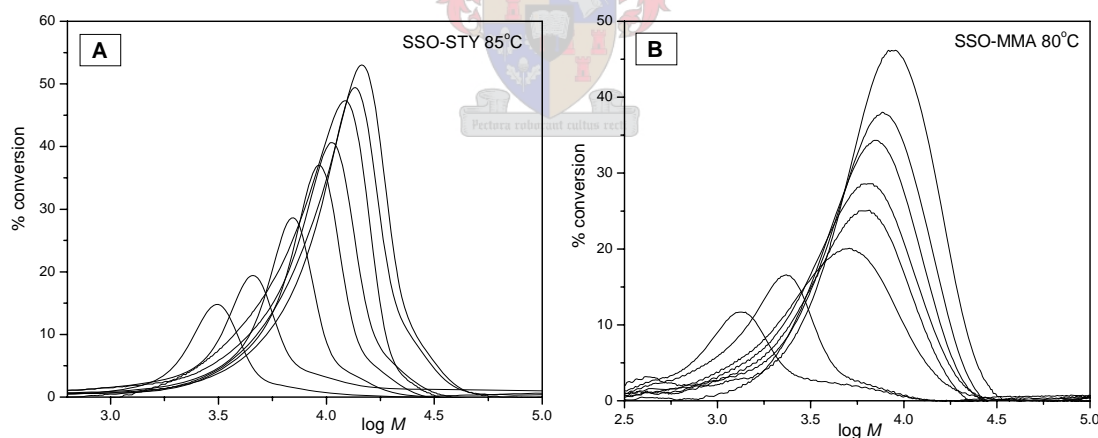


Fig 4.30: Molecular weight distribution for SSO stabilized RAFT miniemulsion polymerization of: A = styrene at 85°C (reaction 17) and B = MMA at 80°C (reaction 18)

The molecular weight increased with increasing conversion in RAFT mediated miniemulsion polymerizations of both styrene and MMA. One of the most interesting observations in the molecular weight distribution of SSO stabilized RAFT miniemulsion polymerization of styrene and MMA is the disappearance of the tri- and bimodal distributions respectively, which were dominant in the SS (monomer of SSO) stabilized miniemulsion reactions. This suggests that the complex distributions found



earlier for the SS stabilized miniemulsions may also be partially due to the reactivity of the surfmer during polymerization. The author postulates that homo/copolymerization of the sulfate surfmer in the aqueous phase as well as in the existing particles played a significant role in producing the multimodality. Copolymerization in the aqueous phase is more likely to occur in MMA than in styrene because MMA is highly water soluble and the chances of finding monomer in the aqueous phase are high. By using SSO as an emulsifier we only expect chain extension to occur, leading to the formation of blocks.

However further investigation needs to be carried out to determine the feasibility of chain extension of oligosurfmers. HPLC that is tolerant to a solvent system of water/THF (approximately 30:70) can be used to analyze the blocks. The solvent system is capable of dissolving the homopolymers (PMMA or polystyrene), copolymers and oligosurfmers synthesized in this project. The molecular weight distribution of oligosurfmers can also be observed i.e. whether the chains are increasing in length with conversion. The problem associated with analysis of oligosurfmers is that a high load of water is required in the solvent system. Moreover, chromatography at critical conditions can not be done and an HPLC column which tolerates a high load of water is required.

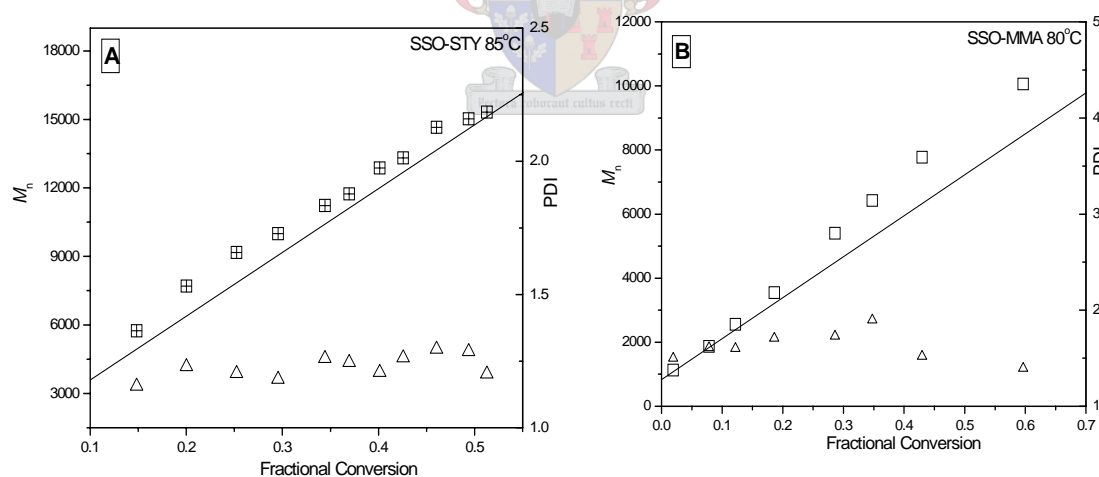


**Fig 4.31: Evolution of  $M_n$  and PDI for SSO stabilized RAFT miniemulsion polymerization of: A = styrene at 85°C (reaction 17) and B = MMA at 80°C (reaction 18)**

The experimental  $M_n$  of the SSO stabilized RAFT miniemulsion polymerization of styrene and MMA increased with increasing molecular weight, showing that the reactions demonstrated a “living” characteristic. The GPC  $M_n$  values are close to the theoretical  $M_n$  values. The deviation of GPC  $M_n$  from theoretical  $M_n$  can be explained

in terms of the underestimation and/or termination which is responsible for the high molecular weight shoulder.

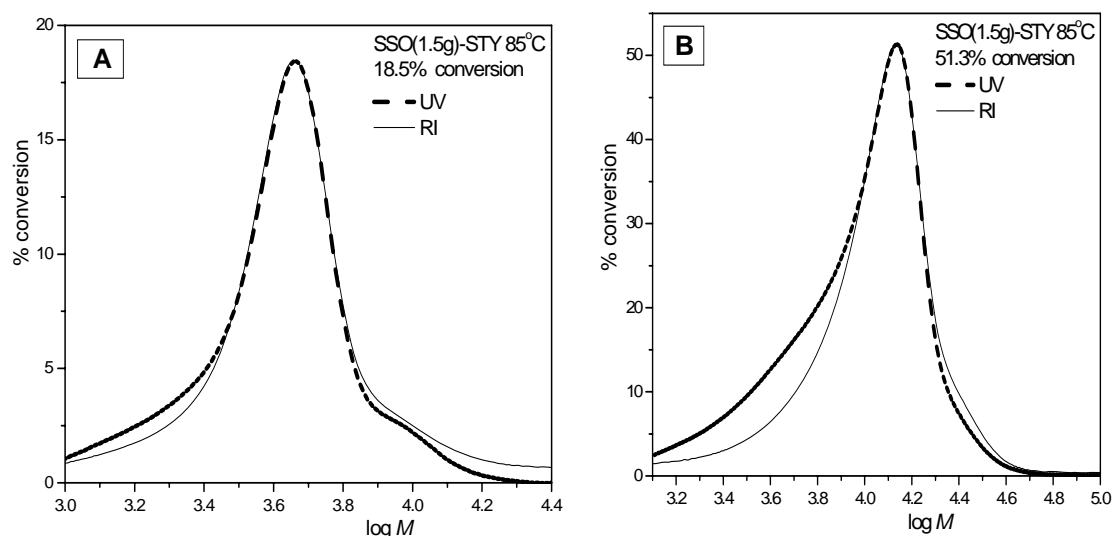


**Fig 4.32: UV-RI overlays for SSO stabilized RAFT miniemulsion polymerization of styrene at 85°C (reaction 17) at two different conversion: A =18.5% and B = 51.3% conversion**

The graphs in Fig 4.31A and B show that most of the polymer chains had the RAFT moiety, as indicated by the UV-RI overlays. In contrast to what was found for SS (monomer of SSO), SSO gave no bimodalities and better control over molecular weight distribution and polydispersity. From GPC curves and UV-RI overlays, it can be concluded that the appearance of the trimodal distribution is due to the reactivity of the SS in the aqueous phase. The presence of reactive species in the aqueous phase would probably aid homogeneous nucleation and, consequently, there is likely to be no control in the aqueous phase nucleated particles because the aqueous phase transport of the RAFT agent is normally low<sup>19</sup>, resulting in high molecular weight polymer being formed in the aqueous phase. Thus oligomerization of the SS will eliminate the presence of the reactive species in the aqueous phase as well as the possibility of homopolymerization of the surfmer. This does not eliminate secondary particle formation in the aqueous phase, which is supported by the presence of free surfactant.

### **4.6.3: Ammonium surfmer oligomer (ASO) in RAFT mediated miniemulsion polymerization of styrene**

#### **4.6.3.1: Rates of reaction**

The rates of reaction and final monomer conversion in the ASO stabilized RAFT miniemulsion of styrene were lower than those found with the monomer (AS surfmer). The rate of reaction increased with increasing ASO concentration, which is analogous to what was observed when surfactant concentration was increased in miniemulsion polymerization.<sup>20</sup> When 1.5 g of oligosurfmer was used, the number of initial monomer droplets formed would be higher compared to when 1 g of oligomer was used, resulting in higher rates of reaction. The average particle size was smaller in miniemulsion stabilized by 1.5 g of oligosurfmer compared to miniemulsion stabilized by only 1.0 g of oligosurfmer.

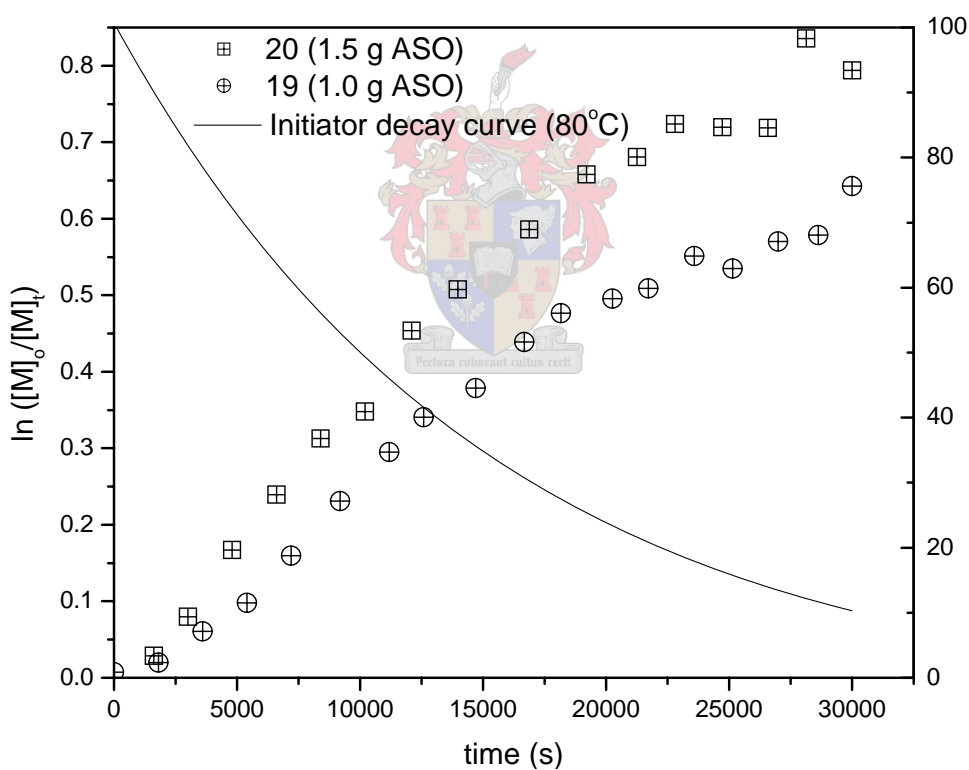


**Fig 4.33: 1st order rate kinetics for AS oligomer stabilized miniemulsion polymerization of styrene**

4.6.3.2: Molecular weight distribution curves for RAFT miniemulsion polymerization of styrene with ASO as the emulsifier

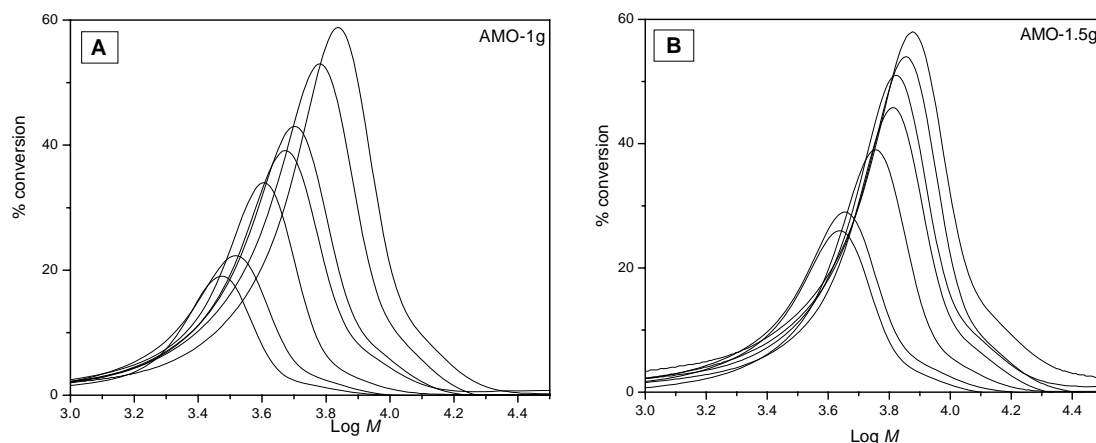


Fig 4.34: Molecular weight distribution for ASO stabilized RAFT miniemulsion polymerization of styrene at 85°C: A = 1 g ASO and B = 1.5 g ASO

The ASO was also efficient in stabilizing the RAFT mediated styrene miniemulsion polymerization. The molecular weight increased with increasing conversion. The chromatograms have a shoulder at high molecular weight, due to termination by coupling, as previously mentioned.

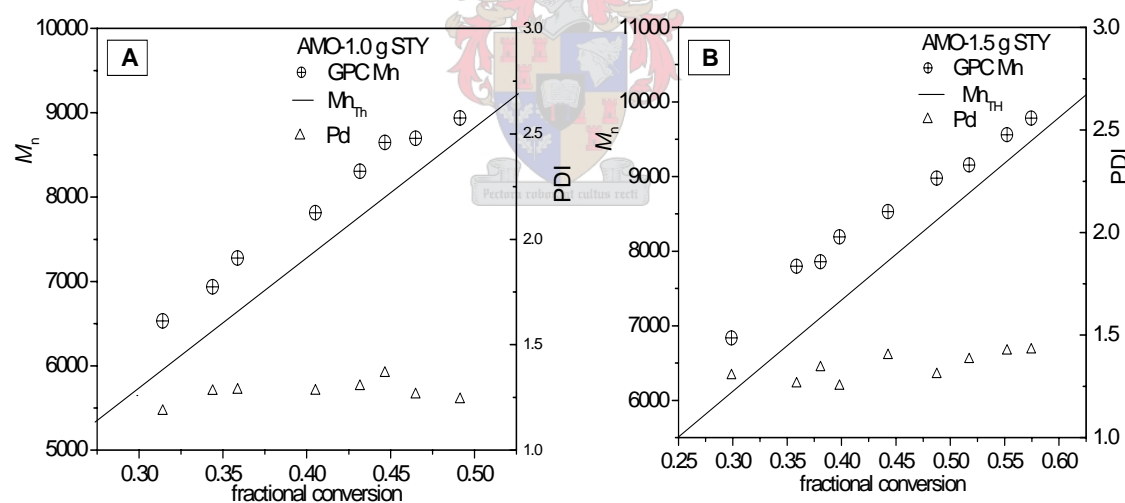


Fig 4.35: Evolution of  $M_n$  and PDI for ASO stabilized RAFT miniemulsion polymerization of styrene at 85°C: A = 1 g of ASO and B = 1.5 g of ASO

In reactions carried out using 1.0 g and 1.5 g of ASO, the number average molecular weight increased with increasing conversion (Fig 4.34A and B) and the polydispersities were below 1.5 throughout the reaction. The deviation of GPC  $M_n$  from theoretical can be due to underestimation and/or termination.

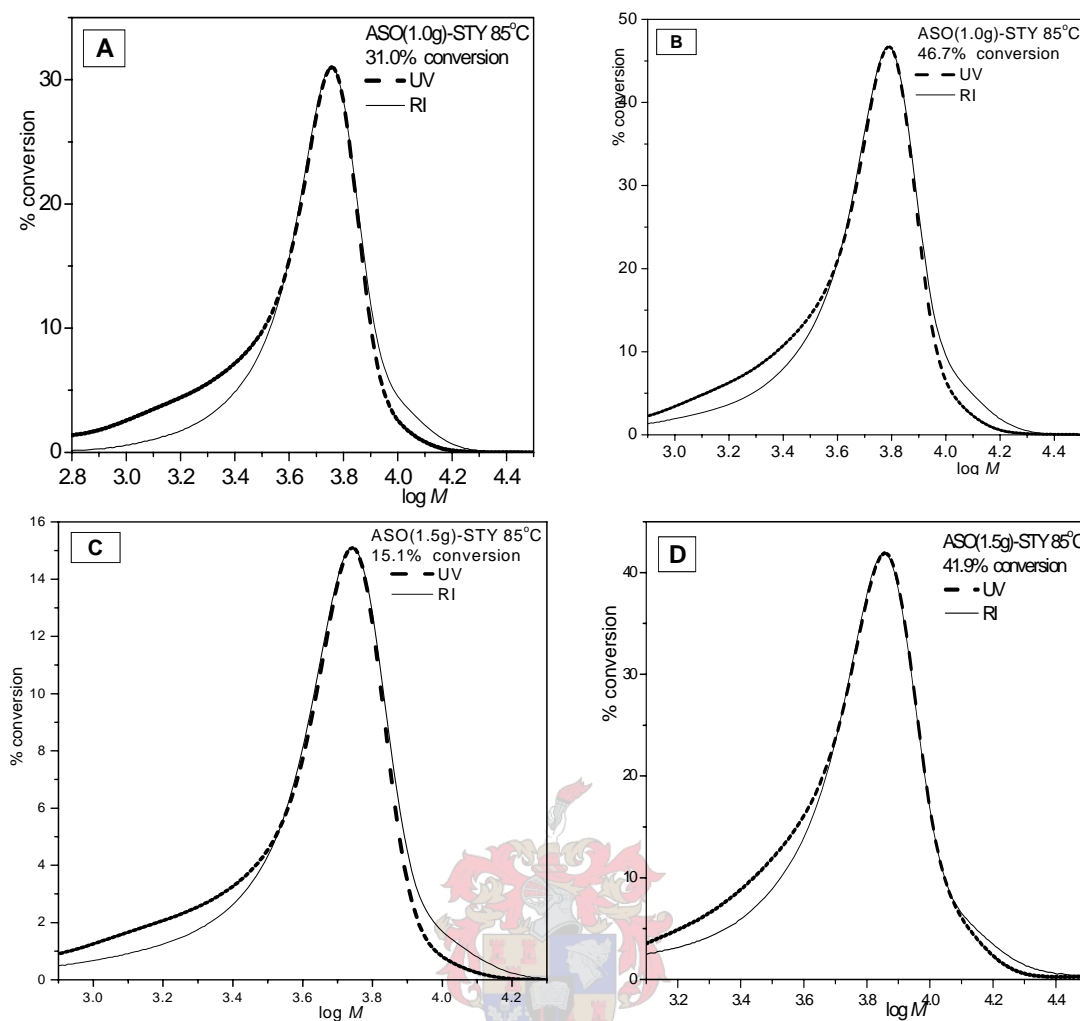


Fig 4.36: UV-RI overlays; A, B and C, D for 1.0 g and 1.5 g ASO respectively in RAFT mediated miniemulsion polymerization of styrene at respective conversions

The UV-RI curves show that most of the polymer chains were RAFT terminated, meaning that the chain growth mechanism was via the RAFT process. There was no significant difference between the AS and ASO stabilized reactions in terms of the molecular weight distribution but the rate of reaction was faster and higher conversions were found in the AS stabilized system than in the ASO stabilized miniemulsion polymerization. This could be due to different initial droplet sizes, as reflected in the final particle sizes (see Section 4.5.2.)

#### 4.6.4: ASO in RAFT mediated miniemulsion polymerization of MMA

##### 4.6.4.1: Rates of reaction

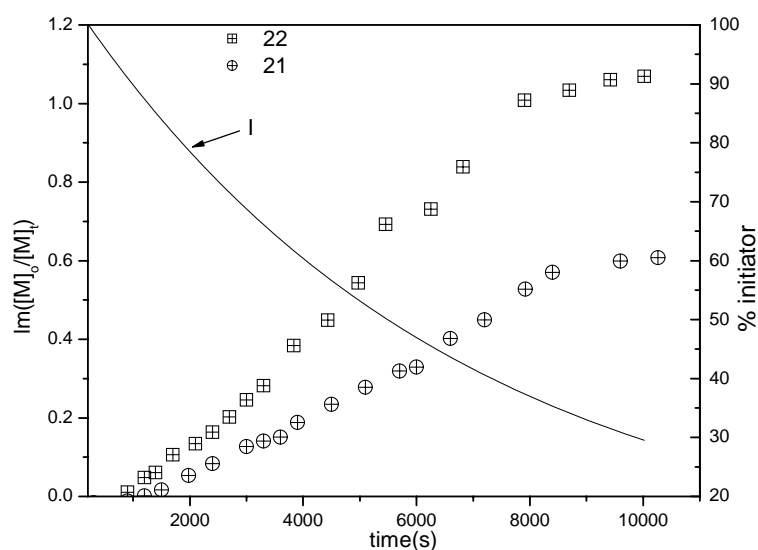


Fig 4.37: 1st order rate kinetics for AS oligomer stabilized miniemulsion polymerization of MMA: 22 = 1.5 g ASO, 21 = 1.0 g of ASO and I = initiator decay curve at 80°C

The ASO was successfully used in RAFT mediated miniemulsion polymerization of MMA. The rates of reaction were however lower when compared to the rates of reaction where the AS surfmer was used (Section 4.4.2). The final conversions were also lower in oligomer stabilized miniemulsion compared to the surfmer stabilized miniemulsion. This might be because the emulsification efficiency of the oligomers was lower than that of their monomers as they behave as polyelectrolytes in aqueous medium and have a tendency to self assemble even at low concentrations. Self assembly of the oligosurfmers may lead to low surface coverage of monomer droplets, leading to large initial monomer droplets. The large initial droplets result in a fewer secondary reactors/nano-reactors, hence low rates of reactions were observed. The rate of reaction increased when more ASO was used, as expected, since an increase in surfactant results in an increase in the number of initial droplets, in which each droplet will become the reaction locus. This results in an increase in the reaction rates.

4.6.4.2: Stabilization of MMA using 1 g of ASO

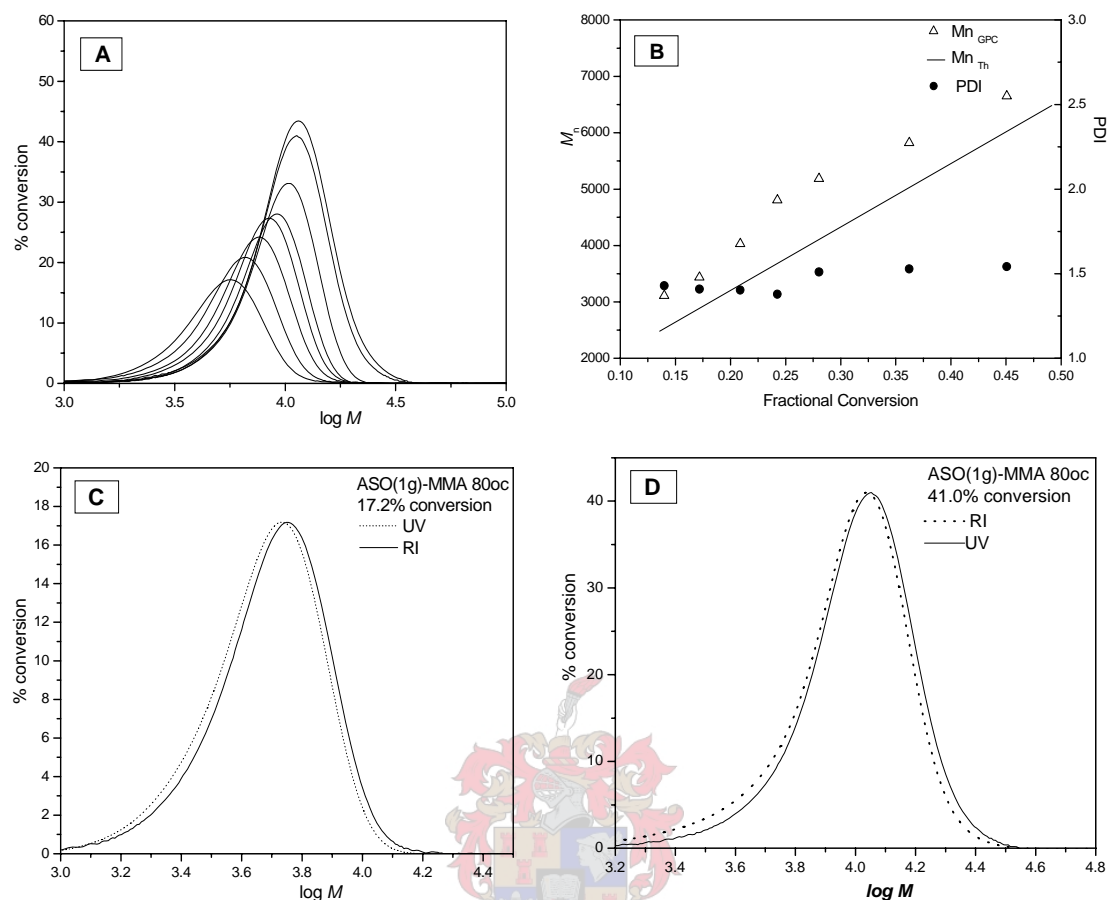


Fig 4.38: A = Molecular weight distribution for AS oligomer (1.0 g) stabilized RAFT miniemulsion polymerization of MMA; B = Evolution of  $M_n$  and PDI for RAFT miniemulsion polymerization of MMA at 80°C; C and D are UV-RI overlays at respective conversions

The number average molecular weight increased with conversion (Figs 4.38A and B), which is the case for controlled free radical polymerization. The polydispersities were around 1.5 throughout the whole reaction. The UV-RI overlays (Figs 4.38C and D) show that most of the chains had the RAFT end group.

4.6.4.3: Stabilization of MMA using 1.5 g of ASO

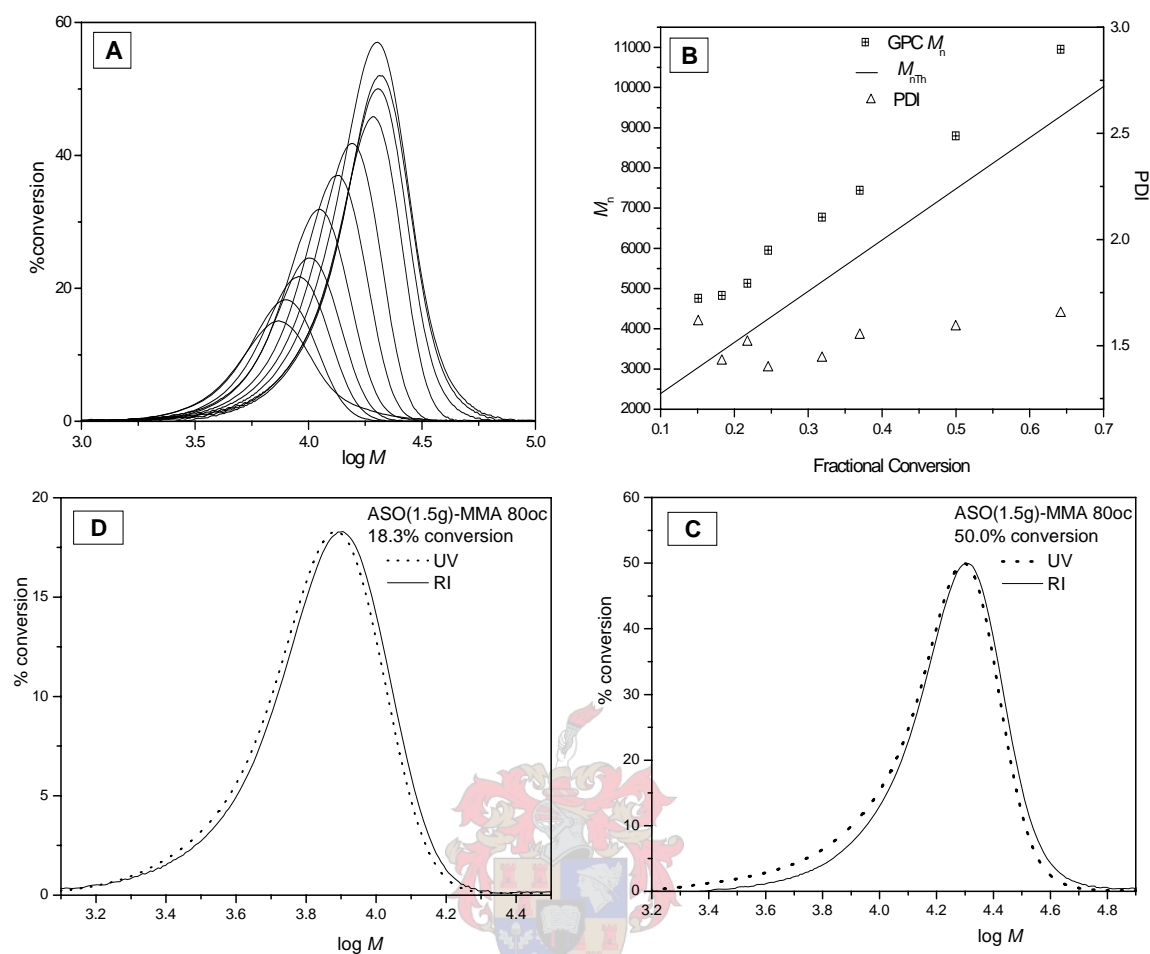


Fig 4.39: A = molecular weight distribution for AS oligomer (1.5g) stabilized RAFT miniemulsion polymerization of MMA at 80°C; B = Evolution of  $M_n$  and PDI for RAFT miniemulsion polymerization of MMA at 80°C; C and D are UV-RI overlays at respective conversions

The  $M_n$  increased with conversion (Figs 4.39A and B), showing that the polymerizations were controlled. The polydispersities were relatively constant, which is expected for controlled polymerization reactions. The UV-RI overlays show that most of the chains are RAFT terminated.

4.6.4.3: Comment on the use of RAFT oligosurfmers as emulsifiers

Since the oligomers were RAFT terminated (see Chapter 3, Section 3.6.2.3), the author expected chain extension to occur in this system. As the oligosurfmers did not dissolve in THF, the chain extension could not be investigated by HPL (THF/H<sub>2</sub>O eluent). It was highlighted in Chapter 2 that the use of these oligomers in aqueous

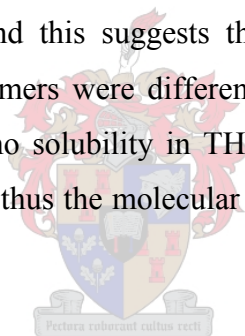


## ***Chapter 4: RAFT mediated miniemulsion polymerization***

---

polymerization can eliminate the problems of surfactant migration as the oligomers themselves are relatively large molecules, which make it difficult for them to migrate. Low rates of reaction, large particle size (see Section 4.7, Tables 4.5 and 4.7), and low monomer conversion have been found for oligosurfmer stabilized miniemulsion polymerization reactions, as described in Sections 3.3 and 4.5.

The SSO and ASO were used as emulsifiers in the miniemulsion polymerization of styrene with no additional RAFT agent added (as was the case in Section 4.3.3). This was done to allow chain extension and molecular weight control through the RAFT end group of the oligosurfmer. The oligosurfmer would be the first block of the block-copolymer. The miniemulsions were prepared as described in Section 4.2 with the exception that no additional RAFT agent was added. The feasibility of chain extension was however not known and full characterization of polymer formed is still ongoing. The block copolymer was not soluble in THF (SEC) but was soluble in a 50/50 mixture of THF/water and this suggests that a block copolymer had been formed. Thus the resulting polymers were different from those obtained in Section 4.3.3 as they showed virtually no solubility in THF. Polymers produced in Section 4.3.3 dissolved well in THF and thus the molecular weights were determined by SEC with THF as the eluent.



## **4.7: Particle sizes of styrene and MMA lattices**

### **4.7.1: Dynamic Light Scattering (DLS) and Transmission Electron Microscopy (TEM)**

#### **Analysis**

Particle sizes of the final latexes were measured using Dynamic Light Scattering (DLS). The instrument was a Zetasizer 1000HS. The cell was a capillary cell and the count rate was in the range 300 to 350 kCps. The detector angle was 90°C, the wavelength was 633 nm and the temperature was 25°C. The transmission electron microscope was a Leo 912 (uracyl acetate stain; dilution 1:50 latex to deionized water).

#### **4.7.1.1: Styrene latex particle sizes**

**Table 4.4: The particle sizes (nm) of styrene miniemulsion latexes for different surfactants and surfmers**

<b>Reaction numbers</b>	<b>Temperature (°C)</b>	<b>Surfactant/Surfmer</b>	<b>Z<sub>average</sub> (nm)</b>
1	85	SDS	64.5
2	75		66.9
5	85	SS	97.9
6	75		88.8
3	85	CTAB	88.3
4	75		86.2
7	85	AS	79.2
8	75		82.6

The final latex particle sizes for the reactions stabilized by SDS were smaller compared to those of SS stabilized latexes for the two reactions conducted at different temperatures. It is expected that there will be more SS in the aqueous phase due to its high water solubility and less SS is available to stabilize the monomer droplets; therefore there is a possibility of homopolymerization of SS in the aqueous phase. The preferential polymerization of the SS in styrene polymerization may lead to formation

## ***Chapter 4: RAFT mediated miniemulsion polymerization***

---

of polysurfmers in the aqueous phase and the droplet/particle stabilization mechanism is likely to deviate from that of classical surfactant to that of polymeric surfactants.

Hence polymerization starts from relatively large monomer droplets, giving larger latex particle sizes in SS than SDS stabilized latexes. However particle sizes obtained for AS stabilized latexes were smaller compared to those of CTAB stabilized latexes but the difference falls within experimental deviation. Generally, the surfmers provide particle sizes that are comparable to that of classical surfactants, SDS and CTAB, when each is used in equimolar ratios in the miniemulsion polymerization of styrene. This can also be related to the rates of reactions where similar behaviors were seen (Section 4.3.1.3). Despite the complexity of the molecular weight distribution of SS stabilized polymers, the final particle size is similar to that of SDS.

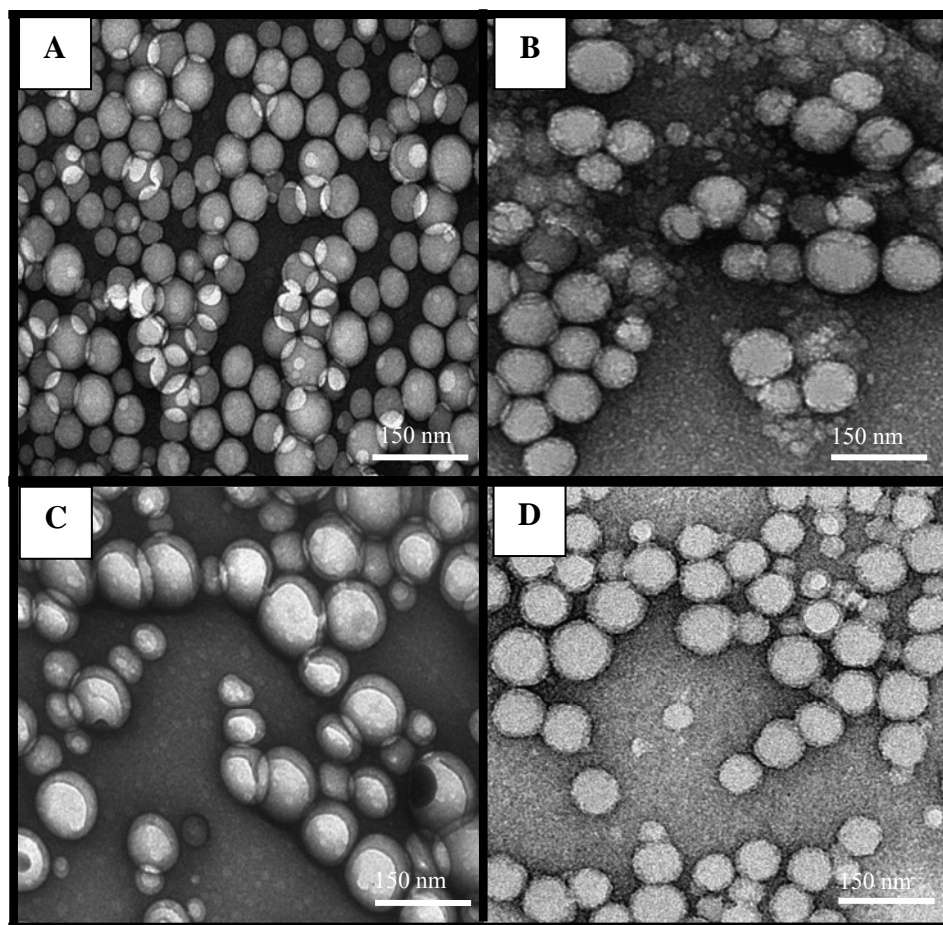


**Fig 4.40: TEM images for polystyrene latexes: A = SDS stabilized polystyrene particles; B = SS stabilized polystyrene particles; C = CTAB stabilized polystyrene particles; D = AS stabilized polystyrene particles (see Table 4.1 for compositions)**

## ***Chapter 4: RAFT mediated miniemulsion polymerization***

The TEM images in Fig 4.40A through D show well define particles. Surfmer stabilized latexes show a broader particle size distribution. However, TEM results resemble dynamic light scattering results. The difference is in Fig 4.40B where many fine particles are found. This is unique to the SS stabilized polystyrene particles and it indicates a much smaller particle, as would be expected for secondary nucleation. What is surprising is the amount of small particles for they are many even though the total volume of these small particles is still small since they were not detected in GPC curves of higher conversion.

**Table 4.5: Styrene miniemulsion latex with SSO and ASO (oligomers) at 85°C**

<b>Reaction number</b>	<b>Oligomer</b>	<b>Quantity of oligomer (g)</b>	<b>Z<sub>average</sub> (nm)</b>
17	SSO	1.5	144.9
23	SSO	1.0	147.5
19	ASO	1.0	157.7
20	ASO	1.5	151.6

The oligosurfmers gave particle sizes that are large compared to those of the particles formed by their monomers. Lim *et al*<sup>23</sup> found particles sizes between 150 and 400 nm when poly (methyl methacrylate-*b*-(diethyl amino) ethyl methacrylate diblock copolymer was used as an emulsifier in miniemulsion polymerization. Chern and Liou<sup>28</sup> used a non-ionic nonylphenol polyethoxylate and particle sizes of between 135 and 280 nm were observed. In miniemulsion polymerization, 1:1 copying of the monomer droplets to polymer particles is obtained in ideal reactions.<sup>12,17,14</sup> It seems likely that the initial droplet size of oligosurfmer stabilized miniemulsion is relatively large and is a function of the emulsification efficiency of the emulsifier when other variables such as energy of sonication, temperature variation during sonication, among other factors, are kept constant. The large particle sizes were also reflected in the rates of reactions, where oligosurfmer stabilized reactions were slower compared to their corresponding surfmer stabilized miniemulsion reactions. Large initial monomer droplets mean that the number of the nano-reactors is less than when the initial droplet size is large and hence a slower rate of polymerization is observed. Slow rates of polymerization lead to lower total conversions and, once the initiator is depleted, polymerization will be minimal. SSO led to smaller particle sizes than ASO. This is in contrast to what was found for their respective monomers; where AS led to

## ***Chapter 4: RAFT mediated miniemulsion polymerization***

smaller particles than that of SS stabilized miniemulsion latexes. Smaller particle sizes obtained in SSO stabilized miniemulsions can be explained by the fact that, in oligosurfmers, the mass of oligosurfmer was used rather than equimolar equivalents and 1 g or 1.5 g of SSO has more SS moieties than the comparable mass for ASO which will have less AS moieties. The fact that the two oligosurfmers might have different degrees of polymerization (still under investigation), can also affect the overall particle size of the latexes, meaning that, direct comparisons are not elementary.

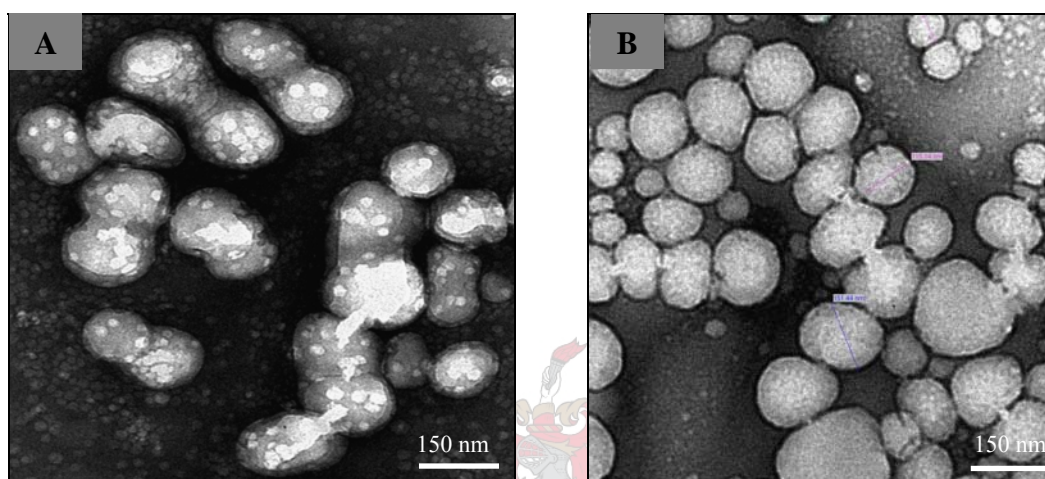


**Fig 4.41: TEM images for polystyrene latexes: A = SSO stabilized polystyrene particles; B = ASO stabilized polystyrene particles. (see Table 4.3 for compositions)**

The SSO stabilized polystyrene particles show a film-forming effect whereas the ASO stabilized particles do not show film formation. The difference might be due to the fact that the samples were not prepared on the same day; hence time might play a role in film formation. It is also observed from the TEM images that the ASO stabilized polystyrene particles have a broad particle size distribution. The SSO stabilized polystyrene latex (Fig 4.41A) shows very small particles. These could arise from secondary particle nucleation, which is less in the ASO stabilized polystyrene latex. This was also observed in the SS and AS stabilized polystyrene latexes where the TEM image of the SS stabilized polystyrene latex showed many small particles compared to that of the AS stabilized polystyrene latex (see Figs 4.40 B and D).

### 4.7.1.2: MMA latex particle sizes

**Table 4.6: The particle sizes (nm) of MMA miniemulsion latexes for different surfactants and surfmers**

Reaction number	Temperature (°C)	Surfactant/ Surfmer	Z <sub>average</sub> (nm)
9	80	SDS	89.8
10	75		93.0
13	80	SS	141.4
14	75		140.5
11	80	CTAB	95.0
12	75		99.6
15	80	AS	167.5
16	T5		170.4

For the MMA system, there is a considerable difference in the final latex particle sizes between latexes stabilized by classical surfactants and those stabilized by surfmers. Surfmers gave larger particle sizes than the classical surfactants did. The rates of reaction were therefore faster in miniemulsions stabilized by classical surfactants than in miniemulsions stabilized by surfmers. This is in contrast to the latex particle sizes obtained in the surfmer stabilized miniemulsion polymerization of styrene where surfmers gave approximately the same particle sizes as those of classical surfactant stabilized miniemulsion styrene latexes. The difference can be explained in terms of the solubility of MMA in the aqueous phase. MMA is more soluble in water than styrene and thus suffers more particle degradation by Oswald ripening.<sup>14</sup> The result of this degradation is that the initial monomer droplets are large, and hence relatively large particles are formed. Surfmers are more water soluble than the classical surfactants due to the ester group present at the tail end. Thus we can postulate that the net result is that surfmers cannot effectively stabilize a more water soluble monomer (MMA compared to styrene). In the styrene miniemulsions stabilized by SS, particle destabilization due to surfmer units being buried inside the particle is unlikely to occur due to preferential polymerization of the sulfate surfmer (SS). The stabilization in styrene-SS miniemulsion changes partially from that of a small molecule surfactant to that of a polymeric surfactant. The AS stabilized styrene miniemulsions do not show any particle destabilization (i.e. comparable particle sizes to those of classical surfactant were obtained) and there is no evidence of preferential addition of the AS. Thus incorporation of the AS is likely to occur on

## Chapter 4: RAFT mediated miniemulsion polymerization

the surface of the droplet and because no increase in initial droplet size as the particle grows is expected in miniemulsion polymerization (1:1 copy of droplet to particle size), the particle remains stable throughout and after the reaction. Further investigation needs to be done to find whether there is any reduction *per se* in surface tension when a water soluble monomer droplet is surrounded by the surfmer by measuring and comparing the surface tension of surfmer stabilized droplets to those of classical surfactant stabilized monomer droplets. Thus, for the classical surfactant, the hydrophobic tail might be the driving force in surface coverage of the MMA monomer droplet, which leads to a considerable net reduction in the surface energy of the system, resulting in the formation of smaller initial monomer droplets.

A significant difference between classical surfactants and surfmers in terms of TEM images as well as particle sizes was observed. Classical surfactants gave well defined particles (Figs 4.42 (A & C)) whereas surfmers gave particles that showed some coalescence. Negative staining was also observed in surfmer stabilized particles.

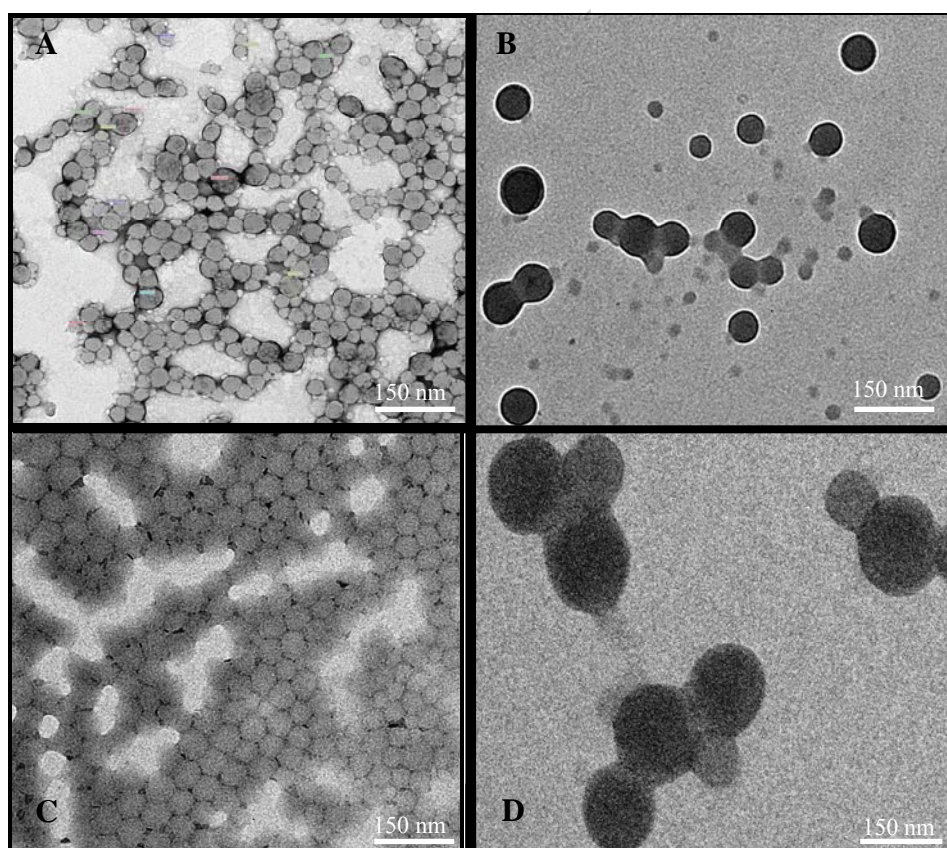


Fig 4.42: TEM images for MMA latexes: A = SDS stabilized PMMA particles; B = SS stabilized PMMA particles; C = CTAB stabilized PMMA particles and D = AS stabilized PMMA particles. (see Table 4.2 for compositions)

## Chapter 4: RAFT mediated miniemulsion polymerization

The particle sizes of latexes stabilized by oligosurfmers were larger compared to particle sizes that were obtained for their monomers (surfmers) in MMA miniemulsion polymerization. Fig 4.42B shows some fine spots which are due to secondary nucleation.

**Table 4.7: MMA miniemulsion latex with SSO and ASO oligomers at 80°C**

Reaction number	Oligomer	Amount of oligomer (g)	Z <sub>average</sub> (nm)
24	SSO	1.0	178.1
18	SSO	1.5	155.1
21	ASO	1.0	198.7
22	ASO	1.5	175.9

A similar trend was also found in oligosurfmer stabilized styrene latexes (Section 4.7.1.1, Table 4.5) and literature<sup>23,28</sup> indicates that particle sizes for polymeric surfactant stabilized miniemulsion polymerization are usually large. Oligomerization in this case results in less effective emulsifying agents. This might be due to inefficient droplet coverage of oligosurfmers due to their bulkiness, hence polymerization starts from relatively large monomer droplets.

### 4.7.2: Capillary Hydrodynamic Fractionation (CHDF)

Capillary hydrodynamic fractionation (CHDF) was used to determine particle size. The instrument used was a Matec Applied Science CHDF 1100, calibrated using polystyrene standards. Analysis was carried out by the "Key Centre for Polymer Colloids, University of Sydney".

#### 4.7.2.1: General

Capillary hydrodynamic fractionation (CHDF) is a hydrodynamic method for the measurement of nanometer-sized particles. A slurry containing the particles is forced through capillaries at high pressure. Flow rate through the capillaries is highest in the center of the capillary. Larger particles extend into the high-flow region while smaller particles travel closer to the wall of the capillary. Thus, larger particles are swept through the capillary ahead of the smaller particles, effecting particle size "fractionation". The particles are detected at the



## Chapter 4: RAFT mediated miniemulsion polymerization

end of the capillary by ultraviolet absorption. Resolution, sensitivity, and size range are dependent on the fractionation cartridge. Particle size data obtained by the CHDF method are tabulated in Tables 4.8 and 4.9.

### 4.7.2.2: Results and discussion

**Table 4.8: Particle sizes (nm) of styrene miniemulsion latexes for different surfactants and surfmers**

Reaction number	Surfactant/Surfmer	Reactions at 85°C Number data (nm)	Reactions at 85°C Weight data (nm)
1	SDS	55.0 ± 14.7	66.0 ± 14.2
5	SS	83.3 ± 20.8	97.7 ± 20.1
3	CTAB	66.2 ± 12.4	81.7 ± 14.0
7	AS	61.3 ± 12.2	75.6 ± 12.7

**Table 4.9: Particle sizes (nm) of MMA miniemulsion latexes for different surfactants and surfmers**

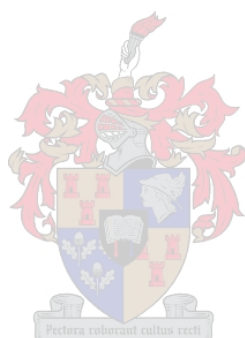
Reaction number	Surfactant/Surfmer	Reactions at 85°C Number data (nm)	Reactions at 85°C Weight data (nm)
9	SDS	54.3 ± 13.0	56.4 ± 15.7
13	SS	59.4±37.5	147.3 ± 54.2
11	CTAB	45.3±14.0	60.6 ± 20.0
15	AS	70.1 ± 22.4	92.5 ± 26.9

The weight overlaid data determined by CHDF (Tables 4.8 and 4.9) resemble the particle sizes obtained by light scattering. The light scattering data is within the standard deviation of the weight average data in most cases. The overlaid number data (Tables 4.8 and 4.9) did not match with the results obtained from light scattering. The reason is that light scattering is

## ***Chapter 4: RAFT mediated miniemulsion polymerization***

---

weight sensitive, as is the CHDF, in measuring by weight mode (weight overlaid data), whereas measuring using overlaid number data mode is not weight sensitive.



### 4.7.2.3: Typical CHDF chromatograms

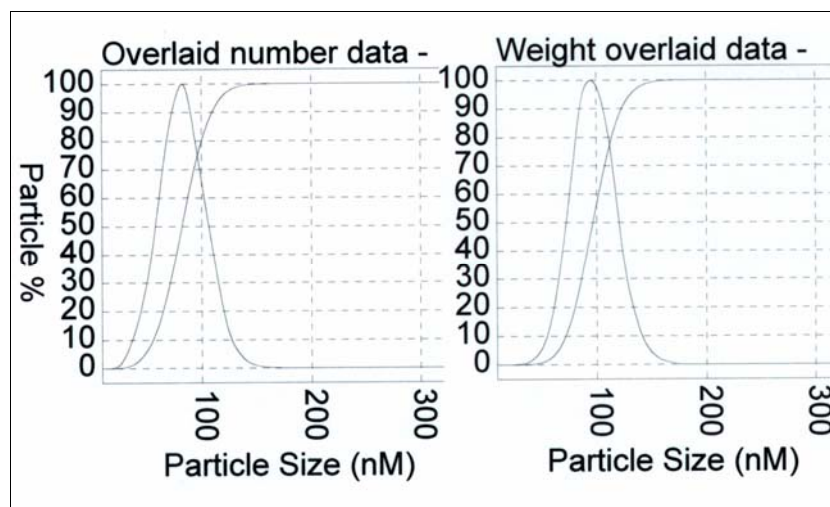


Fig 4.43: Overlaid number data and weight overlaid data (as labeled) for polystyrene latex stabilized by the sulfate surfmer (SS)

The particle size distribution for SS stabilized RAFT miniemulsion polymerization of styrene (Fig 4.43) appears unimodal but is broad. The bimodality observed in the molecular weight distribution is not reflected in the CHDF chromatogram, indicating that the particles are similar in size irrespective of the nature of their formation mechanism.

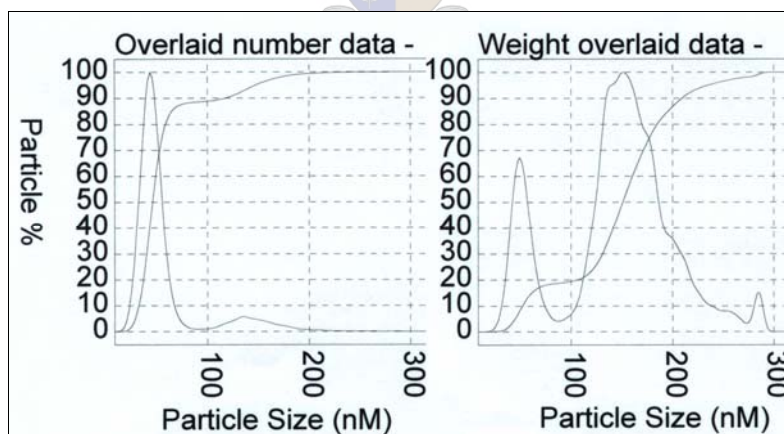
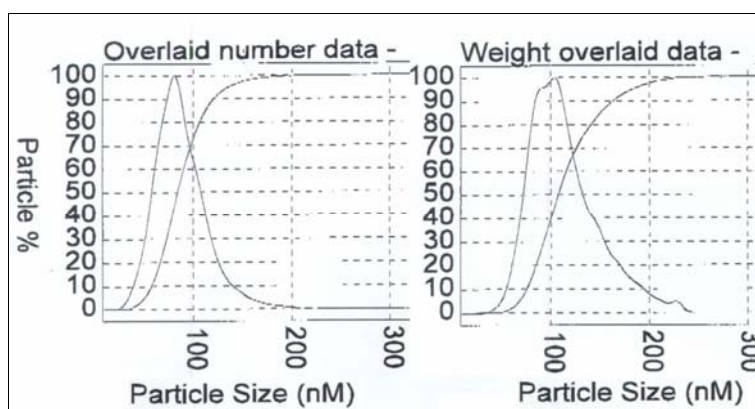


Fig 4.44: Overlaid number data and weight overlaid data (as labeled) for PMMA latex stabilized by the sulfate surfmer (SS)

Fig 4.44 presents both overlaid number data and weight overlaid data. It is observed that there are two particle size distributions for PMMA latex stabilized by SS, unlike the previous particle size distribution for the polystyrene latex stabilized by SS (Fig 4.43) which does not

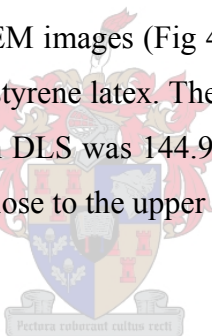
## Chapter 4: RAFT mediated miniemulsion polymerization

show bimodality. The bimodal distribution in PMMA can potentially be attributed to coagulation of particles, as was observed in TEM images (Figs 4.41B & D).



**Fig 4.45: Overlaid number data and weight overlaid data (as labeled) for polystyrene latex stabilized by the ammonium surfmer (ASO)**

The particle size distribution for ASO stabilized styrene (Fig 4.45) is unimodal, broad and skewed towards larger particle size. TEM images (Fig 4.40B) also show the presence of very large particles for ASO stabilized polystyrene latex. The weight overlaid particle size was  $114 \pm 34.5$  nm, while the particle size from DLS was 144.9 nm. The particle size from DLS falls within the standard deviation but it is close to the upper limit.



### **4.8: Conclusions**

#### **4.8.1: General**

Several reactions have been compared (surfactant versus surfmer with the same head group) and from these results it has been shown that the behavior of surfmers SS and AS in terms of the rates of reaction in miniemulsion polymerization is similar to that of classical surfactants SDS & CTAB in certain reactions (reactions 1&5, 2&6, 3&7, 4&8, 9&13, and 10&14). Thus, the efficiency and size dependent coverage<sup>21</sup> of the surfmers and classical surfactants are similar in these reactions. The final latex particle sizes were expected to be similar; however this was not the case in some reactions (see Tables 4.4 and 4.6), indicating that there are other factors affecting particle size. The droplet coverage is a function of the hydrophilic head and the droplet stability is a function of the charge density (or polarity in non-ionic surfactants) of the hydrophilic head. The SDS hydrophilic head is smaller and more polar than that of CTAB and hence, in principle, SDS offers better prevention of coalescence by electrostatic repulsion than CTAB. In the RAFT mediated miniemulsion polymerization of MMA there is a substantial difference in the rates of polymerization, with the SDS stabilized reaction system giving higher rates of reaction than the CTAB stabilized reaction system. MMA is more water soluble than styrene and thus SDS can more efficiently stabilize MMA monomer droplets against coalescence than CTAB can. It must be remembered that the rate of polymerization depends to a large extent on the number of nano-reactors. The greater the number of initial droplets, the faster is the reaction rate. The same conditions were used in both the SDS and CTAB miniemulsion polymerization of MMA, implying that the CTAB stabilized miniemulsion had relatively larger monomer droplets. This was confirmed by the particle sizes obtained for CTAB that were larger compared to those obtained for SDS latexes.

The surfmers SS and AS were successfully applied in miniemulsion polymerization of both styrene and MMA. In the miniemulsion polymerization of MMA the sulfate surfmer behaved in a similar fashion to SDS; higher rates of reaction were obtained when compared to those of AS stabilized miniemulsions. A comparison of SS and SDS in the miniemulsion polymerization of MMA shows that the efficiencies of the two surface active compounds are similar in terms of rates of reaction. The classical surfactant CTAB showed better efficiency in RAFT miniemulsion polymerization of MMA than AS did. This is explained in terms of

## ***Chapter 4: RAFT mediated miniemulsion polymerization***

---

the different hydrophobic tails. The AS surfmer has a short and partially polar hydrophobic tail, meaning that its solubility in water is higher than that of CTAB and this may result in AS being less efficient in monomer emulsification than CTAB. CTAB was shown to be a better emulsifier in miniemulsion polymerization of MMA, but with styrene the efficiency of the two (AS and CTAB) is even similar. From this the author concludes that a more water soluble monomer requires a more efficient emulsifier for the rates of reaction to be high, whereas there is not much difference in the rate of reaction between classical surfactant and surfmers in the stabilization of miniemulsion polymerization of a relatively low water solubility monomer (styrene). However, the fact that SS shows relatively similar rates as well as final conversion to SDS in MMA miniemulsion brings the nature of the hydrophilic head in droplet stabilization to the center of discussion. The SDS and SS miniemulsion polymerizations of MMA show that irrespective of the nature of the hydrophobic tail, whether it is partially polar as previously stated above or not, does not have a major effect if a sulfate head is used. In other words, the effectiveness of a sulfate head group supercedes the effects of the hydrophobic tail. Thus different rates of reactions have been obtained in CTAB and AS RAFT miniemulsion polymerization of MMA whereas the same surfactants gave similar rates of reaction in the RAFT miniemulsion polymerization of styrene. Although the hydrophilic head is the same, the difference in the rates of reactions in MMA polymerization was attributed to the difference in the nature of the hydrophobic tail of CTAB and AS (i.e. C<sub>16</sub> versus C<sub>11</sub>). The author concludes that the effectiveness of the AS surfmer as an emulsifier depended also on the solubility of the monomer. The CTAB and AS styrene RAFT miniemulsions showed relatively comparable rates irrespective of the difference in their hydrophobic tail. This implies that the solubility of MMA is also playing a role in giving different rates of reactions.

Generally, the rates of reactions were relatively similar. This is in contradiction to the results obtain by Guyot *et al.*,<sup>3</sup> who found that the rates in T-type surfmer stabilized polymerization reactions were lower than those of classically stabilized reactions. They further reported that adding classical surfactant to the T-type surfmer stabilized miniemulsion improved the rates of reaction. In this work, the surfmer and surfactant were used in relatively comparable amounts in terms of number of the moles of the emulsifier. We can also conclude that H-type surfmers are better emulsifiers than the T-type since they gave similar rates of reaction to those of classical surfactant stabilized miniemulsion polymerization reactions. The surfmer stabilized miniemulsion reactions showed longer induction periods than their corresponding

## ***Chapter 4: RAFT mediated miniemulsion polymerization***

---

classical surfactants. This was attributed to residual inhibitors that were present in the surfmers. During surfmer synthesis, polymerization inhibitors were added to prevent unwanted polymerization. The induction periods are longer in SS compared to AS because more of the inhibitor was used in SS synthesis as one of the step reactions, requires a temperature as high as 100°C (as seen in Chapter 3, Section 3.2.1.2).

### **4.8.3: Molecular mass distributions**

The results presented show that the molecular molar mass distributions are similar in SDS, CTAB and AS stabilized RAFT mediated miniemulsion polymerizations. Fig 4.25 shows that the  $M_n$  found in CTAB and AS stabilized miniemulsion polymerization of MMA increased with conversion and that the  $M_n$  values were similar. The SEC  $M_n$  values correspond with the theoretical  $M_n$  predicted by Equation 2.14. The PDIs were also similar, showing that the behavior of AS in RAFT miniemulsion polymerization of MMA and styrene is similar to that of the classical surfactant CTAB. However for the SS stabilized miniemulsion polymerization, the molar mass distributions were not single distributions but comprised distinguishable Sections (at higher molar mass) of different molar mass compared to the major part of the distributions which is at low molar mass. One of the reasons can be that the SS surfmer is likely to be more highly water soluble than the AS and its CMC is higher than that of AS. The result of this water solubility is that the concentration of free surfmers in the aqueous phase is potentially larger in SS polymerization system than in any of the other systems (CTAB, SDS and AS). We can conclude that SS promotes homogeneous nucleation supported by the TEM data (Fig 4.40B) and CHDF data (Fig 4.44) where the smaller particles formed are observed.

The molecular weight distributions obtained in styrene RAFT miniemulsion polymerization (Fig 4.6A, reaction 5) gave a tri-modal distribution with SS as the emulsifier. This can be explained in terms of the compatibility of the hydrophobic tail with the monomer. In the styrene polymerization system the distribution at high molar mass might be due to the SS induced secondary nucleated particles where there is no control, the middle distribution could then be a copolymer of styrene and SS, whereas the molar mass distribution at low molar mass is most probably due to styrene homo polymer.

## ***Chapter 4: RAFT mediated miniemulsion polymerization***

---

The molecular weight distributions obtained in the MMA RAFT miniemulsion polymerization MMA system gave a mixed modal distribution (Fig 4.18A). It is likely that the partial compatibility between the MMA monomer and the hydrophobic tail of SS led to the formation of copolymers rather than homopolymers in the aqueous phase. We also postulate that the distribution at lower molecular weight is possibly due to polymer chains formed by the droplet nucleation mechanism. The bimodal and trimodal distributions observed are probably due to secondary nucleated particles, observed in the TEM image (Fig 4.42B). However attention has to be given to the potential activity of the sulfate head towards the chromatographic column which can also lead to retention of the polymer chains that had the SS monomer incorporated in them. Column interaction can also lead to the apparent distributions obtained in Figs 4.6A and C. However, the fact that the molar mass distributions are different in styrene and MMA polymerizations shows that the distributions are most probably dependent on the monomer used which means that the most important factors are likely to be differences in reactivity and the solubility of these monomers. It also means that the choice of surfactant is important to create well behaved controlled systems.

### **4.8.3: RAFT in miniemulsion polymerization**

The reactions conducted using the AS surfmer for both MMA and styrene miniemulsion polymerization showed that the increase in  $M_n$  of AS stabilized reactions was similar to that of CTAB stabilized reactions and the experimental SEC values were close to the theoretically predicted values. The molar mass distributions showed the increase in molecular weight with conversion for the distribution at low molecular weight in the multimodal distributions, which is characteristic of a living system. The polydispersity values of the AS stabilized system are comparable to those of the classical surfactant CTAB stabilized system. Direct comparisons between the SS and SDS stabilized systems in terms of  $M_n$  and PDI are not easily carried out because of the complication in the molar mass distribution of SS stabilized systems. However, despite this, the molar mass distributions show an increase in molecular weight with conversion, which means there is a degree of molar mass control.



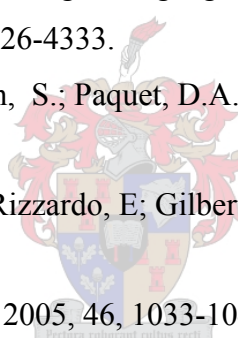
### 4.9: References

- (1) Tsavalas, J. G.; Schork, F. J.; Brouwer, H.; Monteiro, M. J. *Macromolecules* 2001, 34, 3938-3946.
- (2) Luo, Y.; Tsavalas, J. G.; Schork, F. J. *Macromolecules* 2001, 34, 5501-5507.
- (3) Lansalot, M.; Davis, T. P.; Heuts, J. P. A. *Macromolecules* 2002, 35, 7582-7591.
- (4) Butte', A.; Storti, G.; Morbidelli, M. *Macromolecules* 2001, 34, 5885-5896.
- (5) Aizpurua, I.; Amalvy, J. I.; Barandiaran, M. J. *Colloids and Surfaces: Physicochemical and engineering aspects* 2000, 59-66.
- (6) Asua, J. M. *Progress in Polymer Science* 2002, 27, 1283-1346.
- (7) Guyot, A.; Graillat, C.; Favero, C. C. R. *Chimie* 2003, 6, 1319-1327.
- (8) Unzue, M. J.; Schoonbrood, H. A. S.; Asua, J. M.; Gon, A. M.; Sherrington, D. C.; Stahler, K.; Goebel, K.; Tauer, K.; Sjoberg, M.; Holmberg, K. *Journal of Applied Polymer Science* 1997, 66, 1803-1820.
- (9) Joynes, D.; Sherrington, D. C. *Polymer* 1996, 37, 1453-1462.
- (10) Abele, S.; Sjoberg, M.; Hamaide, T.; Zicmznis, A.; Guyat, A. *Langmuir* 1997, 13, 176-181.
- (11) Chern, C.-S.; Chen, T.J.; Liou, Y.C. *Polymer* 1998, 39, 3767-3777.
- (12) Landfester, K. *Macromolecules* 1999, 32, 2679-2683.
- (13) Ghielmi, A.; Storti, G.; Morbidelli, M.; Ray, W. H. *Macromolecules* 1998, 31, 7172-7186.
- (14) Antonietti, M.; Landfester, K. *Progress in Polymer Science* 2002, 27, 689-757.
- (15) De Brouwer, H.; Tsavalas, J. G.; Schork, F. J.; Monteiro, M. J. *Macromolecules* 2000, 33, 9239-9246.
- (16) Tsavalas, J. G.; Schork, F. J.; de Brouwer, H.; Monteiro, M. J. *Macromolecules* 2001, 34, 3938-3946.
- (17) Landfester, K.; Willert, M.; Antonietti, M. *Macromolecules* 2000, 33, 2370-2376.
- (18) Lansalot, M.; Davis, T. P.; Heuts, J. P. A. *Macromolecules* 2002, 35, 7582-7591.
- (19) Charmot, D.; Corpart, P.; Adam, H.; Zard, S. Z.; Biadatti, B. G. *Macromolecular Symposia* 2000, 150, 23-32.

## ***Chapter 4: RAFT mediated miniemulsion polymerization***

---

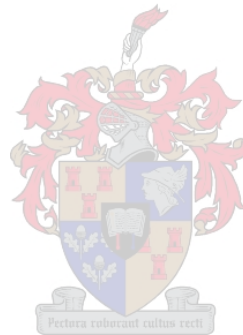
- (20) Landfester, K.; Bechthold, N.; Tiarks, F.; Antonietti, M. *Macromolecules* 1999, 32, 5222-5228.
- (21) Wang, S.; Schork, F. J. *Journal of Applied Polymer Science* 1994, 54, 2157-2164.
- (22) Reimers, J. L.; Schork, F. J. *Journal of Applied Polymer Science* 1996, 60, 251-262.
- (23) Lim, M.-S.; Chen, H. *Journal of Applied Polymer Science* 2000, 38, 1818-1827.
- (24) Merk, Certificate of Analysis, 71727 SDS, Biochemica Ultra  $\geq 90\%$  (GC)
- (25) Saarchem Laboratory Reagents (Specifications and Technical Manual p205)
- (26) Pasch, H.; Trathnigg, B. *HPLC of Polymers*; Springer: Berlin, 1998.
- (27) Baran, K.; Laugier, S.; Cramail, H. J. *Chromatogr. B* 2001, 753, 139-149.
- (28) Zhu, J.; Zhu, X.; Zhou, D.; Chen, J.; Wang, X. *European Polymer Journal* 2004, 40, 743-749.
- (29) Muller; Axel H. E.; Zhuang; Rugang Yan; Deyue Litvinenko; Galina *Macromolecules* 1995, 28, 4326-4333.
- (30) Hutchinson, R.A.; Beuermann, S.; Paquet, D.A.; McMinn, J. H. *Macromolecules* 1997, 30, 3490-3493.
- (31) Prescott, S.W; Ballard, M.J; Rizzardo, E; Gilbert, R.G. *Macromolecules*, 2005, in press
- (32) Nozari, S; Tauer, K. *Polymer* 2005, 46, 1033-1043



## **Chapter 5: Conclusions and recommendations**

### **Abstract**

General conclusions on the findings of this research and possible recommendations for future studies in line with the work presented are provided.



## **5.1: Conclusions**

1. The synthesis of two specific surfmers 11-methacryloyloxyundecan-1-yl sulfate and 11-methacryloyloxyundecan-1-yl trimethyl ammonium bromide (referred to as SS and AS respectively) was successfully carried out as confirmed by NMR, IR and ES/M spectroscopy. The critical micelle concentrations (CMC) of the surfmers were higher than their respective classical surfactants. The high CMC of the surfmers was attributed to the nature of the hydrophobic tail which interacts with water to a certain degree because of the presence of the ester group.
2. Surfmers were used in miniemulsions as emulsifiers. In most cases, the rates of reaction were similar to those recorded with the classical surfactants. In styrene miniemulsion polymerization the two surfmers, SS and AS, showed similar rates in comparison to classical surfactants SDS and CTAB, respectively. In MMA miniemulsion, the anionic emulsifiers SDS and SS showed higher rates of reactions when compared to the cationic emulsifiers CTAB and AS, respectively.
3. Oligosurfmers were successfully synthesized. Polymerization of surfmers was confirmed by the disappearance of the vinylic proton signals in  $^1\text{H}$  NMR spectra. UV spectroscopic analysis of oligosurfmers showed that some of the chains were RAFT terminated. The  $M_n$  of oligosurfmers was estimated using UV spectroscopy and was found to be lower than the theoretical  $M_n$ . However further investigation is required to determine whether the RAFT agent was able to control the molar mass distribution.
4. The synthesized oligosurfmers were used to stabilize styrene and MMA miniemulsion polymerizations. The miniemulsions were stable during and after polymerization. However the rates of reactions were much lower compared to reaction in which their monomers were used. An attempt to form block polymers of oligosurfmer with styrene and MMA was made but the polymers could not be analyzed by molecular weight composition determination techniques such as GPC and HPLC due to lack of suitable conditions and the incompatibility of solvents with the analytical instruments.

5. AS stabilized miniemulsions gave polymers with unimodal GPC molar mass distributions (THF as solvent) whereas SS stabilized miniemulsions gave trimodal distributions in styrene polymerization and mixed-modal distributions in MMA polymerization from GPC (THF). HPLC analysis of SS latexes gave two separate peaks which could be related to polystyrene or random co-polymer of SS and styrene. HPLC analysis of AS latexes showed a single peak at the critical conditions of polystyrene. In this work HPLC analysis of the copolymers was not able to fully elucidate the distributions shown by GPC. Further investigations into this are required. The GPC traces of AS oligomer stabilized polymers showed single distributions.
6. The trimodal and mixed modal distributions obtained for polystyrene and PMMA respectively when SS was used as an emulsifier were attributed to secondary nucleated particles. TEM and CHDF results showed the presents of these secondary particles. Secondary particles were prominent in the SS stabilized systems mainly because of its high solubility in the water phase, thereby supporting secondary particle formation.
7. Particle sizes of the latexes were determined via CHDF, dynamic light scattering and transmission electron spectroscopy. Results were generally in agreement with the kinetic data for most reactions. Surfmer stabilized miniemulsions provided larger particle sizes compared to classical surfactants in the RAFT miniemulsion polymerization of MMA. Oligosurfmer stabilized RAFT miniemulsion polymerization of both styrene and MMA gave larger particle sizes when compared to both their monomers (surfmers) and classical surfactants.
8. The oligosurfmers gave stable miniemulsions both during and after polymerization. The particle sizes were larger compared to those obtained when their monomers were used. It was also observed that the SS oligomer (SSO) gave unimodal molecular weight distribution whereas the monomer (SS) gave trimodal distributions. Thus it can be concluded that the mixed and trimodalities observed in SS systems are primarily due to the participation of SS in polymerization reaction. However, the TEM images of SSO stabilized latexes showed some secondary particles, which was the case with the SS stabilized latexes. The ASO gave unimodal distribution as expected; AS did not

## ***Chapter 5: Conclusions and Recommendations***

---

give any bimodal or trimodal distribution in both styrene and MMA RAFT miniemulsion polymerization.



## **5.2: Recommendations for future research**

A number of questions arose during this study that would benefit from further investigation. In order to further clarify the mechanisms at play in the presented in this thesis, the following recommendations for future research are made:

1. Investigate the kinetics of the SS surfmer in miniemulsion in order to be able to draw tangible conclusions in terms of molar mass distributions.
2. Further investigate the use of RAFT in the synthesis of oligosurfmers and the feasibility of forming block copolymers of oligosurfmers with either MMA or styrene.
3. Investigate the properties of the surfmer stabilized latexes in terms of water absorption of their films as well as their stability towards mechanical agitation, shear and freeze thawing conditions.
4. Carry out 2-D chromatographic analyses of surfmer stabilized miniemulsion polymers (styrene and MMA). (This work was not complete due to lack of suitable HPLC conditions, i.e. column packing materials and suitable solvent systems).
5. Further characterize the block copolymers (oligosurfmers-b-PS or PMMA). (This work was not complete due to lack of suitable HPLC conditions for characterizing the block copolymers). This can be done by using HPLC columns that operate under aqueous conditions as the block copolymers tend to dissolve in a mixture of water and THF in the ratio of 4:5.